VIBRATION OF LIGHTWEIGHT WOODEN FLOORS: EXPERIMENTAL AND ANALYTICAL EVALUATION

by

GREG A. NEUMANN

B.A.Sc., The University of British Columbia, 1990

A THESIS SUBMITTED IN PARTIAL FULFILLMENT OF

THE REQUIREMENTS FOR THE DEGREE OF

MASTER OF APPLIED SCIENCE

in

THE FACULTY OF GRADUATE STUDIES

(Civil Engineering)

We accept this thesis as conforming

THE UNIVERSITY OF BRITISH COLUMBIA

OCTOBER 1992

In presenting this thesis in partial fulfillment of the requirements for an advanced degree at the University of British Columbia, I agree that the Library shall make it freely available for reference and study. I further agree that permission for extensive copying of this thesis for scholarly purposes may be granted by the head of my department or by his or her representatives. It is understood that copying or publication of this thesis for financial gain shall not be allowed without my written permission.

Department of Civil Engineering.

The University of British Columbia

Vancouver, Canada

Date October 15, 1992.

Abstract

An experimental study of two lightweight wooden floors' dynamic response was performed. The objective of this study was to evaluate the applicability of the computer programs, NAFFAP and DYFAP, for the case of lightweight wooden floor vibration. The program NAFFAP solves for the floor system's natural frequencies and mode shapes while DYFAP performs a time domain integration of the equations of motion in response to a specified loading on the floor. DYFAP also has the capacity to model the coupled response of oscillators upon the floor system. These programs employ a T–beam finite strip analysis. The test data of the floors' dynamic response to various impacts were compared with the programs' simulations. One floor used 2x8 sawn lumber joists while the other used composite wood I–Joists. The transient dynamic response of the two floors to three types of excitation were recorded. The three types of excitation were created by a hammer tap, releasing a sand filled bag and a standard human heel drop. The modelling of a human occupant with a single degree of freedom oscillator, the International Standards Organization's two degree of freedom oscillator model and a forcing function were investigated with DYFAP. The oscillators were composed of lumped masses, springs and viscous dashpots.

The program NAFFAP was sufficiently successful in predicting the floors' natural frequencies. The floor parameters that were used with NAFFAP were then used with DYFAP to produce displacement time histories that compared well with the test data. DYFAP's modelling of occupants with simple oscillators rather than a forcing function proved to be appropriate.

Table of Contents

List of Tables

List of Figures

Acknowledgement

I wish to express gratitude to my supervisor Ricardo O. Foschi and to Bryan Folz for their advice and assistance throughout this project. Thanks to the Council of Forest Industries of B.C. for their donation of building material. The continuous support of family and friends is appreciated for it was important for the successful completion of this thesis.

Chapter 1

Introduction

Excessive vibrations of lightweight floor systems have become a common design problem now that higher strength materials are becoming available. They allow designs to employ lighter and longer spanning structural members. Lightweight wooden floors constructed for the North American residential market have received an increasing number of consumer complaints. This has prompted a number of studies and has resulted in the NBCC1990 adopting a new, more stringent vibration criteria. Allowable floor joist spans have been reduced in an effort to minimize the number of floors that have natural frequencies which fall within or near the human's primary natural frequencies that lie between 4Hz and 20Hz.

1.1 Human Perception of Floor Vibrations

Much work has been done to identify human vibration threshhold levels. Relationships between acceptable vibrational performance and acceleration, deflection, velocity, or frequency have been explored. A subjective testing procedure has generally been used. Subjects have been asked to evaluate floor vibrations via various scales. Most human senses are believed to be of a logarithmic rather than linear nature, thus Ohlsson believes that vibration perception ought to behave similarly [Ohlsson, 1982]. Y.H. Chui listed a small literature review concerning this area [Chui, 1986]. A short summary of his listings follows:

Onysko and Bellosillo (1978) made a comprehensive literature review;

Russel (1954) and Hanson (1960) correlated discomfort level with deflection under concentrated load;

Polensek (1970) studied human response to impulsive vibrations in terms of their frequency and amplitude;

Lenzen (1962) had human subjects evaluate floor vibrations using the Reiher and Meister Scale (1946);

Lenzen (1962), Polensek (1975), Rainer and Pernica (1981) considered the added damping capacity to the floor system provided by a human occupant;

Lenzen (1966) established that damping strongly influences perception of transient vibrations;

Shaver (1976) attempted to correlate acceleration and displacement with human response

Parks (1962), Wiss and Parmalee (1974) studied the response of subjects to transient vibration tests, and their evaluation of the vibrations via a four or five point scale respectively.

Many threshhold and performance curves have been proposed by a number of the above authors. Grether performed a study to determine to what degree vibration would affect human performance [Grether, 1971]. The results indicate that humans are sensitive to frequencies in the range of $4 - 8$Hz. This conclusion was supported by exposure durations from short time (impulse/transient) to continuous vibrations. The curves of equal tolerance of Fig. 1.1 show a marked dip over this range. The International

Standards Organization (ISO), noted and recognized this and recommended that frequencies be weighted to reflect this sensitivity prior to analysis. Y.H. Chui utilized the RMS of the acceleration to develop the graph of tolerable levels shown in Fig. 1.2. He found that a RMS acceleration of $0.375 m/s^2$ resulting from a heel drop impact test defined a boundary between acceptable and unacceptable floor vibration for a typical person [Chui, 1986]. The Reiher and Meister scale for steady–state vibration is shown in Fig. 1.3. Wiss and Parmalee worked with transient vibrations. Shown in Fig. 1.4 is a plot of their mathematical model that they derived from their transient vibration studies [Wiss and Parmelee, 1974]. Allen and Rainer performed tests on long span floors. Shown in Fig. 1.5 is their plot of peak acceleration versus frequency with damping considered. The lines mark acceptability threshholds [Allen and Rainer, 1976]. Shown in Fig. 1.6 is Polensek's plot, which is similar to that of Reiher and Meister's shown in Fig. 1.3. He was interested in the maximum peak–to–peak displacement of the floor response. This is measured by taking the absolute value of the displacement between a positive peak and the following negative peak [Polensek, 1970].

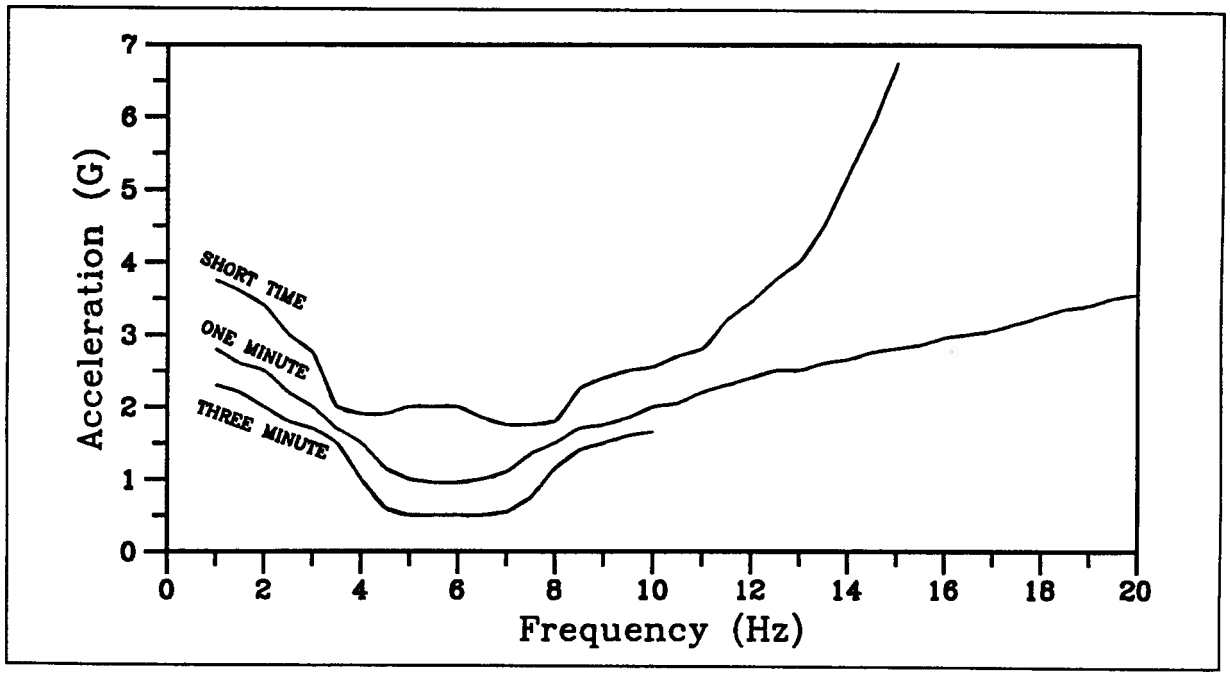

Figure 1.1: Human subjective tolerance to whole body sinusoidal vertical vibrations, standing position (Grether, 1971)

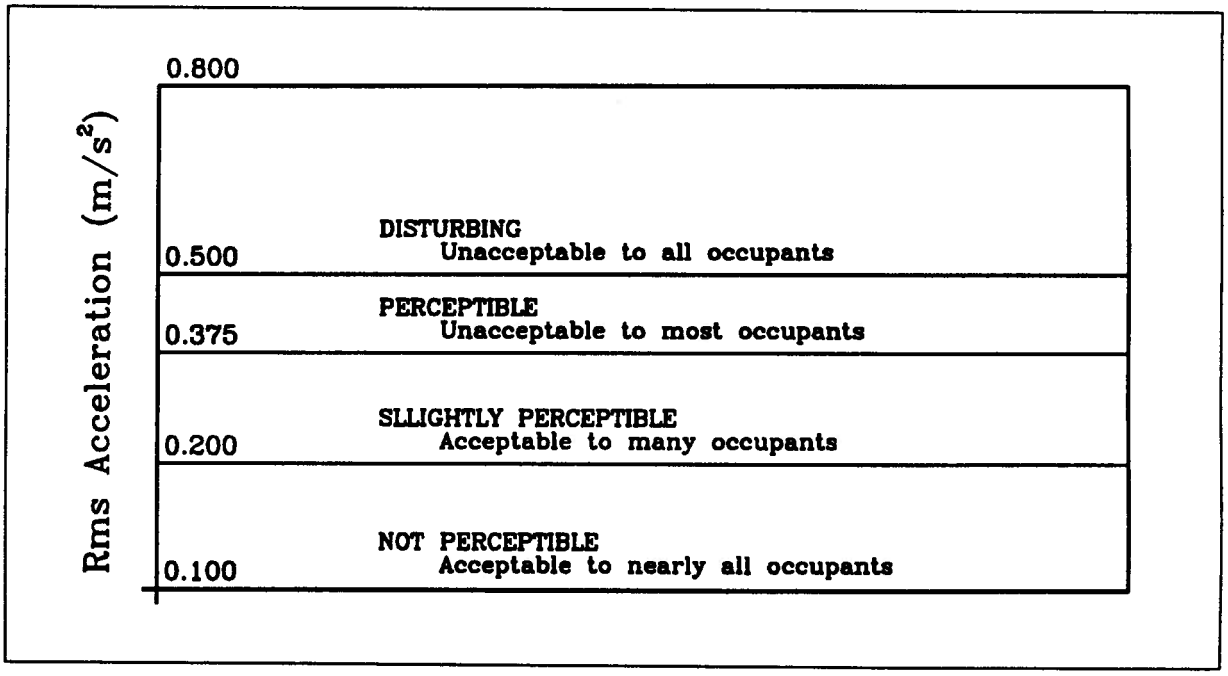

Figure 1.2: Human response to various RMS levels of floor vibration induced by heel drop tests (Chui, 1986)

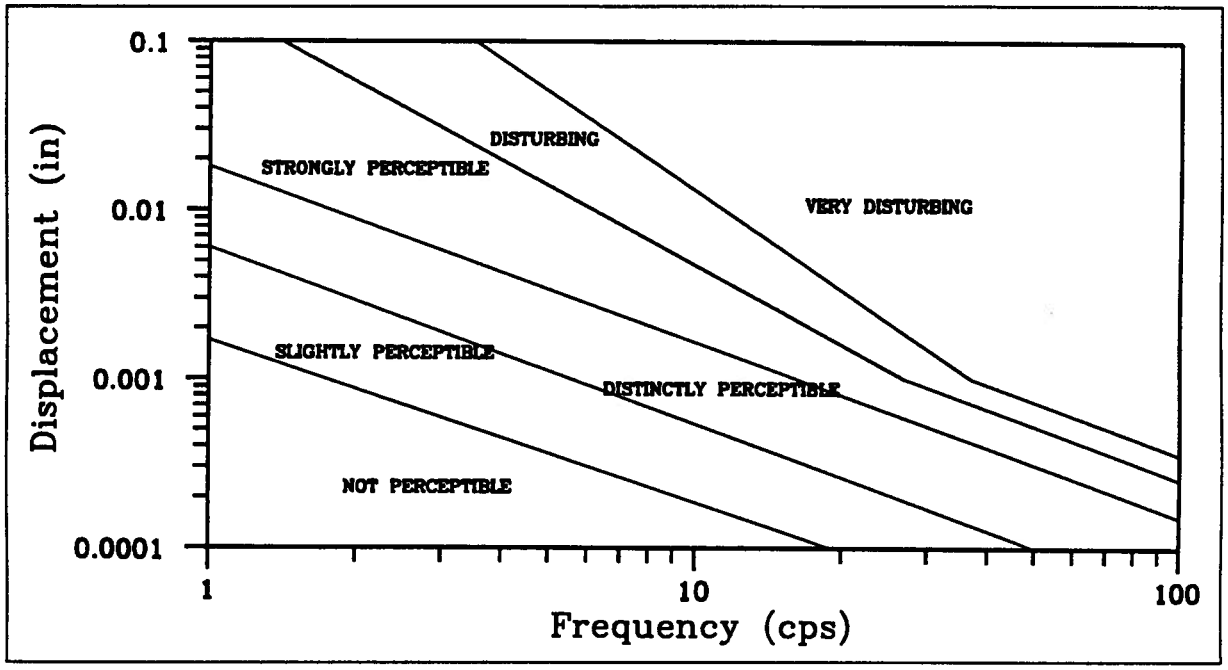

Figure 1.3: Human response to steady-state vibration, vibration vertical (Wiss and Parmelee, 1974)

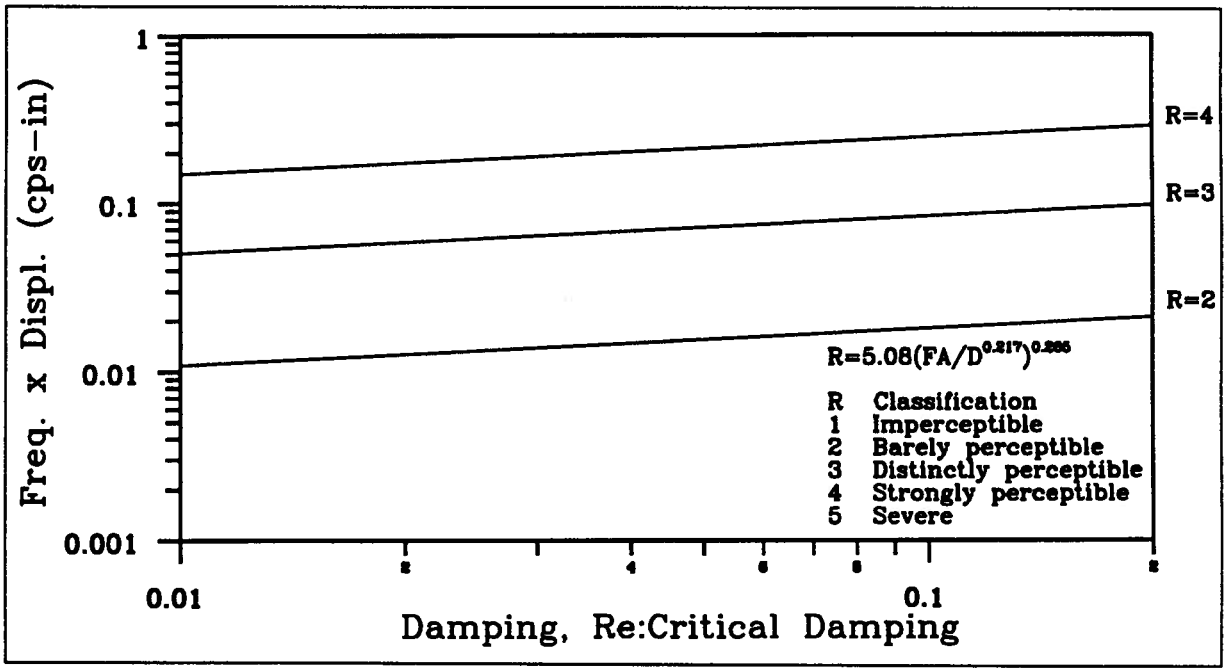

Figure 1.4: Curves of mathematical model for evaluation of transient vertical vibrations (Wiss and Parmelee, 1974)

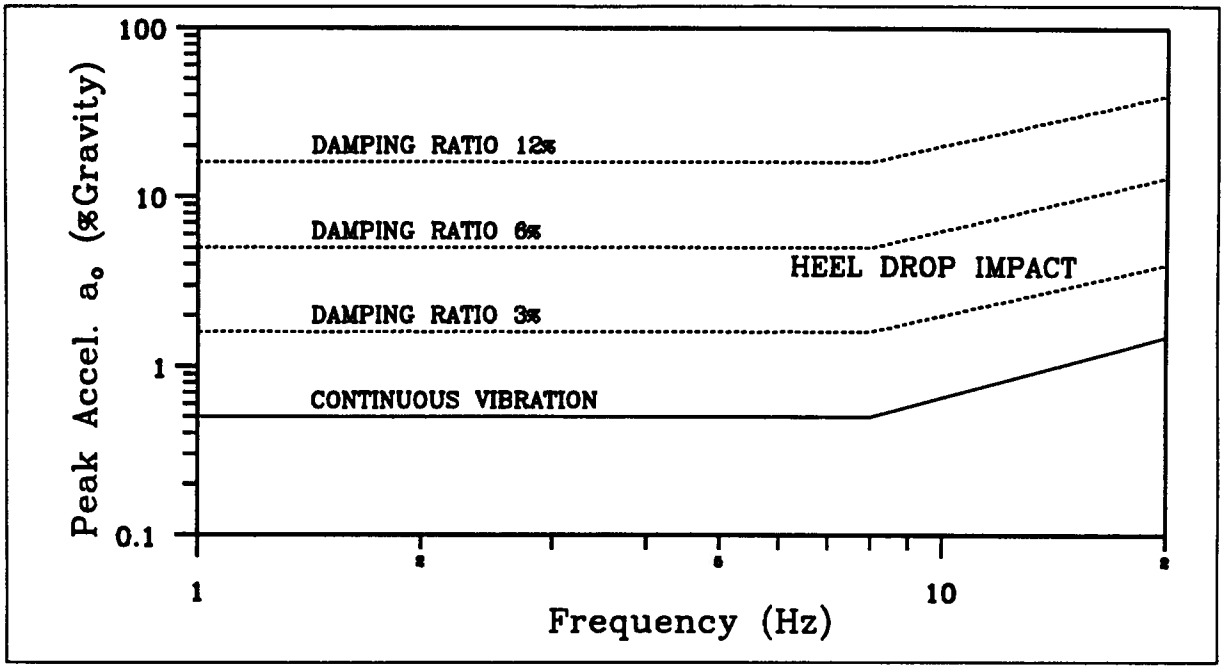

Figure 1.5: Annoyance criteria for floor vibration: residences, offices, and schoolrooms (Allen and Rainer, 1976)

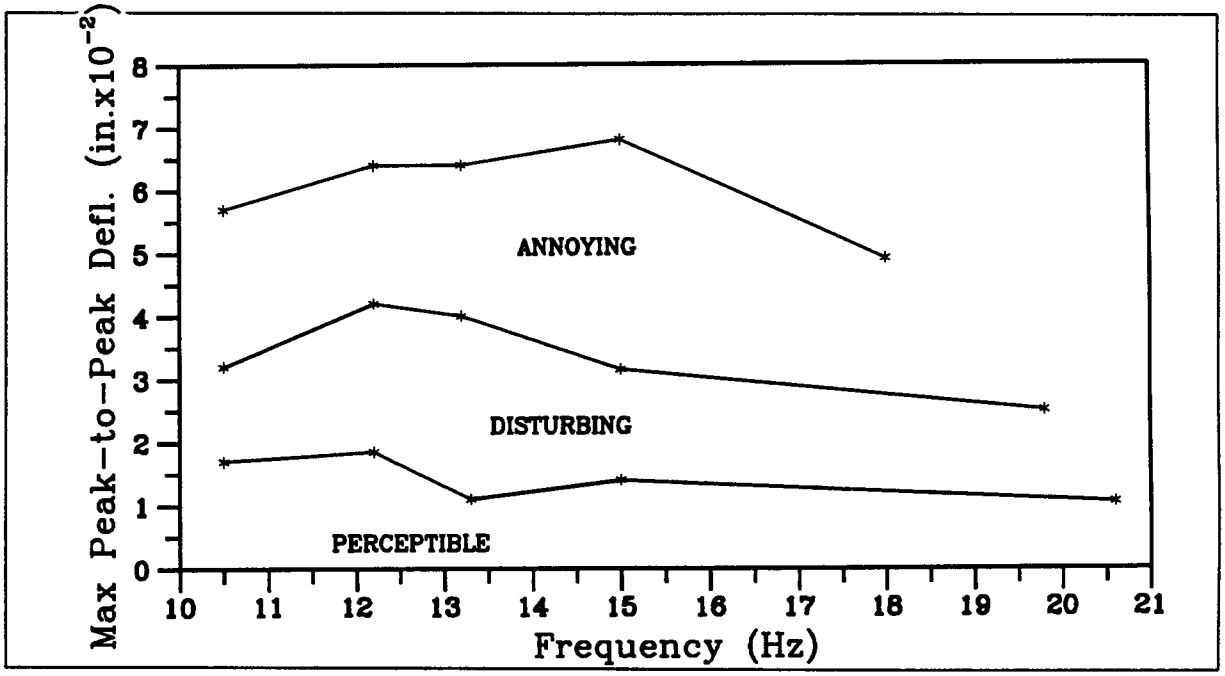

Figure 1.6: Human response to transient vertical vibration induced by dropping a 70*lb* steel weight onto the floor centroid (Polensek,1970)

1.2 Objective and Scope

As previously mentioned, much work has been done to address the floor vibration problem from a subjective testing point of view. From these studies several vibration acceptance criteria have been produced. In an effort to analytically model a floor's dynamic response, two computer programs, (NAFFAP and DYFAP), have been developed at the University of British Columbia [Filiatrault and Folz, 1989] [Filiatrault et al, 1990] [Folz and Foschi, 1991]. The main objective of the investigation reported in this thesis was to study experimentally the applicability of the programs NAFFAP and DYFAP for the case of lightweight wooden floor vibration.

Two wooden floors were constructed as per the NBC1990 guidelines. One used traditional sawn lumber joists while the other used composite wood I–Joists. The I–joist is becoming particularly popular due to its ability to span greater distances with less material than available sawn lumber products.

Currently, the data from in–situ testing of floors takes the form of acceleration time histories. The acceleration time history can be processed and integrated to produce velocity and displacement time histories and frequency spectra. Three types of impact testing were performed on each of the floors: tapping the floors with a common hammer, releasing a sand bag from a predetermined height and a human heel drop.

The three forms of floor excitation were modelled by DYFAP. The hammer impulse was estimated and entered as a discretized forcing function. The bagdrop impulse was recorded and therefore was available for discretization. The human heel drop, however, posed the most difficult problem for DYFAP. Previous research by Folz and Foschi showed that for the case where the occupants' mass is a significant percentage of the floor system's mass, an assumed forcing function was inadequate. An oscillator model of the human was placed upon the floor and was given an initial velocity to simulate the heel drop

action.

The natural frequencies of the floors were determined experimentally. NAFFAP's predicted frequencies and DYFAP's time histories were then compared with the experimental data. In the time domain, such features as peak acceleration, damping and peak displacement were used to evaluate the performance of DYFAP.

Chapter 2

Material Properties

The primary components of the floor systems, the joists and sheathing, were tested before the floors were constructed. The geometrical and mechanical properties that are required by NAFFAP and DYFAP were evaluated. Each joist was tested in flexure, weighed and its physical dimensions measured. Sixteen small plywood samples, assumed to be representative of the plywood stock used for the two floors, were similarly tested.

2.1 Joists

One floor was built with ten SPF No.2 2x8 joists spaced at $400mm$ while the other used nine TTS (Jager Industries) MSR2100 wood I–Joists spaced at $600mm$. The programs required five geometrical properties and two moduli for each joist.

The joists were tested in flexure under 4–point loading. They were cut to length prior to testing so that the test and floor span would be the same. Therefore the ten 2x8 joists spanned $3100mm$ and the nine Jager I–Joists spanned $4200mm$. The loading span was set at $600mm$ for both types of joists. The Jager and 2x8 joists were loaded to $400lbs$ ($1780N$) and $240lbs$ (1070N) respectively. The deflections at these loads were recorded. The bending stiffness was then derived from the standard beam formula of Eq. 2.1.

$$(EI)_y = \frac{Pa(3L^2 - 4a^2)}{24\Delta} \tag{2.1}$$

The elastic modulus for each of the 2x8 joists was calculated directly from Eq. 2.1. The inertia and the torsional constant were calculated from the physical dimensions of

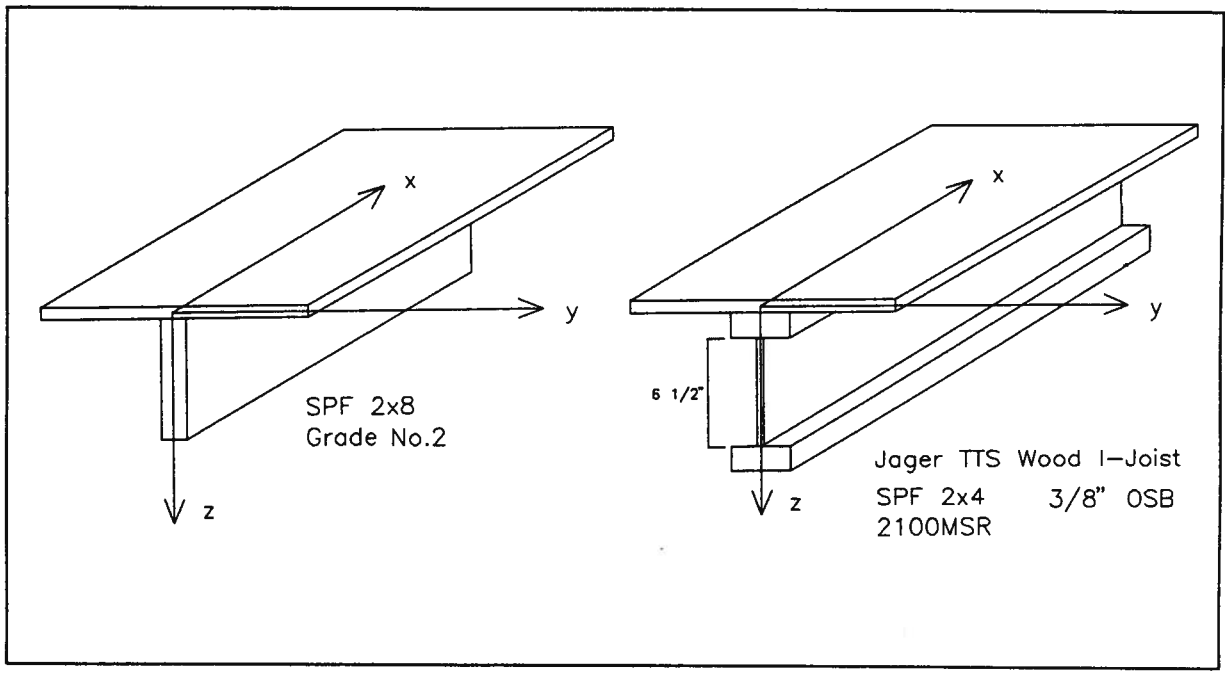

Figure 2.1: Joist cross–sections with coordinate systems

the joists' cross–section. The shear modulus was derived from the elastic modulus. It was assumed that the ratio of elastic to shear modulus was 17. Shown in Table 2.1 are the 2x8 joists' elastic moduli that were used in the programs' data files.

The elastic moduli for the I–Joists were not immediately available from Eq. 2.1. The I–Joists are composite structures. Their bending stiffness can be expressed as

$$(EI)_y = 2E_F I_F y + E_w I_w y \tag{2.2}$$

There are two unknowns in Eq. 2.2. The elastic moduli for the web (E_w), and flanges (E_F), are unknown. The modulus for the web material was assumed. A value of 9653 Mpa ($1.4x10^6$ psi) was taken for the 3/8" OSB web. A poor assumption ought not to have a large effect since the flange inertia ($I_F y$) is substantially larger than the web inertia ($I_w y$). Since $(EI)_y$ was measured, (E_F) was calculated from Eq. 2.2. Equation 2.3 was then used to derive a composite elastic modulus for the z–direction. The programs

Table 2.1: Joist E–moduli obtained from 4–point bending tests

E–Modulus (MPa)		
Joist #	*2x8*	*I–Joist*
1	14982	18016
2	19271	15734
3	15527	15810
4	16685	13886
5	17582	16189
6	14879	16892
7	14162	17271
8	16789	17002
9	15934	14941
10	9425	–

required that the elastic moduli for the y–direction and z–direction be equal. Therefore, from Eq. 2.3, the elastic moduli for the I–Joist became simply E_F.

$$(EI)_z = 2E_F I_F z \tag{2.3}$$

Contribution from the web to Eq. 2.3 was neglected because the flange inertia was very much larger than the web's. Also shown in Table 2.1 are the I–Joists' elastic moduli that were used in the programs' data files. The composite moment of inertia that the programs require was then calculated from Eq. 2.4, using $E = E_F$.

$$I_y^* = (EI)_y / E \tag{2.4}$$

The contribution from the web to the composite torsional constant was neglected since the flange's constants were so much larger. The shear modulus was found by making the same assumption as for the 2x8 joists. The ratio of the composite shear and elastic moduli was assumed to be 17.

Once the joist stiffnesses were determined, the mass density (mass/volume) of the

Table 2.2: Joist mass density at time of floor construction

Mass Density $(mN\ s^2/mm^4, 10^-7)$		
Joist #	*2x8*	*I–Joist*
1	4.27	5.42
2	5.31	5.76
3	4.28	5.39
4	4.62	5.31
5	5.01	5.10
6	5.03	5.73
7	4.50	5.23
8	4.71	5.36
9	5.36	5.46
10	3.83	–

joists were derived. An estimate of their volume via dimensions and their mass was required. Moisture content readings for the 2x8 joists ranged from 12% to 19%. The 2x8 joist floor was then constructed immediately but the mass of the Jager joists dropped $2-3\%$ from the time of flexure testing to floor construction. At the time of construction, the 2x8 and Jager joist floors weighed approximately $490lbs$ ($2180N$) and $820lbs$ ($3650N$) respectively.

Listed below are the joist parameters required by the programs.

RIY ....Moment of inertia of joist around Y-axis.

RIZ ....Moment of inertia of joist around Z-axis.

RIT ....Torsional inertia of joist.

AJ ....Cross-sectional area of joist.

HCJ ....Distance from centroidal axis of joist to bottom of cover.

EJ ....Modulus of elasticity of joist.

GJ ....Shear modulus of joist.

RHOJ ....Mass density of joist.

2.2 Plywood

The programs require a number of parameters to describe the plate action of the plywood sheathing. Eight specimens in each orientation, span parallel and perpendicular to the surface grain, were tested under 3-point bending. Each specimen had nominal dimensions of $275x1188mm$. Only the mass density and bending stiffnesses parallel and perpendicular to the surface grain were determined experimentally. The mass density of the plywood was determined in the same manner as for the joists. All other parameters were derived from the composite plate property equations 2.5–2.12.

$$RKX = \sum_{i=1}^{4} \frac{E_{22}^i I_{11}^i}{(1-\nu_{12}\nu_{21})} + \sum_{i=1}^{2} \frac{E_{11}^i I_{22}^i}{(1-\nu_{12}\nu_{21})} \tag{2.5}$$

$$RKY = \sum_{i=1}^{4} \frac{E_{11}^i I_{11}^i}{(1-\nu_{12}\nu_{21})} + \sum_{i=1}^{2} \frac{E_{22}^i I_{22}^i}{(1-\nu_{12}\nu_{21})} \tag{2.6}$$

$$RKV = \sum_{i=1}^{4} \frac{E_{11}^i I_{11}^i \ \nu_{12}}{(1-\nu_{12}\nu_{21})} + \sum_{i=1}^{2} \frac{E_{22}^i I_{22}^i \nu_{21}}{(1-\nu_{12}\nu_{21})} \tag{2.7}$$

$$RKG = \sum_{i=1}^{4} G^i I_{11}^i + \sum_{i=1}^{2} G^i I_{22}^i \tag{2.8}$$

$$DY = \sum_{i=1}^{4} \frac{E_{11}^i t_{11}^i}{(1-\nu_{12}\nu_{21})} + \sum_{i=1}^{2} \frac{E_{22}^i t_{22}^i}{(1-\nu_{12}\nu_{21})} \tag{2.9}$$

$$DX = \sum_{i=1}^{4} \frac{E_{22}^i t_{11}^i}{(1 - \nu_{12}\nu_{21})} + \sum_{i=1}^{2} \frac{E_{11}^i t_{22}^i}{(1 - \nu_{12}\nu_{21})} \tag{2.10}$$

$$DG = Gd \tag{2.11}$$

$$DV = \sum_{i=1}^{4} \frac{E_{11}^i \nu_{12} t_{11}^i}{(1 - \nu_{12}\nu_{21})} + \sum_{i=1}^{2} \frac{E_{22}^i \nu_{21} t_{22}^i}{(1 - \nu_{12}\nu_{21})} \tag{2.12}$$

where:

RKX ....Bending stiffness of the cover in the direction parallel to the joists. For plywood, this is usually perpendicular to the face grain.

RKY ....Bending stiffness of the cover in the direction perpendicular to the joists. For plywood, this is usually parallel to the face grain.

RKV,RKG ....Parameters for plate bending related to Poisson's effect and torsion respectively.

DX ....Axial (in-plane) stiffness of the cover in the direction parallel to the joists.

DY ....Axial (in-plane) stiffness of the cover in the direction perpendicular to the joists.

DV,DG ....Axial (in-plane) stiffness of the cover related to Poisson's effect and in-plane shear respectively.

In addition, the programs require the following parameters:

TCOV ....Thickness of the cover.

RHOC ....Mass density of the cover.

Table 2.3: Assumptions required by the composite plate property equations

Poisson's ratios	0.02,0.4
E/G	17
E_{par}/E_{perp}	20

Table 2.4: Moduli values obtained from the composite plate property equations

	(MPa)
E_{par} *(exterior)*	13442
E_{perp} *(exterior)*	672
E_{par} *(interior)*	10709
E_{perp} *(interior)*	535
G (exterior)	791
G (interior)	630

A number of assumptions were required in order to apply Eqs. 2.5– 2.12. Listed in Table 2.3 are the values used for Poisson's ratios, elastic to shear modulus ratio and the E–moduli ratio parallel and perpendicular to the grain of a ply. It was also assumed that the interior and exterior plys may be of different species. Using Eq. 2.5 and Eq. 2.6, and the above assumptions the E–moduli parallel to a ply's grain were derived. Table 2.4 provides a summary of the various moduli values derived for the plywood.

2.3 Sheathing–joist Connections

Glue and nails were used for the sheathing to joist connection. The glue, an elastomeric wood adhesive, caused the connection to exhibit a high strength as well as a high stiffness. Shear tests were conducted using $200mm$ long sections of the floors' connections. The dimensions of the available testing apparatus restricted the choice for specimen length

Table 2.5: 2x8 joist floor connection's test results

2x8 Joist			
glue		*1 nail + glue*	
stiffness (N/mm)	*peak load (N)*	*stiffness (N/mm)*	*peak load (N)*
3974	7500	5000	7000
5063	5500	5047	7000
7317	9300	7867	9000
4070	4000	8824	9500
–	–	6410	6000

to $200mm$. An MTS 810 testing machine was used for these tests. A frontal and side view of a specimen clamped in the testing apparatus are shown in Fig. 2.2 and Fig. 2.3 respectively. The lower table was raised thus causing the joist to shear away from the plywood.

Specimens with and without a nail were tested. The tests were displacement controlled. The displacement rate was set at $0.1mm/sec$. Listed in Table 2.5 and Table 2.6 are the connection test results. Over the recorded strain range, the stiffness and peak loads obtained from the tests showed no evidence of whether a nail was present or not. The stiffness distributions for the two types of tests are significantly nested. The stiffness and peak loads from the tests were $3-4$ times higher than that usually expected from typical nailed connections. The connection stiffness was quite variable. An average stiffness of $5706N/mm$ was calculated from all of the tests with the high and low values removed. They likely depended upon the glue thickness and contact area. The three specimens shown in Fig. 2.4 illustrate how the glue connection varied in thickness and bond width. At failure, only the residual strength of the nail remained, the glue–wood bond had been entirely destroyed.

The mechanical properties of the glued connections during low amplitude vibrations

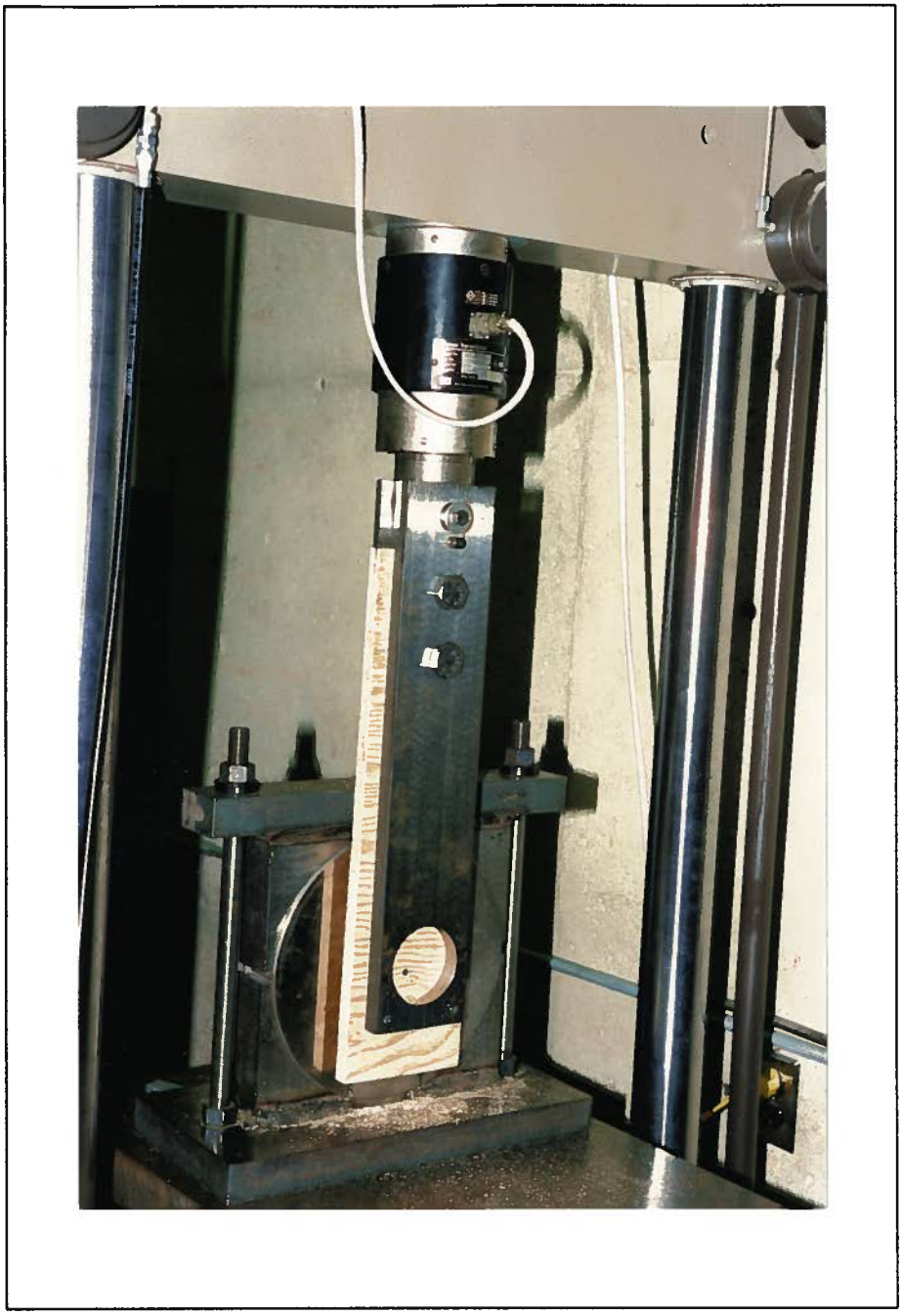

Figure 2.2: Test setup for testing the joist/plywood connection in shear; front view

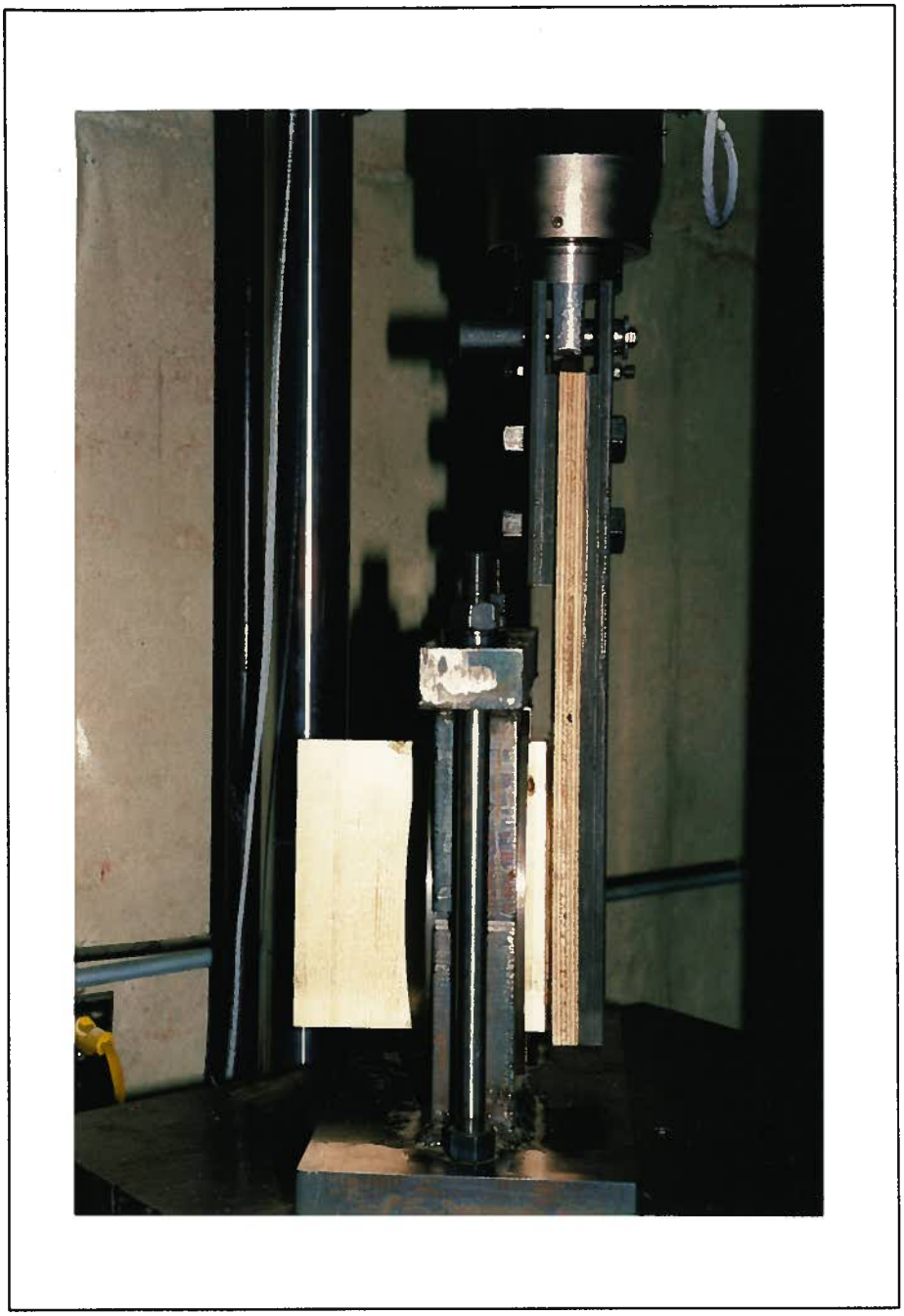

Figure 2.3: Test setup for testing the joist/plywood connection in shear; side view

Figure 2.4: Cut away samples of typical joist to plywood glue connection

Table 2.6: I–Joist floor connection's test results

I–Joist			
glue		*1 nail + glue*	
stiffness (N/mm)	*peak load (N)*	*stiffness (N/mm)*	*peak load (N)*
12380	15000	3846	9000
3015	5000	5908	8000
8714	14000	1390	4000
6430	11500	2140	7500
4100	5500	9280	9500

may differ from that of a nailed connection. The connector strains incurred during low amplitude vibrations are low enough that it is believed that only the nail is contributing significantly to the connection stiffness. Y. H. Chui noted in his tests with glued floors that the fundamental frequency was virtually unchanged by the addition of glue to a nailed connection [Chui and Smith, 1991]. If the high stiffness of a glued connection is utilized then the frequency distribution ought to reflect it.

The characteristics of the stress–strain relationship of the 3M adhesive may explain why the apparent high stiffness of the glued connection is not activated during low amplitude vibrations. The 3M adhesive is an elastomeric adhesive. Its properties are listed in Table 2.7. Its structure is analogous to rubber, a polymeric material. A polymer is a large molecule built up by the repetition of small simple chemical units. These polymers can be linked as a linear, branched or network system. By definition, the 3M adhesive exhibits a rubber–like elasticity. Small scale motion is allowed by local movement of chain segments but any large scale motion is restricted by the previously mentioned polymer linking or network systems [Billmeyer, 1984].

For a material of polymeric structure, the elastic modulus is simply a measure of the resistance to the uncoiling of randomly oriented chains. The application of a stress

Table 2.7: Material properties for 3M wood adhesive

Base:	Synthetic elastomer
Solvent:	None
Colour:	Rose–tan
Net weight:	15.0, 0.3 N/L
Flash point:	None
Solids content:	100% by weight (approximately)
Consistency:	Gun grade, Thixotropic paste
Caulk rate:	45 g/min (using 3 mm orifice, 350 kpa at 20C)
Shear modulus:	770 kpa (20C under stress level 0–32 kpa)

eventually tends to untangle the chains and align them in the direction of the stress [Cowie, 1973]. The load-slip curves from the connection tests are quite linear. It has been reported that for some polymer materials, up to 10% strain can be quite nonlinear [Pechhold, 1973]. Shown in Fig. 2.5 is a stress–strain curve of a drawn polyamide fiber that exhibits an initial low modulus region. If the 3M adhesive has a similar stress–strain relationship then one could consider the vibration strain domain to be dominated by the nail's modulus.

Listed below are the connection parameters required by the programs.

ENL ....Connector spacing along the joists.

RKPAL,RKPER ....Connector load-slip stiffness (modulus) in the parallel and perpendicular directions to the joists respectively.

RKROT ....Connector rotational stiffness between the cover and the joists.

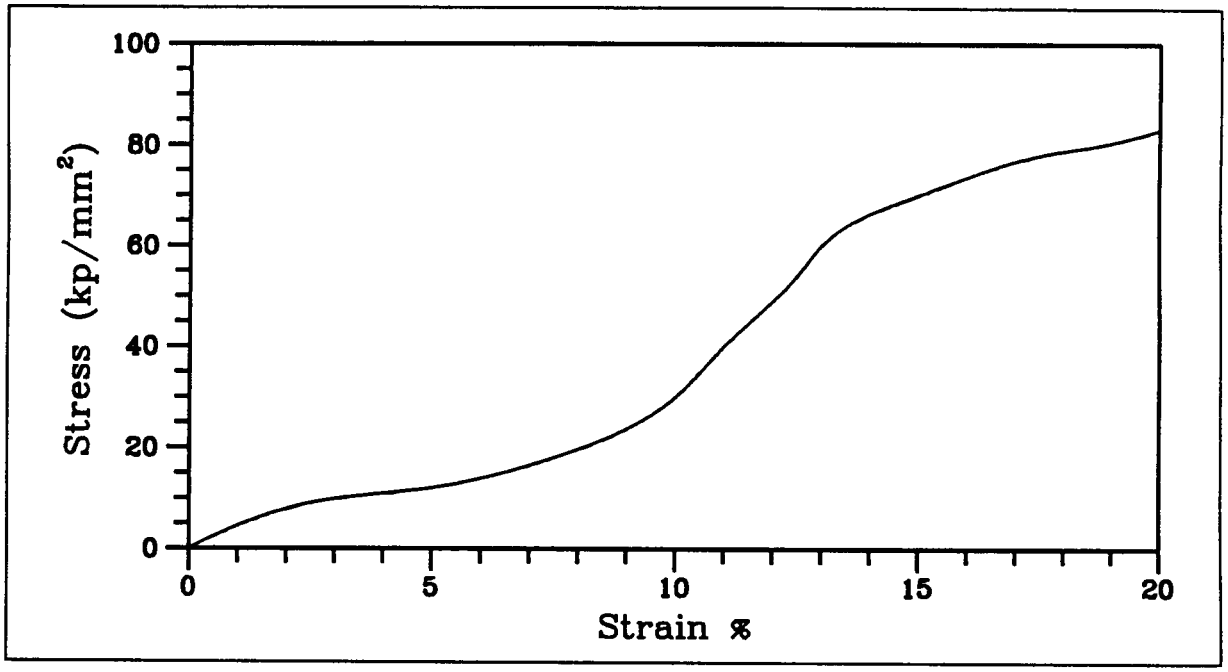

Figure 2.5: Load deflection curve for a drawn polyamide fibre (Pechhold, 1973)

Chapter 3

Experimental Setup

In order to plan the testing setup, a preliminary study of the influence of some key floor parameters was undertaken. There were a number of geometric and material parameters to be considered during the design of the lightweight wooden floors. Each of the parameters have some effect upon the floor's dynamic response. Two important response characteristics are the natural frequencies and their degree of separation.

Vibration modes which are poorly spaced can interact to produce higher amplitude vibrations. This is particularly important for lightweight residential floors, which are strongly orthotropic structures, because their lowest frequencies are generally closely spaced.

3.1 Floor Parameter Study

Supporting the rim joists

Often the perimeter joists are supported in some manner. The inclusion of rim joist support systems in the design is not difficult or expensive. A floor with its rim joists supported is less orthotropic, thus its dynamic response is improved. Tests performed by Chui indicated a high damping value in the first mode when the rim joists were supported. The high damping in the first mode would indicate that its contribution to the floor's response has been significantly reduced [Chui and Smith, 1991].

Generally, the introduction of rim joist support causes an increase in all modal separations. The results from NAFFAP simulations indicate that separation between the

first and second and between the fourth and fifth frequencies are somewhat less affected by the addition of rim joist support [Filiatrault et al, 1990].

Joist end fixity

End fixity can range from simple supports to fully fixed. Joist hangers and built in construction are common examples. However, in practice, most construction can be considered as simply supported. Chui tested a floor by doubling the clamping force on the joist ends. The results showed negligible change. It was concluded that for usual clamping loads acting on the joist ends,the natural frequencies were insensitive to changes in end fixity [Chui, 2/86].

Aspect ratio

The aspect ratio is defined by the floor's width divided by its length (joist span). The sheathing sheets are always laid with their longer length, the dimension parallel to surface grain, spanning the joists. Studies of the effects of aspect ratio upon a floor's response showed that if the aspect ratio is greater than or equal to 1 for a floor simply supported on all four sides the floor's frequency distribution was improved.

The aspect ratio, of course, can be changed by either changing the floor's span or width. These two methods do not affect the frequencies in the same manner. NAFFAP studies showed that any increase in the number of joists past nine had no effect on the fundamental frequency and generally does not affect the modal separation. Increasing the span caused a dramatic decrease in the fundamental frequency and an increase in modal separation. Modal separation improvement was especially evident for the lower frequencies [Filiatrault et al, 1990].

Joist spacing

Reducing the joist spacing has the effect of increasing the floor's bending stiffness per unit width. The floor's stiffness perpendicular to joist span is dependent upon sheathing stiffness, joist spacing and the type of between joist bridging. The ratio of bending

stiffnesses for the floor's width and length increases with modal separation. Generally, for a decrease in joist spacing the fundamental frequency increases and the modal separation decreases.

Nail spacing

A nailed joist to sheathing connection can be considered as semi-rigid. Most construction practices fall well within the code's specifications. The NBCC suggests a maximum spacing of $300mm$ at interior supports and $150mm$ at the sheathing's end supports. Altering the nailing density does not affect the distribution of frequencies. NAFFAP runs have shown that an increase in nail spacing of $3 - 4$ times is required before the frequency distribution is significantly changed [Filiatrault et al, 1990]. This was supported by Chui's test where doubling of the nail density had virtually no effect upon the fundamental frequency [Chui, 2/86]. He did find that damping had increased slightly as a result of the stiffened connection.

Nail stiffness

The load–slip moduli of the joist to sheathing connection has a large effect upon the stiffness and the dynamic response of the floor system. An increase in the nail horizontal slip stiffness will increase the fundamental frequency but the modal separation is relatively unaffected. An increase in connector stiffness reduces the system's ability to dissipate energy through friction. The introduction of an elastomeric adhesive improves the durability of the connection. It is believed that the adhesive has a negligible effect upon the floor's dynamic response but that it significantly reduces the "squeakiness" of the floor [Chui and Smith, 1991].

3.2 Floor Design

Currently common residential floor construction involves either sawn lumber joists or composite wood I–Joists. One floor of each type was designed and tested. SPF No.2 2x8s and TTS Jager Industries wood I–Joists were used.

Parameters that were chosen to be common between the two floors include the sheathing to joist connection nail spacing, sheathing thickness and aspect ratio. The joist span and spacing were chosen so that the floors were designed to approximately the same percentage of the NBCC1990 span table limits. The nail spacing for the sheathing to joist connection was chosen to be $300mm$. The floors' sheathing was $18.5mm$ D–fir plywood. The aspect ratios were 1.13 and 1.12 for the 2x8 joist floor and the I–Joist floor respectively.

The NBCC1990 has incorporated new vibration criteria for determining allowable joist spans. The new criteria are supposed to improve the serviceability of wooden floors by moving the floor's fundamental frequency away from the human sensitive frequency range of $4 - 20$Hz. The NBCC1990 suggests a span limit of $3.36m$ for 2x8 joists spaced at $400mm$. To satisfy a reasonable aspect ratio, ten joists at a span of $3100mm$ were chosen.

Relying upon the manufacturers span tables for the I–Joist, nine Jager joists at a spacing of $600mm$ and spanning $4200mm$ were chosen. The larger joist spacing was used to reduce the stiffness of the floor. It was anticipated that this would cause an increase in between joist "bounciness", but the majority of the tests were performed over joist lines.

3.3 The Floor's Support System

The system that supports the floors had two functions. Firstly, it was to simulate typical boundary conditions found in common residential construction. Secondly, the frame was not to participate with the wooden floor's response in addition to isolating the floor system from the lab floor. The conceptual design for the support system followed the work of Chui, as it appeared to be successful in obtaining clean dynamic responses from lightweight wooden floors. This permitted the identification of a significant number of the floors' natural frequencies [Chui and Smith, 1991].

Platform framing is the most common form of floor joist construction used over a foundation wall. The box–sill method is common in platform framing [CMHC, 1984]. As shown in Fig. 3.1, the 2x8 header and both the 2x4 plate and sill were included in the floor system. The 2x4 sill was bolted to the W–shape. The floors were then built upon these sills as per the NBCC1990 and CMHC recommendations. Threaded steel rods were used as a clamping system to apply some pressure to the top of the floor. Fig. 4.3 and Fig. 4.4 illustrate how the clamping system was applied. This loading could represent partial roof or wall loading. The 2x8 joist floor had each of its joist ends clamped but the I–Joist floor had only eight of its joist ends clamped. Since the bottom flanges of the I–Joists were nailed directly to the 2x4 sills, it was believed that it would be unlikely that the floor would lift from the steel frame. It is believed that the clamping system did not significantly restrain rotation of the joist ends.

The floor was supported on all four sides by the steel W–shapes as shown in Fig. 3.2. The perimeter joists were restrained from vertical and lateral movement by toe-nailing the joists to the 2x4 sill that was bolted to the steel frame. Particularly for the 2x8 joists, this nailing may have restrained joist rotation significantly. The web of the I–Joist was flexible enough to allow significant rotation at its top flange.

Figure 3.1: Connection details at joist ends for the I–Joist joist floor

Figure 3.2: A view of the floor framing and the steel support system

Generally, house construction allows the transmission of vibrations from one structural system to another. As a simplification, the test floors were isolated. The 2x4 sills acted as dampers between the floor and the stiff steel W–shapes. These were laid upon the lab's concrete floor. Shims were used to ensure a stable and level foundation for the floor. Floor anchors were used to eliminate any movement of the steel frame relative to the lab floor. Shown in Fig. 3.3 is the anchoring system consisting of HSS square sections and channels. Vertical threaded rods embedded in the floor were the root of the system. The channels received the vertical anchor loads from the HSS square sections and then transmitted them laterally to the lab floor and the lower flange of the W–shapes.

3.4 Data Acquisition

The raw data from the floor vibration tests were recorded as acceleration records. Two $2g$ IC Sensors accelerometers were used to capture the response of the wooden floors to the various excitations. The accelerometers were firmly screwed to the plywood sheathing.

Care was taken to ensure that all cables were suspended above the floor's surface. Vibrations of the laboratory floor could be detected by the accelerometers since the testing apparatus was not isolated from the general lab floor. Analysis of the noise traces identified frequencies that may become amplified and be mistakenly identified as floor frequencies. The real component of the complex valued spectral "Energy" density of a noise trace for the two accelerometers is shown in Fig. 3.4. Multiples of 60Hz appear to be the only frequencies of concern.

A $100lb$ Lebow load cell, securely screwed to the floor's surface, recorded the impulse imparted to the floor by the bag drop test. Full scale output for the $100lb$ load cell was 7.559 volts. Calibration of the load cell was set at $6.0075kg/V$ or $58933.575mN/V$. The mass of the load cell assembly was $1.08kg$.

Figure 3.3: Anchoring system for the W–shape frame

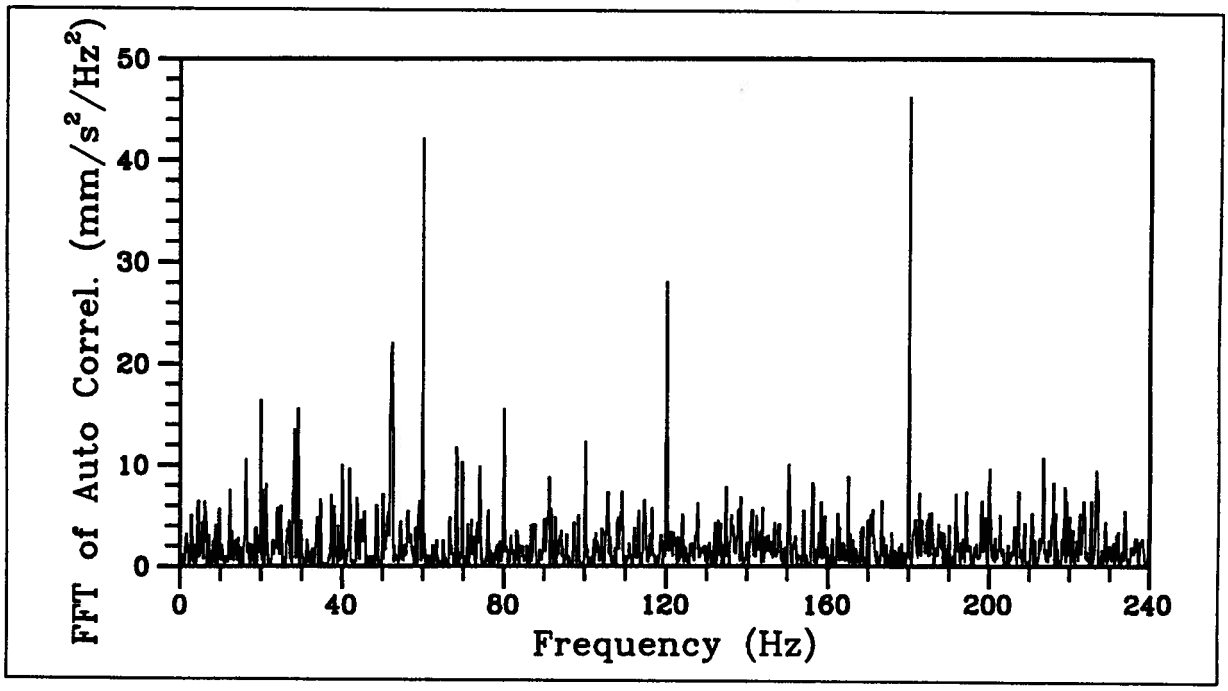

Figure 3.4: Real spectral "Energy" density of a noise trace

The Labtech Notebook version 6.0 software package was used to manage the recording of the data. The data acquisition system was limited to a sampling rate of approximately 370Hz for four channels. Generally, the hammer and heel drop tests were recorded at 0.002 seconds per sample while the bag drop tests were limited to 0.0027 seconds per sample.

Chapter 4

Testing

The series of tests that were performed on the two floors involved simple hammer impacts, sandbag and heel drop impacts with or without a passive occupant. The four series of tests were performed upon each of the floors. Each test was recorded by two accelerometers located at the positions indicated in Fig. 4.1 and Fig. 4.2. Each of the test series followed the common testing grid of ten impact sites shown in Fig. 4.1 and Fig. 4.2.

4.1 Hammer Impact Tests

The hammer impact is a convenient, efficient and fast method of vibration testing that produces a clean response with a very clear frequency spectrum. For this reason the hammer test responses were used to identify the floor's natural frequencies. The hammer test data were used for NAFFAP's verification.

A common hammer was used to tap the floor surface. To avoid saturating the accelerometers, given that high accelerations are associated with very sharp impacts, a $12mm$ thick piece of porous rubber was placed on the floor at the impact site. This was sufficient to keep the maximum accelerations close to $2g$. Fig. 4.3 shows the 2x8 joist floor and the equipment in place for a hammer impact test at site number 2.

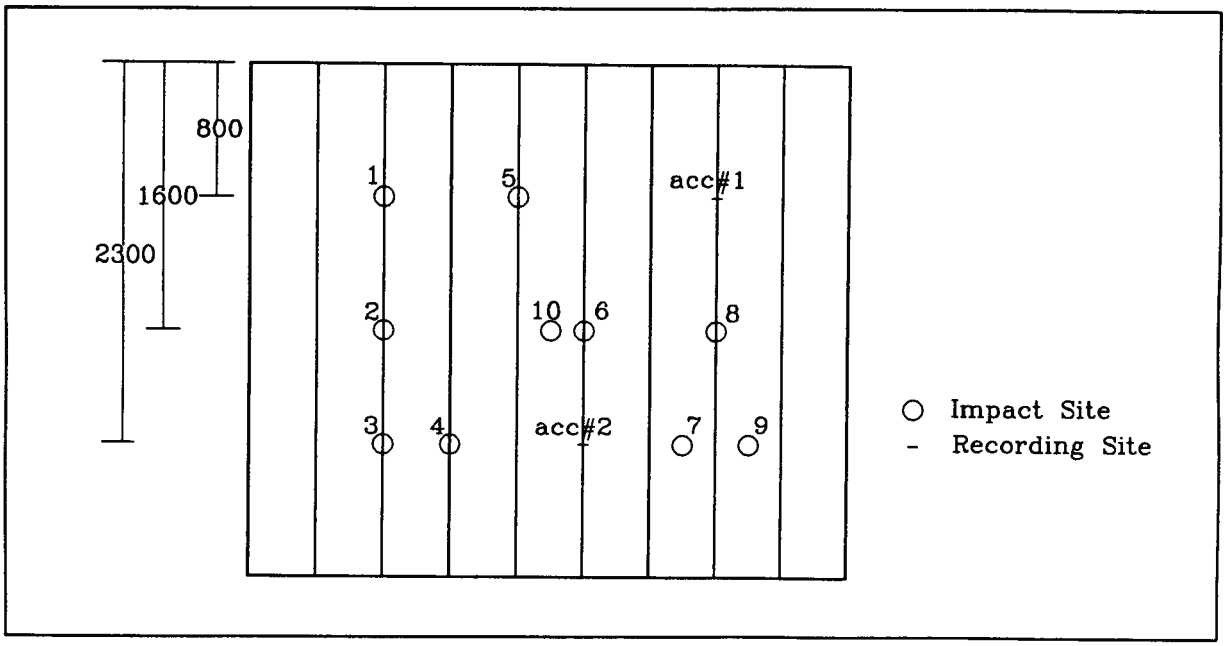

Figure 4.1: Impact and recording locations used on the 2x8 joist floor

4.2 Sandbag Impact Tests

The sandbag impact was chosen for its repeatability and for DYFAP's verification. The load time history is similar to that of a heel drop but the $15lb$ ($66.7N$) sandbag imparted far less energy to the floor. Its duration falls within the range $25 - 30ms$. Fig. 4.4 and Fig. 4.5 illustrate the test setup for a typical bagdrop test. The bag was of circular cross-section. Its diameter matched that of the impact platform that was attached to the load cell. This ensured a balanced loading, reducing error due to a moment that could develop between the loading platform and the load cell. The drop height and bag mass were limited by the $100lb$ ($445N$) capacity of the load cell. A $15lb$ ($66.7N$) bag released from a height of $27mm$ produced peak loads of $105 - 115lbs$ ($467 - 512N$). The bag was released by sliding the looped string over a nail that was attached to the post of the spanning frame.

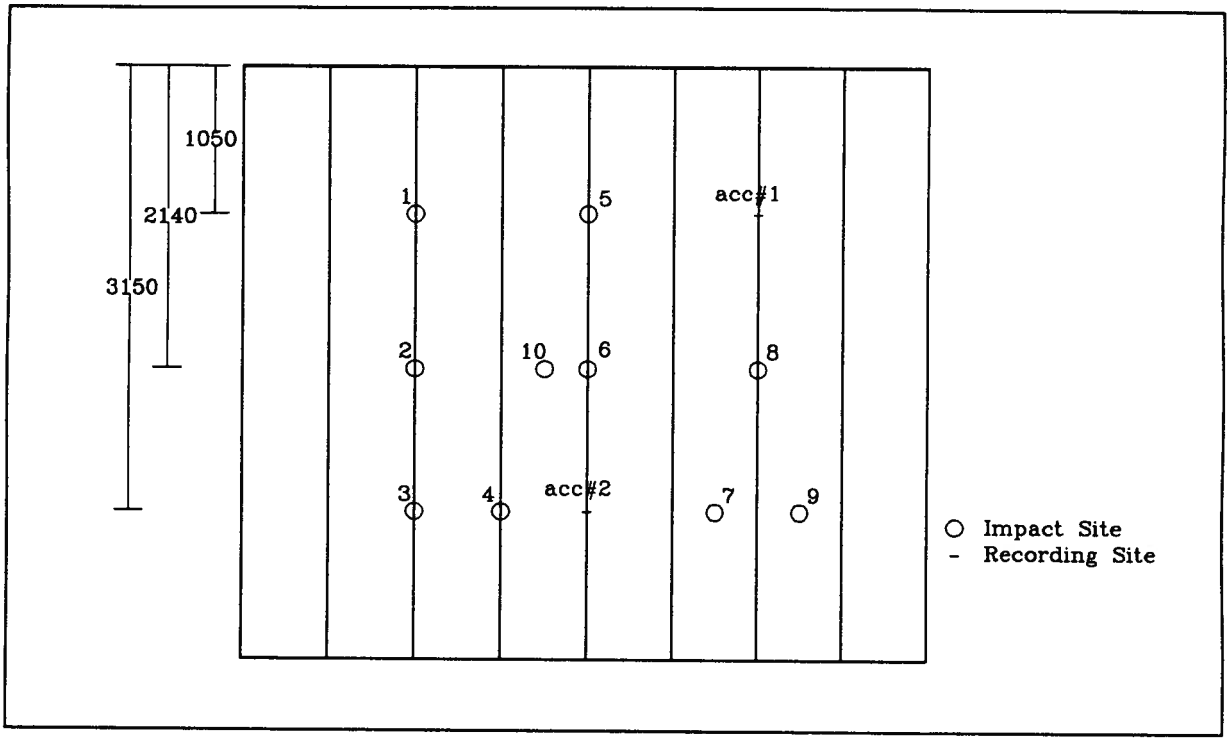

Figure 4.2: Impact and recording locations used on the I–Joist floor

Figure 4.3: The hammer impact test

Figure 4.4: The bagdrop impact test

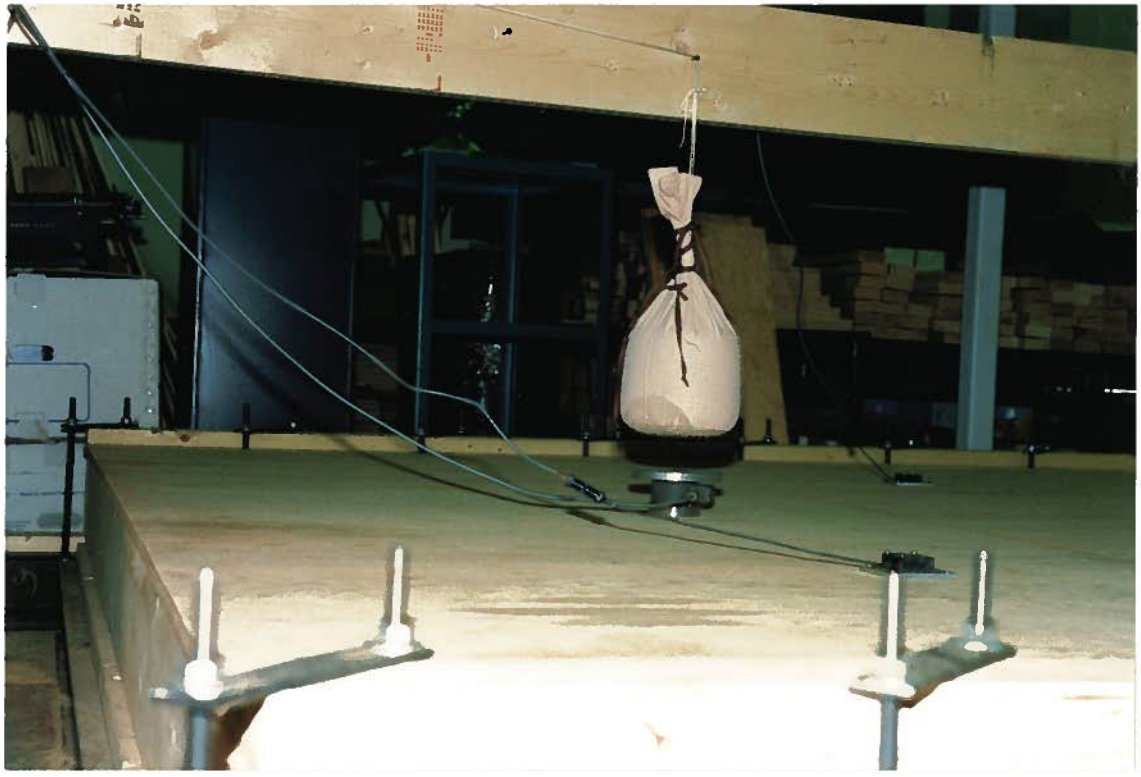

Figure 4.5: A closeup of the bag, load cell and accelerometers (Photograph shows a drop height approximately twice that of the $27mm$ test height)

4.3 Heel Drop Tests

Walking and running are two common sources of dynamic excitation. The human footstep induced vibration is the most common type of serviceability problem for lightweight wooden floors. Running differs from walking in that both feet will lose contact with the floor. The force–time history for running most resembles that of an impulse. Generally, with only marginal error, the vibration can be treated as transient if only one person is active on the floor. The type of occupancy will dictate what level of activity would be tolerable. For most domestic uses, the heel drop impact has been shown to be adequate as an upper limit for evaluating floor performance. The heel drop test performs well against the more expensive Random, Sweep and Discrete frequency methods [Rainer, 1980].

The heel drop test was performed by a $200lb$ ($890N$) man. Shown in Fig. 4.6 is a person in position to demonstrate a heel drop test. All tests were performed with shoes removed. The person rises up on his toes, raising his heels approximately $65 - 75mm$ before suddenly shifting his weight over to his heels. He hits the floor, impacting with his heels, while remaining as relaxed as possible. Each part of the human body vibrates at its own particular frequency. Movement of the shoulder girdle and arms can impart a significant amount of momentum to the floor. Although the load histories of the heel drops were not recorded, a plot of the average force versus time from Lenzen and Murray shown in Fig. 4.7 indicates that a $50ms$ duration could be expected [Allen and Rainer, 1976]. The peak load, depending upon floor stiffness, is generally $2 - 4$ times the heel dropper's weight [Allen and Rainer, 1976] [Chui, 2/86].

Series #4 involved a second person standing on the floor while a heel drop was performed. As shown in Fig. 4.6 the second person, the observer (passive occupant), stood $500mm$ behind the impact site on the same joist. Each test was then repeated with the observer now standing on the adjacent joist. The same two persons were used for these

Figure 4.6: The starting position of a typical heel drop test with an observer standing on the same joist as the tester

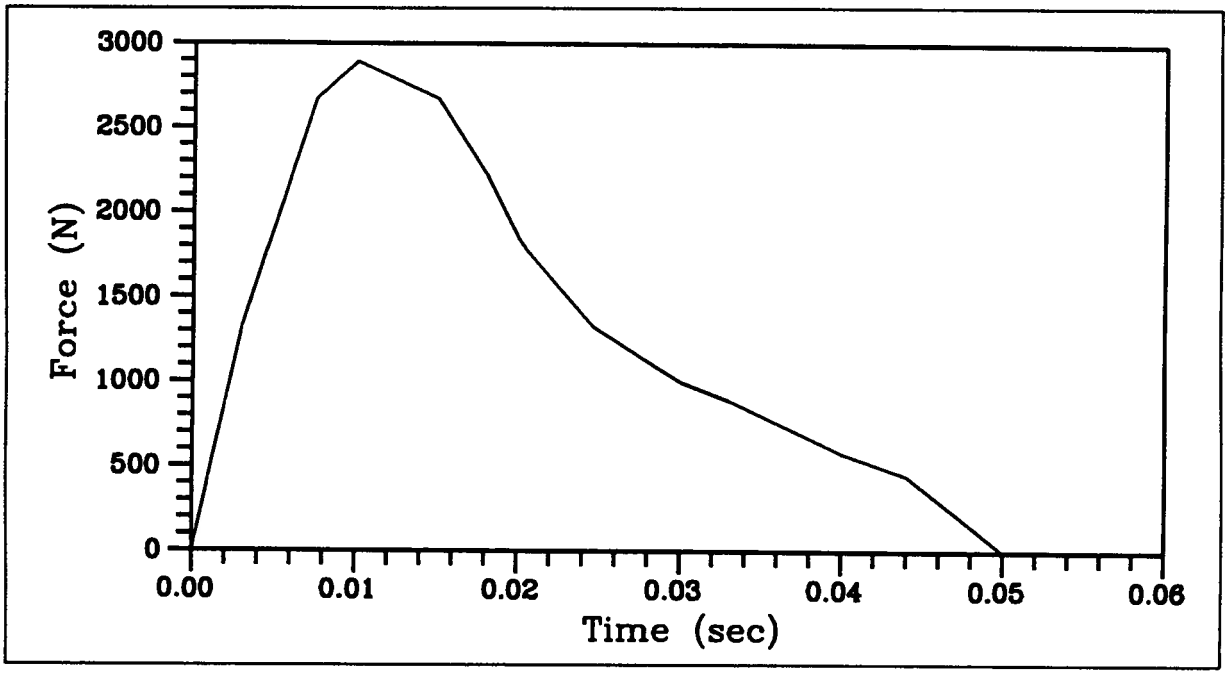

Figure 4.7: Averaged plot of force versus time for heel drop impact (Folz and Foschi, 1991)

tests, as observer and heel dropper. The observer was a $215lb$ ($957N$) man.

The data files for all of the tests are referenced by a coded label of the form FTI-R where F=type of floor (SL, 2x8 sawn lumber floor or IJ, TTS Jager I–Joist floor), T=type of impact (H, hammer, B, bag, F, heel drop, S, heel drop with observer located on same joist, N, heel drop with observer located on adjacent joist), I=location of impact (see Fig. 4.1 and Fig. 4.2) and R=which accelerometer, #1 or #2, recorded the signal (see Fig. 4.1 andFig. 4.2 for location). For example, IJH6-2 denotes the test on the I–Joist floor with the hammer impact at location #6 and the signal was recorded by accelerometer #2.

Chapter 5

Dynamic Response of Test Floors

5.1 Evaluation of Damping Ratios

Wooden floors exhibit a moderate level of damping. Each connection has some capacity to dissipate energy by friction or in the case of glued connections by elastic deformation. The material itself can deform elastically under the applied loadings.

The raw test data are acceleration records. An equivalent viscous damping ratio (ζ) can be derived directly from an acceleration time history. A common method is by logarithmic decrement, using Eq. 5.1. To gain greater accuracy the equation is expanded to consider two positive peaks separated by m positive peaks.

$$\frac{A_n}{A_{n+m}} = e^{2\pi m\zeta} \tag{5.1}$$

where:

A.....trace amplitude

n,m.....counters for the trace's positive peaks

ζ.....viscous damping ratio

Since the acceleration records include the full spectrum of frequencies, it is necessary to filter the records for the floor's natural frequencies. Applying band pass filters one can isolate particular frequencies thus creating time histories for specific frequencies. Shown in Fig. 5.1 is the decay curve for the I–Joist floor's second frequency. The vertical scale

has been changed to show only the positive peaks. Not shown is the rising portion where the particular frequency is growing in participation from the time of the impact. The participation of the lower frequencies do not peak until much of the floor motion has been completed. The damping of the higher frequencies has a much larger influence upon the higher levels of motion that occur soon after the impact.

The damping ratio for a frequency is dependent upon where on the decay curve the measurements are taken. Shown in Fig. 5.1 are the damping ratios expressed as a percent of the critical damping for four regions, bounded by dashed lines, along the decay curve. The ratios generally increase with time. The low damping early in the trace likely has a minimal influence upon the floor's response. Approximately the second half of the decaying portion of the free vibration trace was used to estimate the damping ratio. The first peak A_n was taken at half the trace's peak value. The second peak A_{n+m} was taken as near as possible to the lowest peak. Generally this meant that m was taken as $30-50$ positive peaks. For the particular example of Fig. 5.1 $m = 51$ and the damping ratio was calculated to be 0.81%.

The programs do not allow the user to specify a viscous damping ratio for any particular frequency. They will only accept Rayleigh proportional damping as defined by Eq. 5.2. The constants for mass and stiffness proportional damping, β and α respectively are program inputs.

$$[C] = \alpha[K] + \beta[M] \tag{5.2}$$

$$\zeta = \frac{1}{2}(\alpha\omega + \frac{\beta}{\omega}) \tag{5.3}$$

The Rayleigh factors are related to damping ratio by the relation defined by Eq. 5.3. The damping ratios (ζ_1, ζ_2) associated with the frequencies that bound the frequency range of interest, first natural frequency to one close to 65Hz, were calculated. Using these two damping ratios, a system of two Eqs. 5.3 were then used to solve for the Rayleigh factors

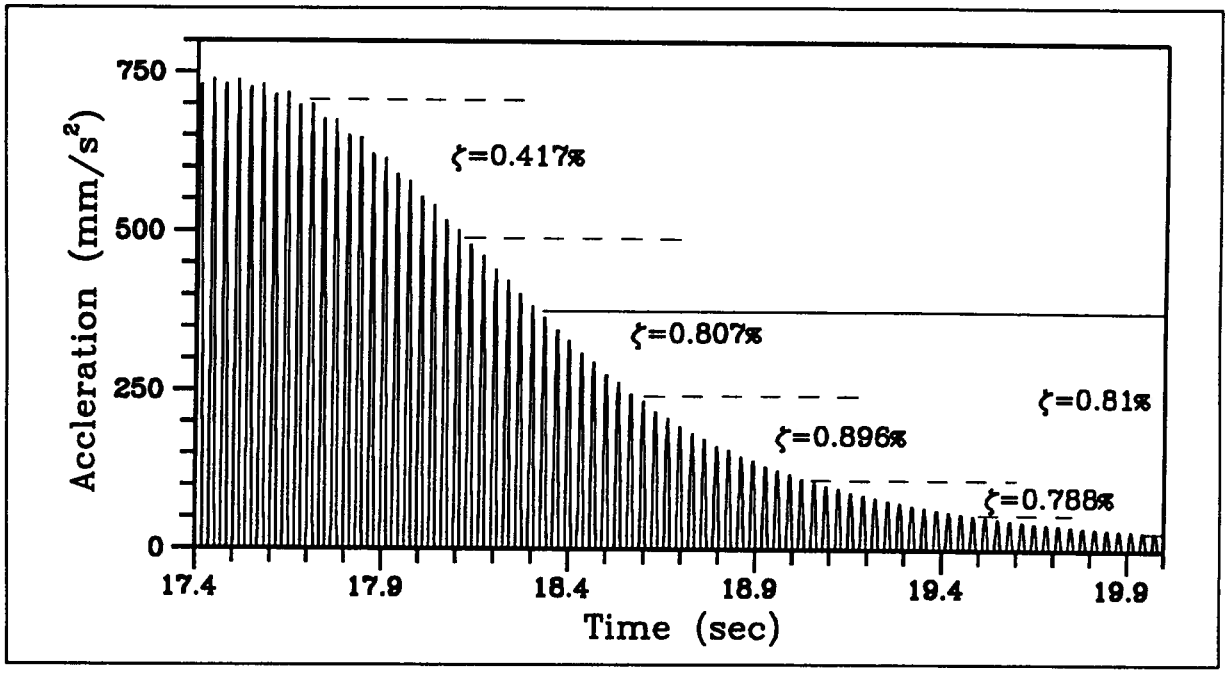

Figure 5.1: The decay curve from an acceleration trace filtered to isolate 30.4Hz, IJH6-2

α and β.

Listed in Table 5.1 are a few of the bounding damping ratios (ζ_1, ζ_2) and their corresponding α and β values that were calculated for the I–Joist floor. The 2x8 joist floor required only mass proportional damping because the higher frequencies had lower damping than the first frequency's which required unacceptable negative α values. Table 5.2 lists a few of the bounding damping ratios and the β values that were calculated for the 2x8 joist floor. Only the average β and α values for each floor were inputted into the programs.

The calculated damping ratios were not sufficient for use in DYFAP to represent actual damping effects. DYFAP is restricted to the Rayleigh damping equation. Variation in damping by floor location or frequency were not modelled by DYFAP. Variation by floor location is particularly evident in the results of Table 5.2. The averaged damping ratios

Table 5.1: A selection of proportional damping constants for the I–Joist floor

Record	α	β	$\zeta_1\%$	$\zeta_2\%$
IJH1-2	0.000051	1.33493	0.84	1.24
IJH5-1	0.000050	1.6495	0.91	1.25
IJH8-1	0.000034	2.56253	1.05	1.01
IJH8-2	0.000041	1.70527	0.84	1.07
IJH6-1	0.000058	1.41435	0.92	1.38
IJH6-2	0.000055	1.10364	0.81	1.28
average	0.000047	1.7329	0.91	1.19

Table 5.2: A selection of proportional damping constants for the 2x8 joist floor

Record	β	$\zeta_1\%$	$\zeta_2\%$
SLH6-1	8.63898	2.01	1.35
SLH6-2	22.17317	4.41	1.54
SLH8-1	10.70202	2.49	1.14
SLH8-2	6.06018	1.41	1.07
SLH4-1	10.05732	2.34	1.70
average	9.8854	2.3	1.36

were increased in order to produce traces that reasonably matched the duration and amplitude of the experimental traces. The damping ratio ζ for the 2x8 joist floor was set at 4%. The I–Joist floor required its ζ_1 and ζ_2 to be 2% and 2.5% respectively.

5.2 Identifying the Floors' Natural Frequencies

The natural frequencies of the floor systems were identified from Fourier spectra derived from the hammer test's acceleration records. The hammer impact seemed to do well in exciting the entire range of frequencies of interest. The hammer test did not involve adding any additional masses to the floor systems that could have altered the systems' frequency distributions. Spectra from all ten test locations were used to identify the predominant frequency peaks.

The complete data record for any particular test included: a 1.5 second leader of ambient noise, a $0.5 - 1$ second response and about another 3.5 seconds of ambient floor vibration following the floor's response. The passage of time associated with the floor's response was only 15% of the entire record. Performing a Fast Fourier Transform on the entire record produced a significant amount of clutter in the Fourier spectrum, particularly at the higher frequencies. The frequency content of the ambient noise leader was significant and not necessarily representative of the floor's response. In order to be able to compare the Fourier spectrum amplitude levels with those obtained from DYFAP runs, only 4.1 seconds of recorded data were analysed. This made the DYFAP output and the experimental data record of the same duration. The lower time bound for the analysis began at the beginning of the floor's response, excluding the leading noise. By comparing Fig. 5.2 and Fig. 5.3 one can see how much activity was present in the ambient noise leader and tail. The floor's predominant natural frequencyies are now clearly evident. The high frequency content was all but eliminated. The drop in Fourier

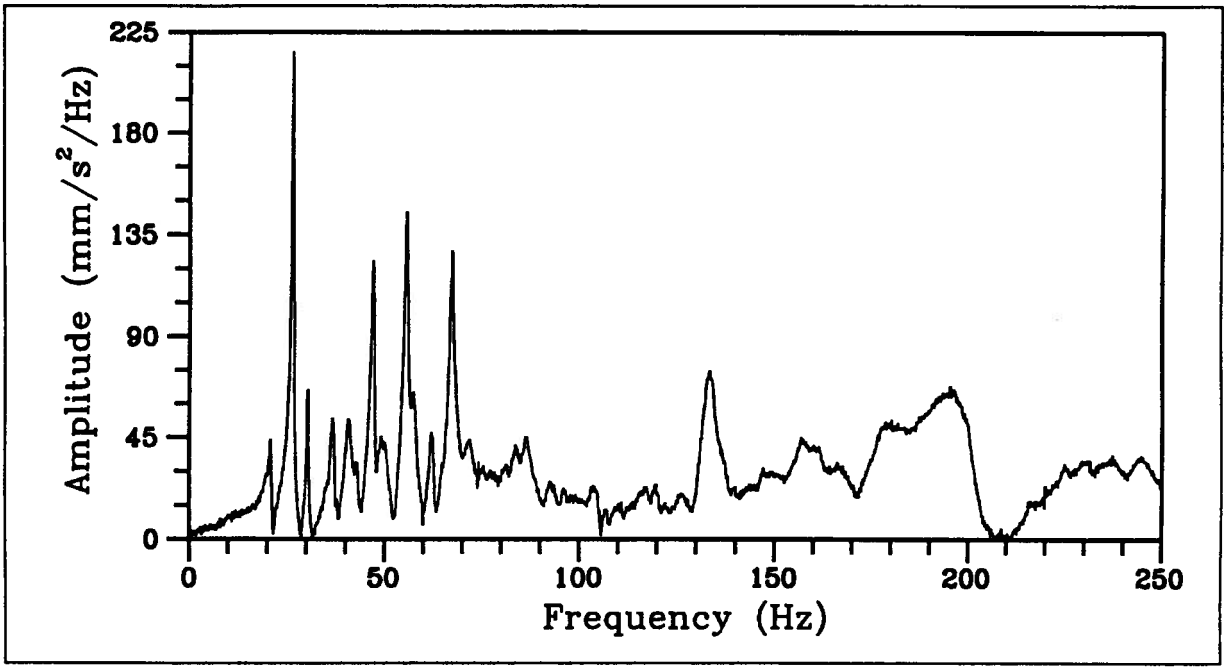

Figure 5.2: Fast Fourier Transform of a six second acceleration record

spectrum amplitudes indicate that as expected, the ambient floor vibration included the floor's natural frequencies contaminated with noise frequency components. Even for a record clipped to 4.1 seconds in duration, a lot of the record was just ambient vibration but the longer duration was necessary in order to achieve a reasonable 0.24Hz frequency increment for the Fourier spectra.

Each test location produced its own unique Fourier spectrum. At any particular test location, the frequencies that strongly participated in the response depended heavily upon the location of the impulse and the receiver on the floor. This was particularly evident when comparing the response at two locations due to the same impulse. As an example, Fig. 5.4 and Fig. 5.5 show the Fourier spectra from two accelerometer locations produced by the impact at test location #5. These figures show that even though acceleromter#2 was located near the center of the floor, it would be wrong to assume that the strong

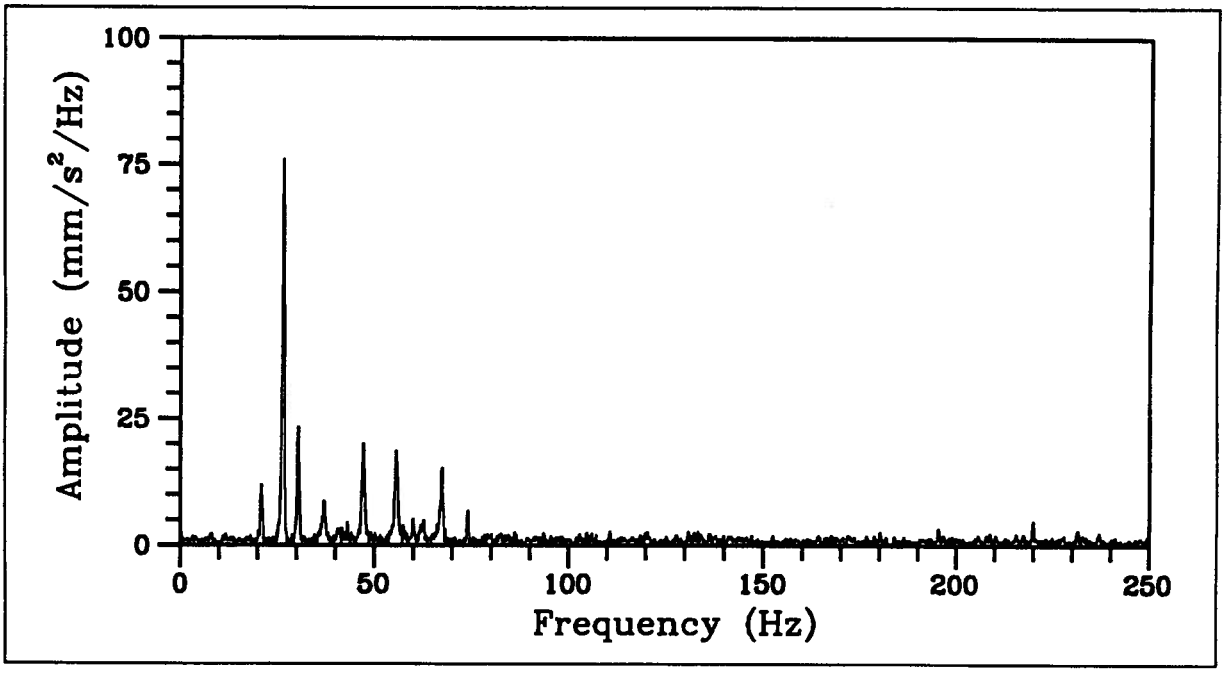

Figure 5.3: Fast Fourier Transform of a bounded acceleration record, time bounds of 5.35 – 9.45 seconds

peak at 40Hz was the floor's fundamental frequency. Therefore, it is important to analyze responses at a number of locations to allow one to evaluate how significant a particular peak is to the floor's general response.

For both floors, only the frequencies from 0 – 100Hz were considered since the very high frequencies are not important for the free vibration of the floor. They do contribute to the extreme spikiness of the high peak accelerations during the first 2 – 3 cycles but they dampen out very quickly. A floor's lowest three or four frequencies typically dominate its response.

For the identification of natural frequencies, a simple approach was used. For the purpose of this investigation, it was only necessary to be able to identify the predominant frequencies. The many other frequencies that could be identified by more sophisticated techniques are of little interest since their level of participation do not significantly effect

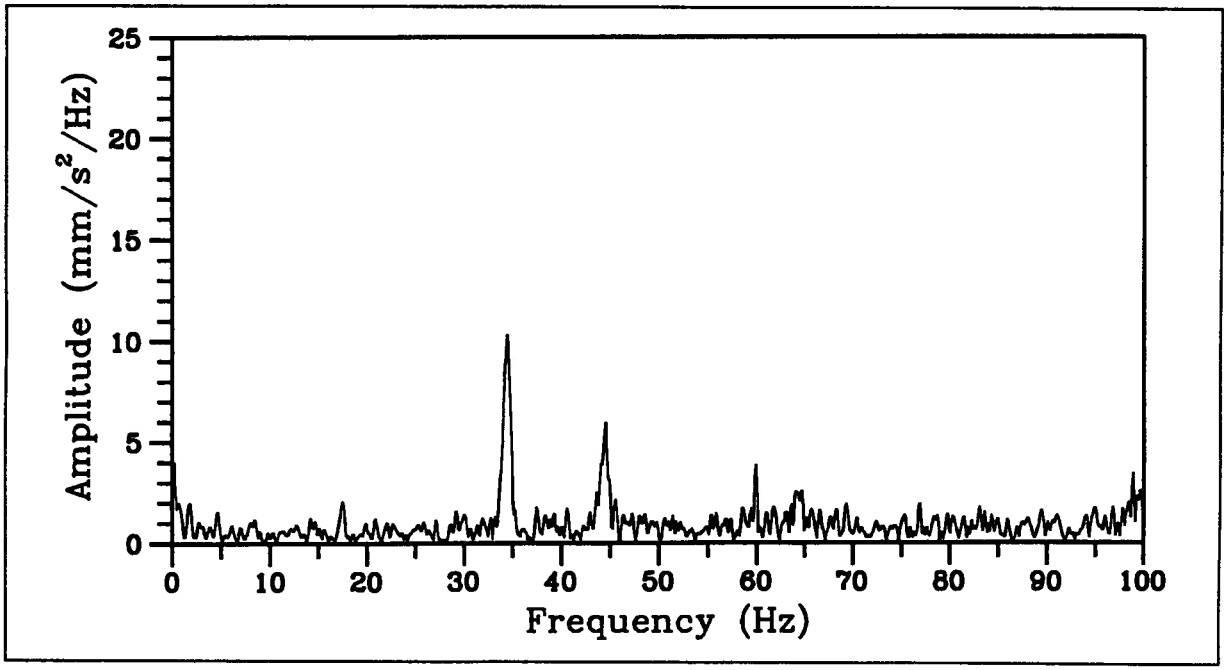

Figure 5.4: Fourier spectrum for hammer test, SLH5-1

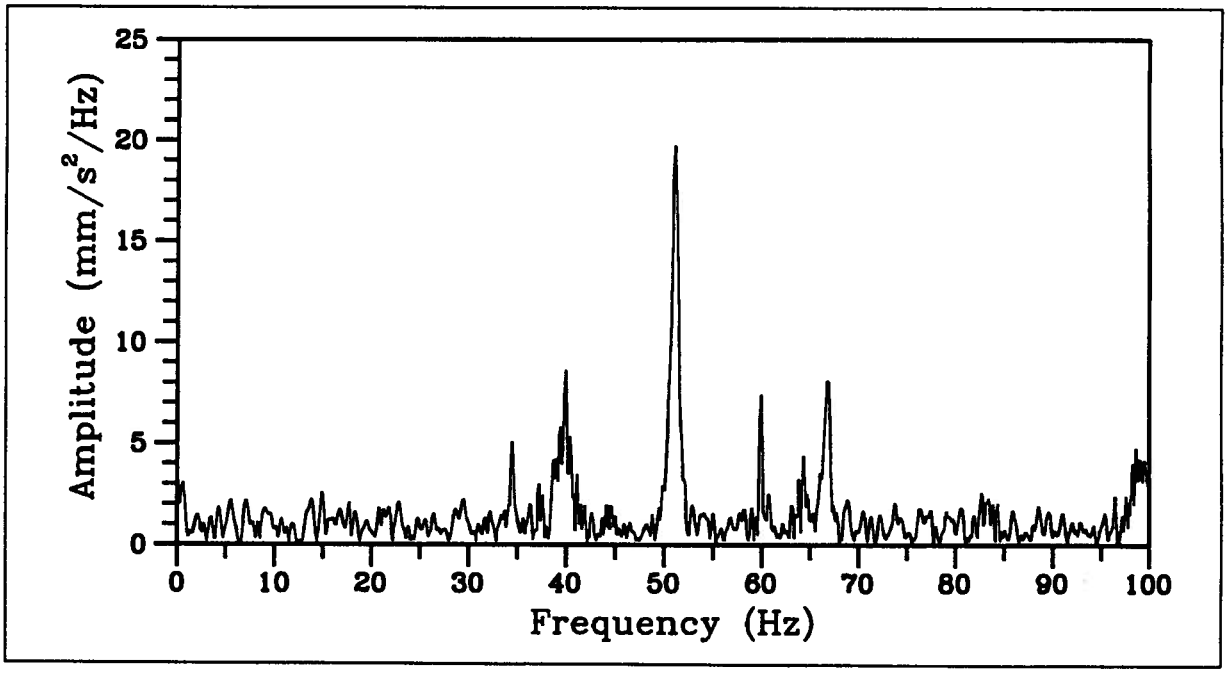

Figure 5.5: Fourier spectrum for hammer test, SLH5-2

Table 5.3: Natural frequencies for the test floors

	Natural Frequencies (Hz)	
Mode Number	*2x8 Joist*	*I–Joist*
1	34.2	26.4
2	40.0	30.4
3	44.2	34.7
4	50.9	37.0
5	55.6	47.1
6	64.2	50.4
7	66.7	55.5
8	83.3	67.0

the floor response time traces. A peak of moderate amplitude was considered as a likely frequency if it occured on a number of the records. The strongest one or two peaks for any record were automatically considered to be natural frequencies. These criteria were sufficient to safely identify six frequencies and to allow a couple more to be tentative.

Samples of spectral densities for the 2x8 joist floor are shown in Figs. 5.4 – 5.9. These plots show strong peaks for 7 of the 8 frequencies listed in Table 5.3. The peak at 55Hz occurs in only four of the 20 records and never very strongly. It was the weakest of all the identified frequencies and was much stronger than the next possible candidate.

Samples of Fourier spectra for the I–Joist floor are shown in Figs. 5.10 – 5.14. Eight frequencies are listed in Table 5.3 for the I–Joist floor but only four had consistently strong and sharp peaks in the spectra. The peak at 37.0Hz marked the pass fail boundary like 55Hz did for the 2x8 joist floor.

As previously mentioned, electrical noise at 60Hz was not to be mistaken for a floor frequency. A narrow spike at 60Hz appears in all cases for both floors as shown in the following spectral density plots. At times it may not be evident but the magnitude of the spikes are consistently between $4 - 8$ units. This frequency was not filtered out prior to

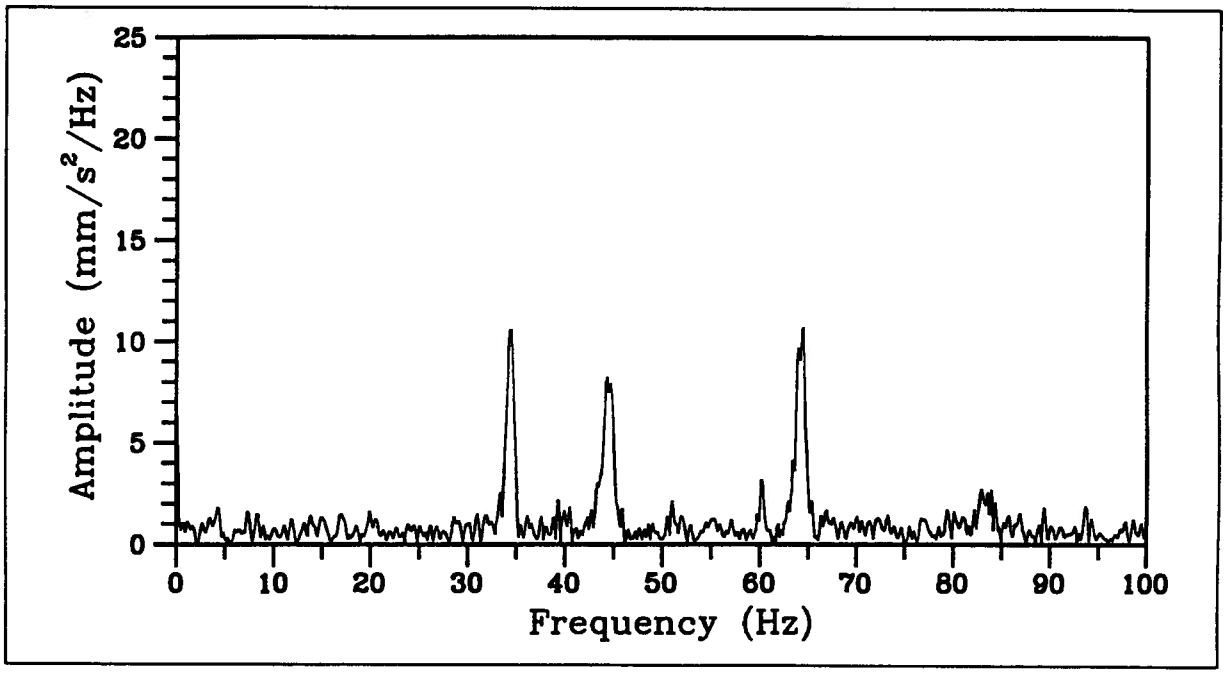

Figure 5.6: Fourier spectrum for hammer test, SLH6-1

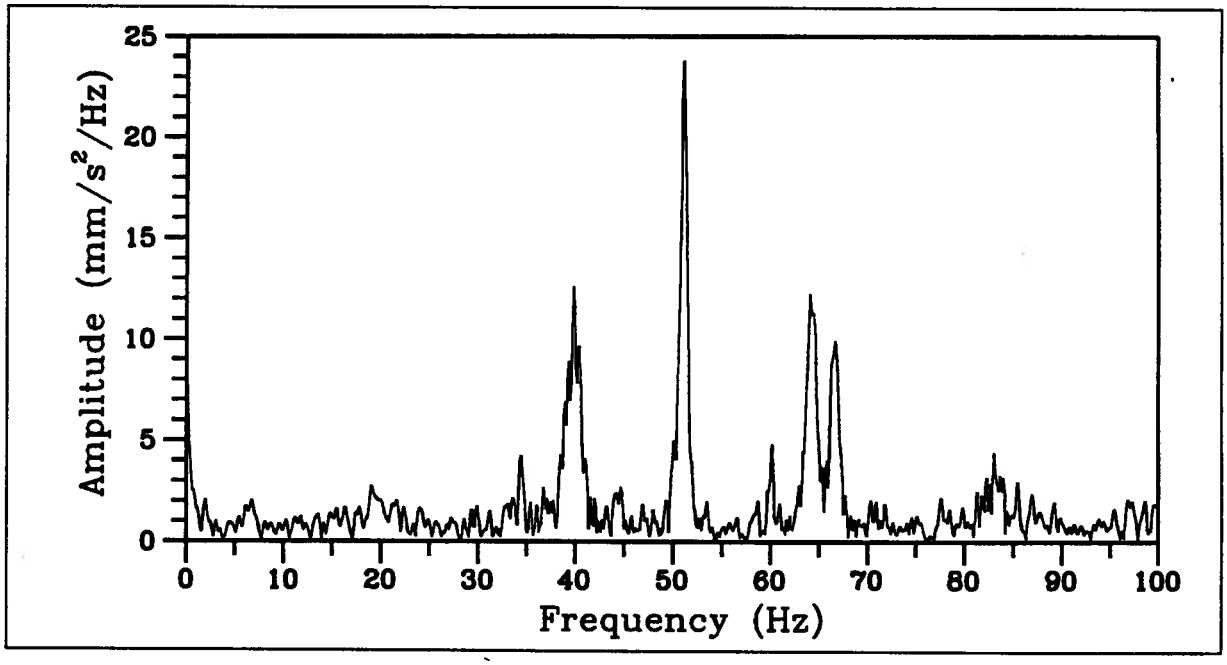

Figure 5.7: Fourier spectrum for hammer test, SLH6-2

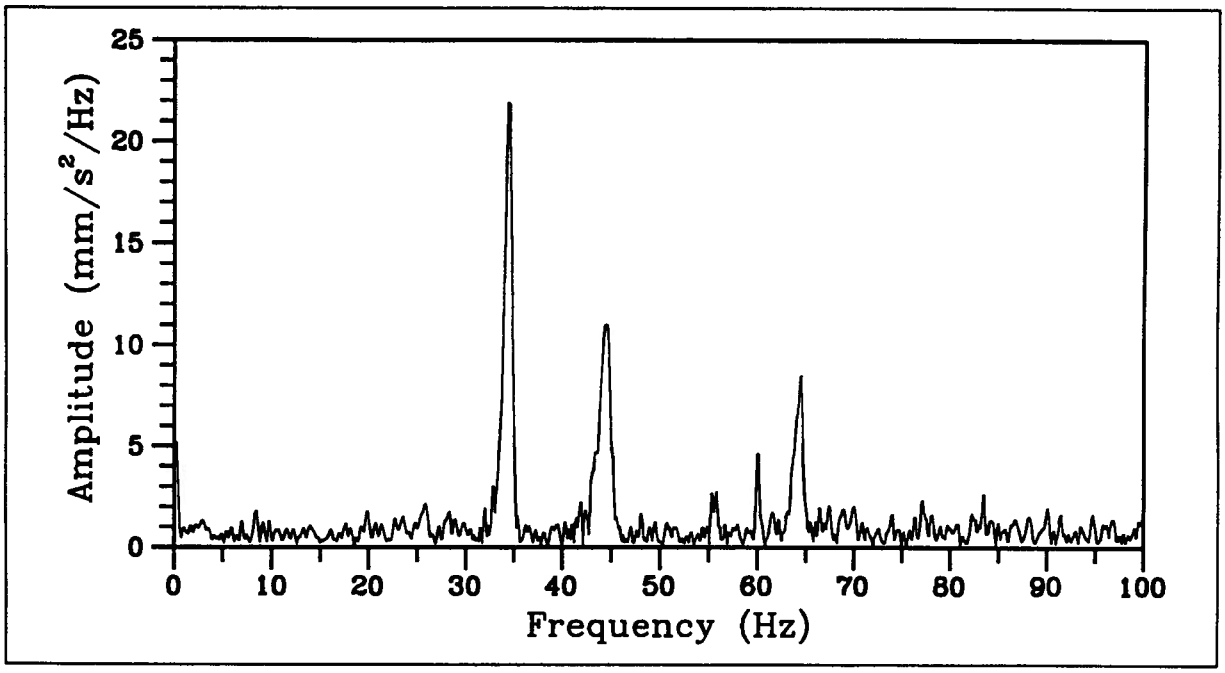

Figure 5.8: Fourier spectrum for hammer test, SLH7-1

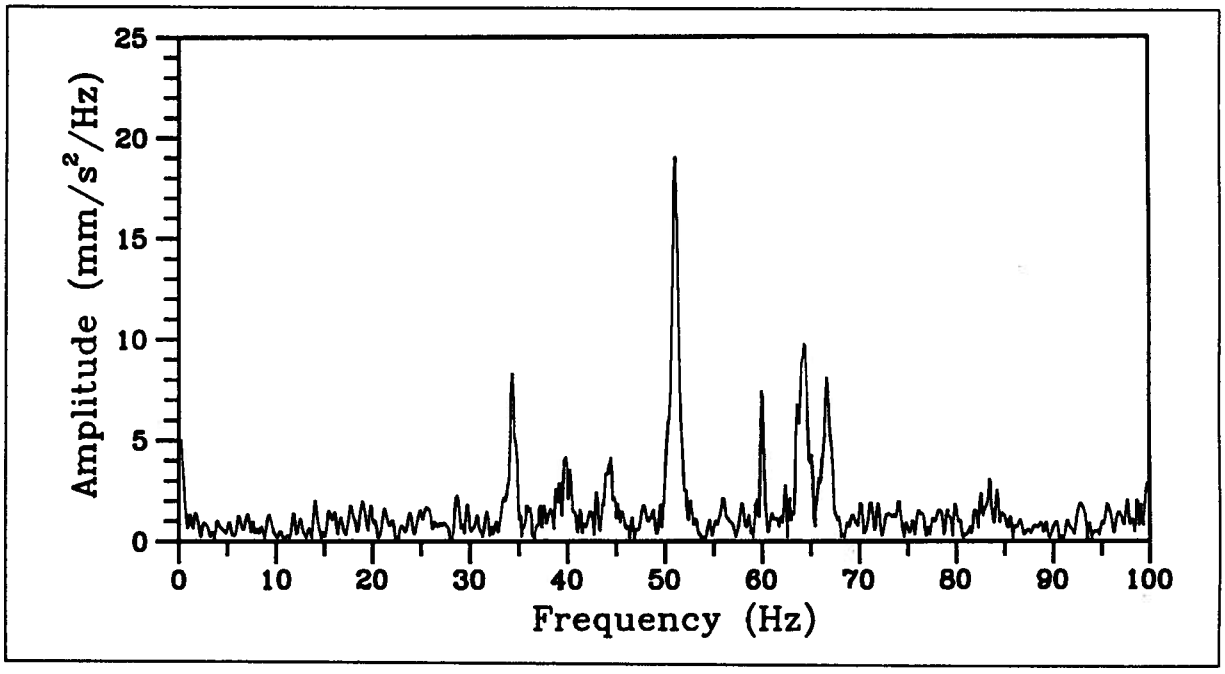

Figure 5.9: Fourier spectrum for hammer test, SLH7-2

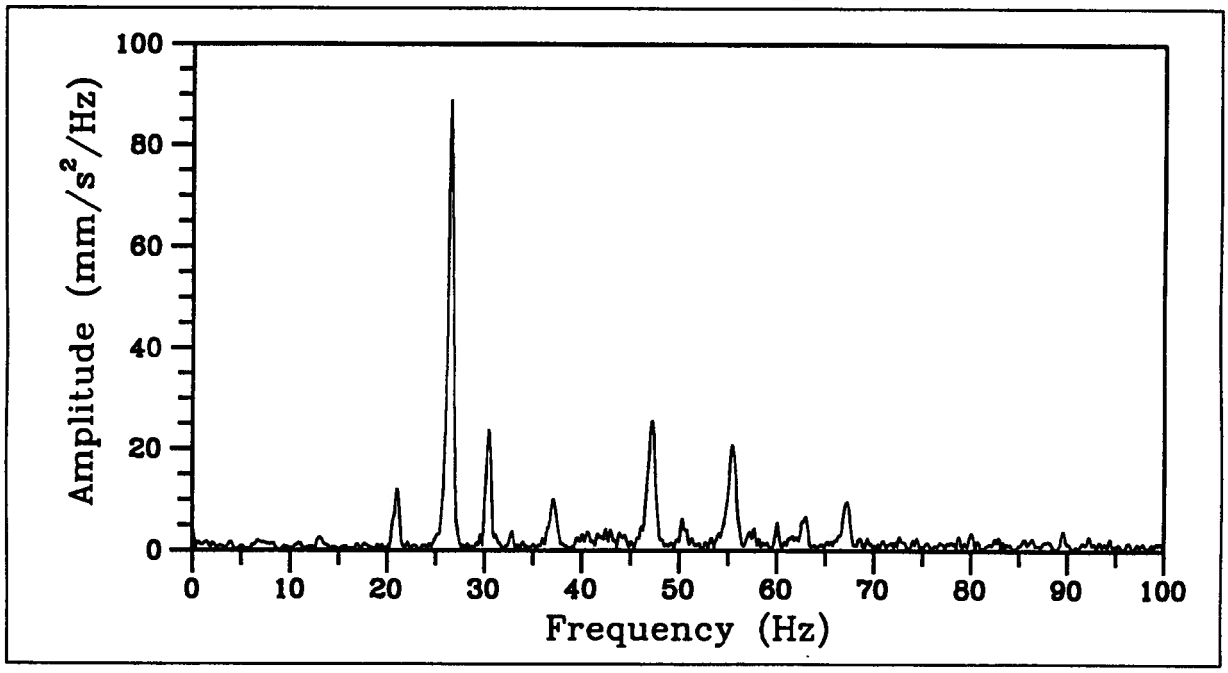

Figure 5.10: Fourier spectrum for hammer test, IJH2-1

the investigation of the acceleration and displacement time histories. The low amplitude high frequency did not significantly alter the characteristics of the traces. The I–Joist floor had an additional extraneous frequency at 21Hz. It is likely due to some form of floor–frame interaction that was allowed as a result of some irregularity that may have occured during the reconstruction of the frame for the I–Joist floor. It became significant during the heel drop tests and therefore, it was necessary to apply a narrow band pass filter to the raw acceleration records. The larger peak displacements during the heel drop tests are likely the cause for the increased participation of the 21Hz component.

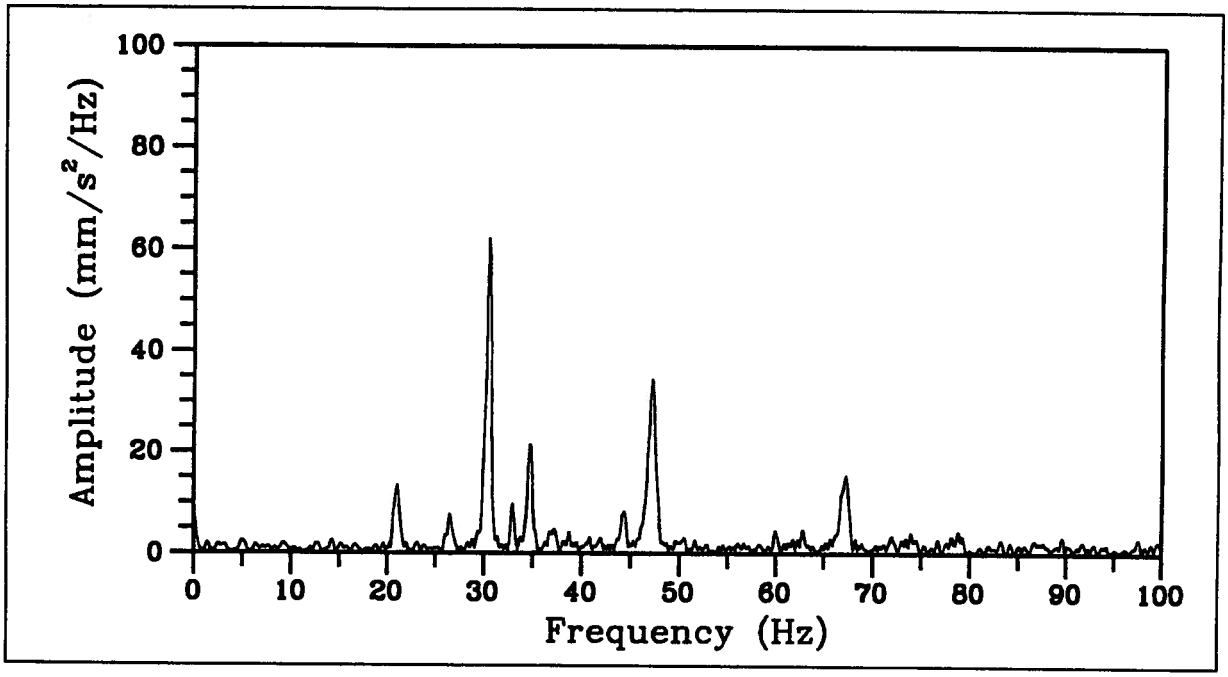

Figure 5.11: Fourier spectrum for hammer test, IJH2-2

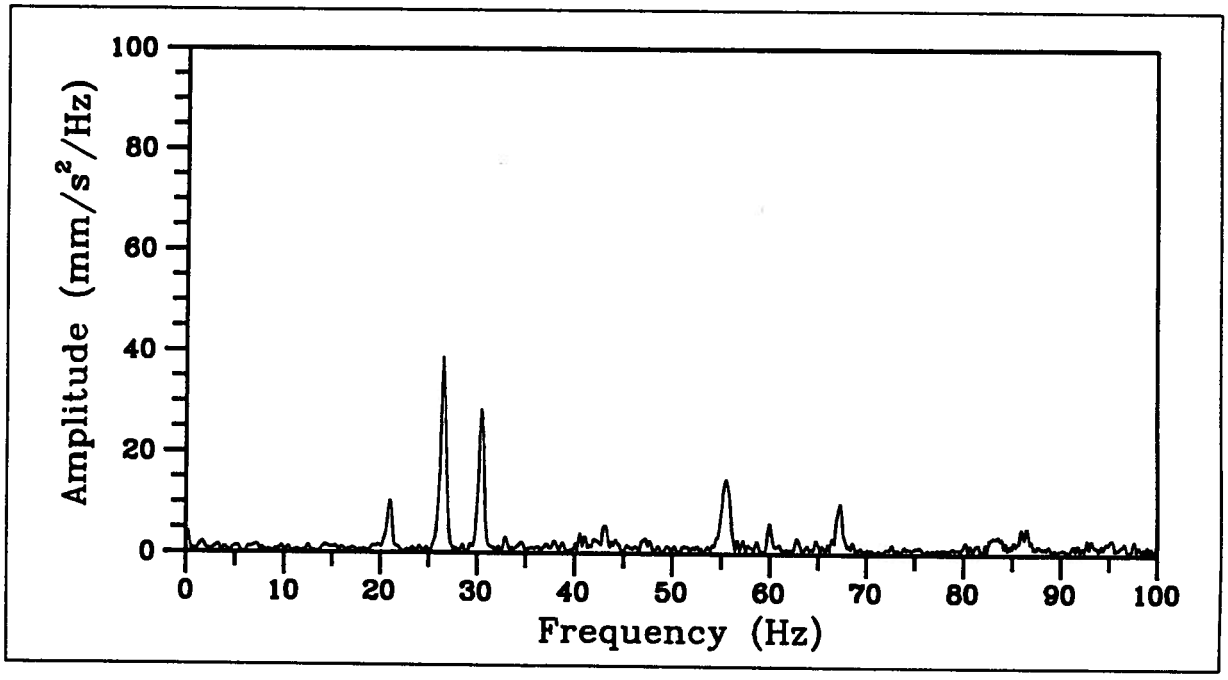

Figure 5.12: Fourier spectrum for hammer test, IJH4-1

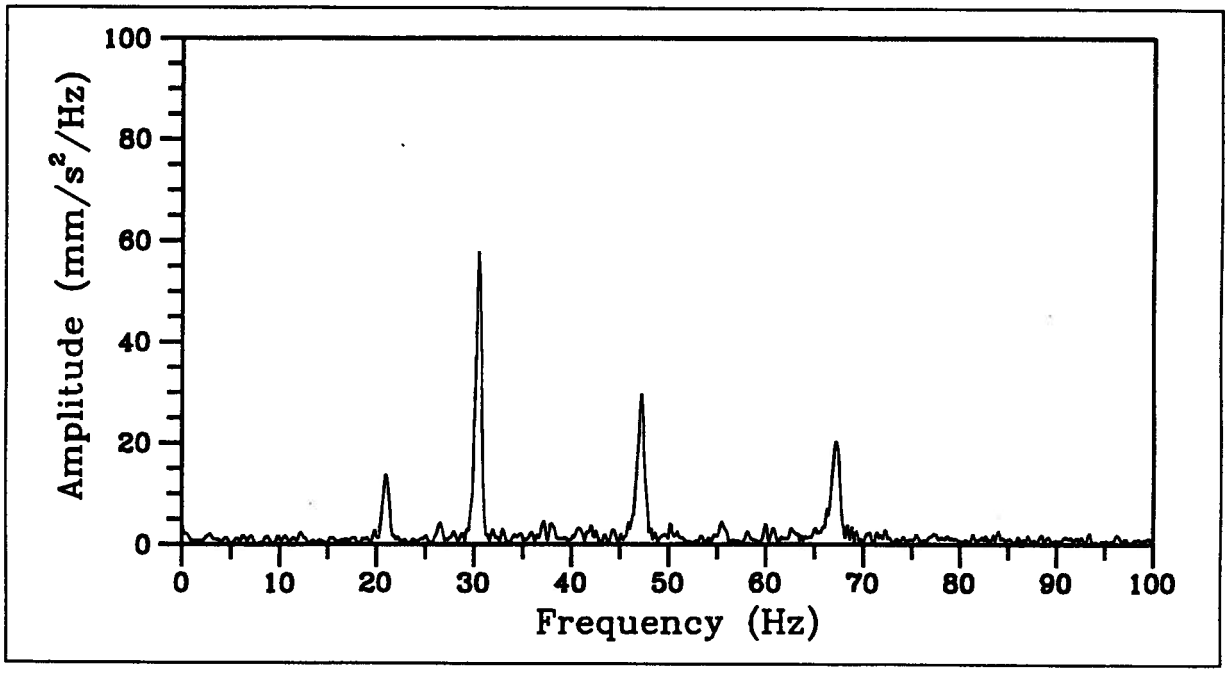

Figure 5.13: Fourier spectrum for hammer test, IJH6-1

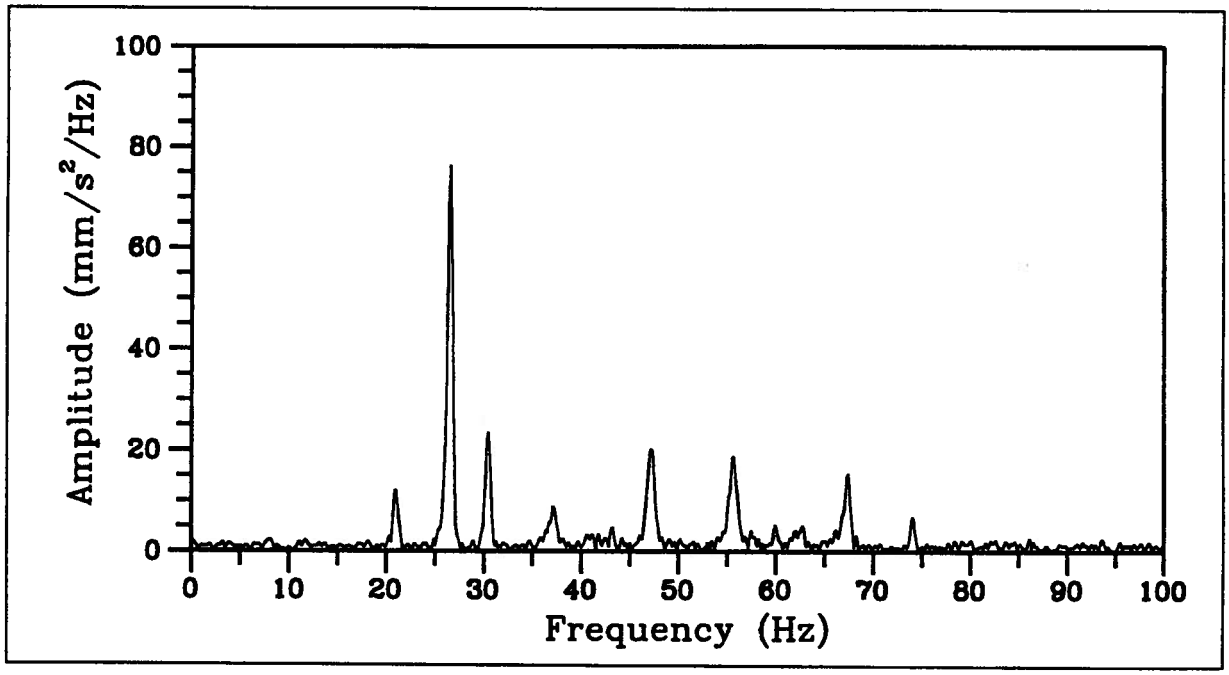

Figure 5.14: Fourier spectrum for hammer test, IJH8-1

Chapter 6

NAFFAP

6.1 Introduction

The program NAFFAP, NAtural Frequency Floor Analysis Program, was developed by Andre Filiatrault and Bryan Folz at the University of British Columbia in 1989 [Filiatrault and Folz, 1989]. It solves for the natural frequencies and mode shapes of an undamped one–way stiffened floor system. The floor system is restricted to one with equidistant simply supported stiffeners attached to an orthotropic plate. Semi–rigid stiffener–to–plate connectors are allowed. The program's solution employs a T–beam finite strip analysis that was developed by Foschi [Foschi, 1982]. Each strip, as shown in Fig. 6.1, consists of 4 nodes with 19 degrees of freedom. The DOF associated with node 4 are as shown while nodes $1-3$ take u,v,w and the first derivitives of u and v. The current version can handle a floor with up to 12 stiffeners.

6.2 Data File

The boundary conditions for the perimeter joists were different for the two floors. Although their construction were essentially the same, the difference in torsional rigidity of the two types of joists warranted differences in how the degrees of freedom could be defined. The longer spanning deeper I–Joist allowed for significant rotation about its x–axis at midspan. By definition, the perimeter I–Joists were more closely modelled by a simple rather than a fixed support. The lower flanges were nailed to the sills but their

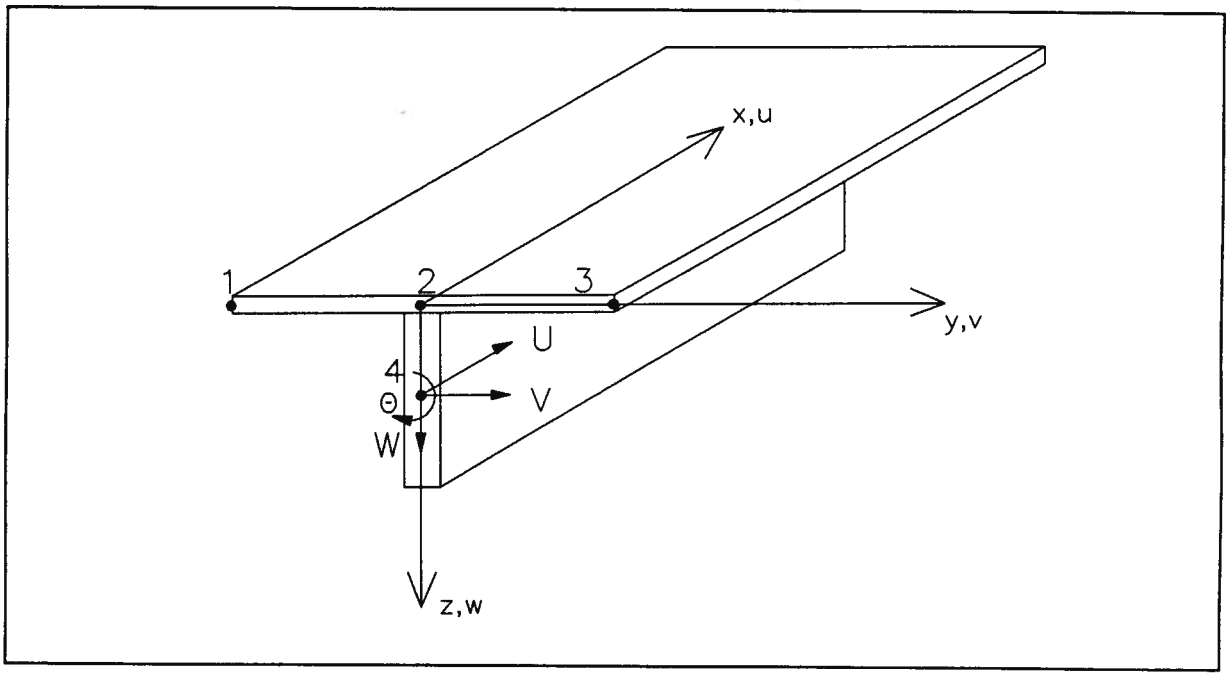

Figure 6.1: A T–beam finite strip

thin webs provided little torsional stiffness. The 2x8 joists were $57.2mm$ shallower and had a 60% larger torsional constant than the I–Joists. The 2x8 joist floor had a shorter span and a smaller joist spacing than the I–Joist floor, thus joist rotation was better controlled. Here the perimeter joists were best modelled as fixed supports.

The floor parameters required by NAFFAP and DYFAP to model the floors were discussed in chapter 2. Values were either measured directly or were derived from equations except in the case of nail stiffness. Tests were not performed for nailed connections. The tests that were performed only provided evidence for disregarding the stiffness contribution from the elastomeric glue.

It was assumed that the test floors' connector stiffness could be modelled by a nailed connection. A value for nail stiffness of approximately $10000lb/in$ ($1750N/mm$) would be acceptable. To determine what value of nail stiffness would work best with NAFFAP,

a minimization procedure was followed. NAFFAP runs were done for stiffness values ranging from $7000 - 34000 lbs/in$ ($1230 - 5950 N/mm$). The upper limit was the average stiffness obtained from the glued connection tests.

The percentage error in matching frequencies with the test results was used as a minimization parameter. Not all frequencies were used. The higher modes are more difficult to model accurately than the first couple of modes. Besides which the lower frequencies generally dominated the acceleration traces. An additional acceptance criteria was applied to the first three frequencies. They were all to be within 5% of the test frequencies. Listed in table 6.1 are the percentage error for the 2x8 joist floor's first three frequencies. The table shows that a nail stiffness of $8000 - 13000 lb/in$ ($1400 - 2280 N/mm$) allows NAFFAP to do fairly well in matching the frequencies of the tests. Values in this range are all acceptable for an $8d$ common nail connection. As the nail stiffness values approach that of a glued connection one can see how NAFFAP diverges from the first and third frequencies. Only the $10000-12000 lb/in$ ($1750-2100 N$) nail stiffnesses satisfied the sub 5% criteria. Of those, $10000 lb/in$ ($1750 N/mm$) provided the best combined fit for the first and second frequency.

The values taken for the 2x8 and I–Joist floors' connector rotational stiffness (RKROT) were $6000 lb/in$ ($1050 N/mm$) and $12000 lb/in$ ($2100 N/mm$) respectively. These were minimum values to ensure that NAFFAP did not produce an overabundance of "joist wiggling" frequencies. The low torsional rigidity of the I–Joist required the large connector rotational stiffness.

NAFFAP had difficulty in capturing the I–Joist floor's first frequency at 26Hz but it did well with the strong frequencies at 30Hz, 47Hz, 55Hz and 67Hz. The frequencies above 45Hz were not very sensitive to changes in the nail stiffness parameter but unwanted frequencies between 38Hz and 45Hz were developing more pronounced mode shapes. Straying too far above the nail range of $7000 - 13000 lb/in$ ($1230 - 2280 N/mm$) caused

Table 6.1: Percentage difference between 2x8 joist floor tests' and NAFFAP frequencies

Nail Stiffness	*% Difference*		
(lb/in)	*Mode1 (34.2Hz)*	*Mode2 (40.0Hz)*	*Mode3 (44.2Hz)*
7000	2.08	6.08	2.19
8000	2.63	5.63	1.81
9000	3.16	5.18	1.45
10000	3.65	4.75	1.11
11000	4.15	4.33	0.77
12000	4.62	3.93	0.45
13000	5.09	3.53	0.14
20000	7.87	1.10	1.88
30000	10.91	1.65	4.16
34000	11.90	2.55	4.95
1000lb/in = 175N/mm			

NAFFAP's first frequency to increase its error from 14% to 20%.

6.3 NAFFAP's Results for the Test Floors

NAFFAP produced a number of frequencies for both floors. Some of these are a result of the inclusion of a rotational degree of freedom. Most often these "rotational" or "joist wiggling" modes are associated with very low vertical motions, and therefore are of little interest. The I–Joist floor was most susceptible to this type of mode shape. The lower torsional rigidity of the joists coupled with the larger joist spacing were responsible. Listed in table 6.2 are the complete lists of NAFFAP frequencies and the frequencies identified from the tests for both floors.

The mode shapes that NAFFAP suggested for the two floors are shown in Fig. 6.2 and Fig. 6.3. They were drawn from the values for the vertical and rotational degrees of freedom for nodes 1, 3 and 4. The mode numbers shown in Fig. 6.2 and Fig. 6.3 correspond to those listed in Table 6.2. Only the first few mode shapes for each floor

Table 6.2: NAFFAP results compared with frequencies identified from floor tests

	Natural Frequencies (Hz)				
Mode	*2x8 Joist Floor*		*Mode*	*I-Joist Floor*	
Number	*Test*	*NAFFAP*	*Number*	*Test*	*NAFFAP*
1	34.2	35.5	1	26.4	30.3
2	40.0	38.1	2	30.4	31.0
3	44.2	43.7	3	34.7	31.3
4	50.9	51.2		–	32.3
	–	52.4		–	33.1
5	55.6	53.3		–	33.9
	–	54.5		–	34.9
	–	55.4		–	35.0
	–	55.6		–	35.7
	–	56.7		–	36.5
	–	56.9		–	37.5
6	64.2	59.1	4	37.0	38.5
7	66.7	72.8	5	47.1	41.1
8	83.3	93.0	6	50.4	46.5
			7	55.5	54.5
			8	67.0	65.1

were drawn. The first mode shape for either floor was not symmetrical because the joists were of different stiffnesses.

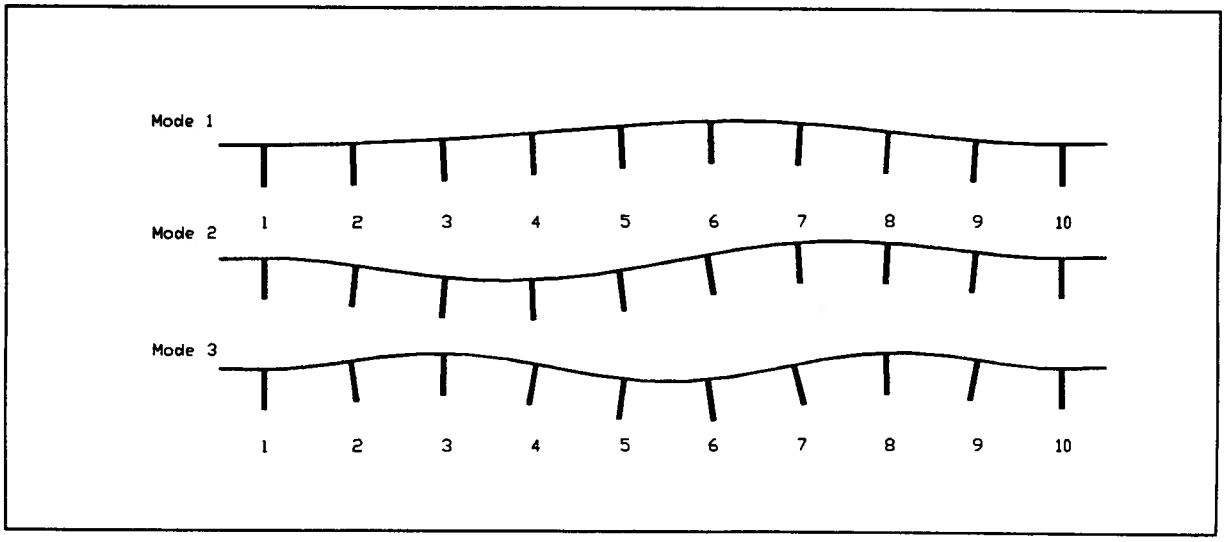

Figure 6.2: NAFFAP mode shapes for the 2x8 joist floor

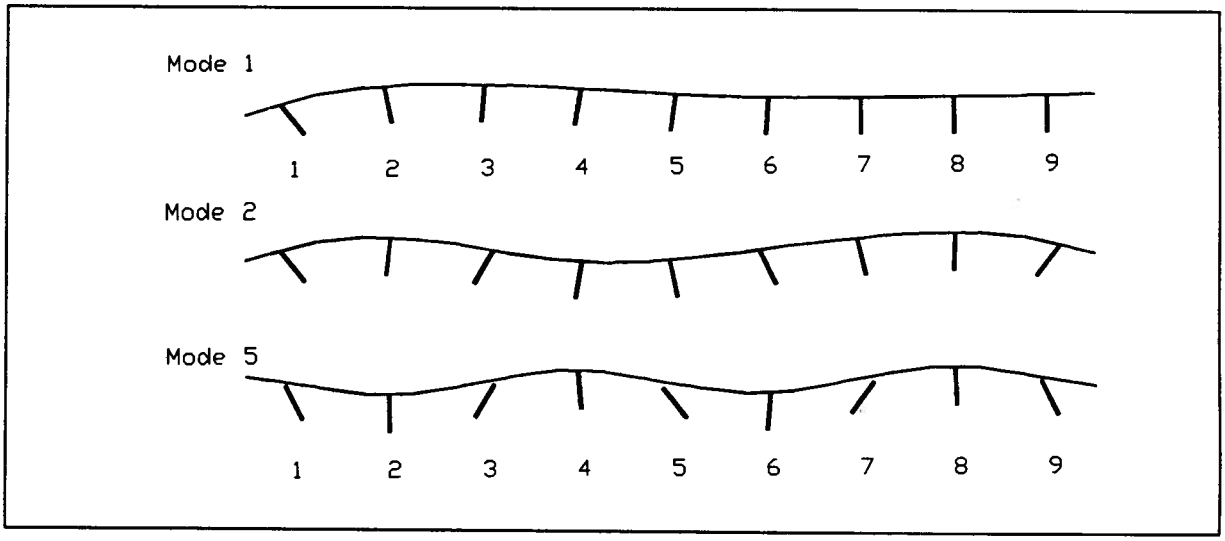

Figure 6.3: NAFFAP mode shapes for the I–Joist floor

Chapter 7

DYFAP

7.1 Introduction

The program DYFAP, DYnamic Floor Analysis Program, was developed at the University of British Columbia by Bryan Folz, Andre Filiatrault and R.O. Foschi in 1990 [Filiatrault et al, 1990]. It employs the same structural modelling as NAFFAP. The input data file is almost identical to that of a NAFFAP input file. The difference lies in that DYFAP performs a time domain integration of the equations of motion in response to a specified loading on the floor. The loading can take the form of a sinusoidal forcing function, step load, discretized forcing function and/or impulses from an oscillator that is attached to the floor surface. DYFAP output consists of displacement, velocity and acceleration time histories for a designated floor location. Such an output is of course influenced by the form and level of loading that is applied to the floor.

7.2 Modelling of a Hammer Impulse

Since the impulses imparted to the floor by the hammer impact tests were not recorded, it was necessary to derive an estimate of a typical hammer impulse from the literature. Scaling from a trace reported in Chui's paper, a duration of approximately 16ms and a peak load of $230N$ were measured [Chui, 2/86]. The peak accelerations measured from his floor due to the hammer impulses were roughly $0.5g$. The peak accelerations for the tests reported in this thesis were on the order of $2g$. To obtain the larger response one

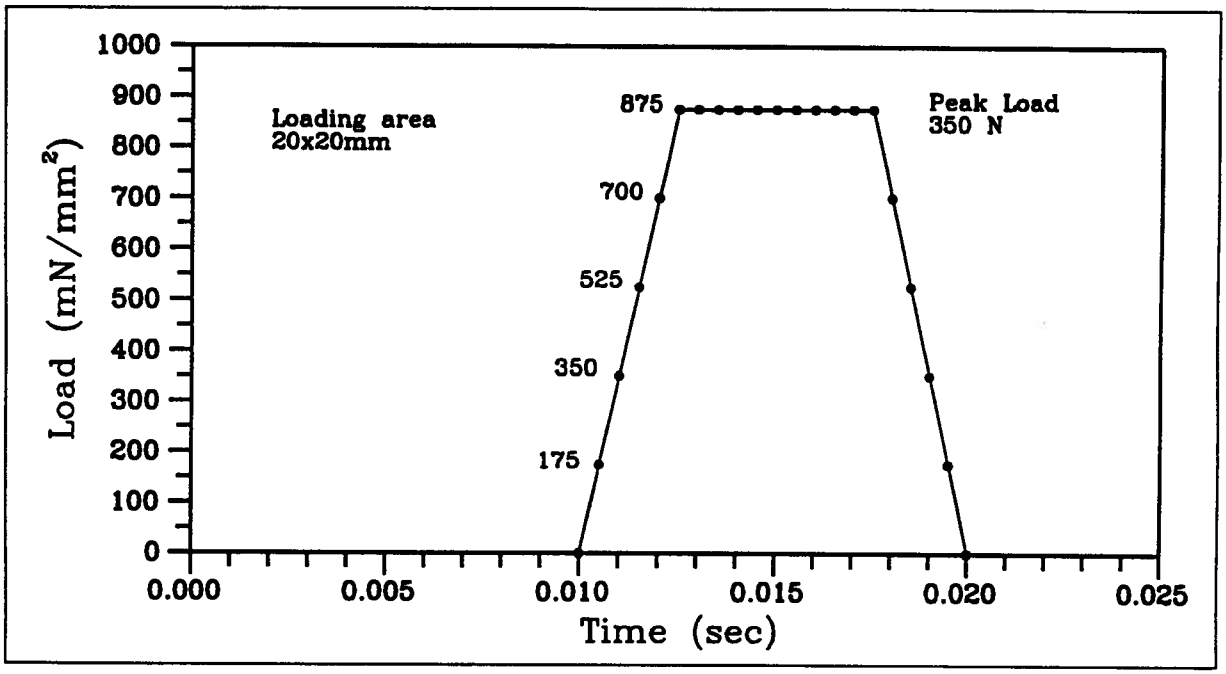

Figure 7.1: Modelling of a hammer impulse

can increase the peak load and decrease the duration. The influence of changing the peak and duration was noted and compared with the acceleration peaks of test SLH6-2. The combination of $350N$ and $10ms$ was sufficient in order for DYFAP to match the test's peak accelerations. This loading was applied over a $20x20mm$ area. For DYFAP, the loading was discretized as shown by Fig. 7.1. The time scale of Fig. 7.1 has been magnified so that the plateaued peak of the impulse model would be visible. Rather than increasing the peak load substantially in order to increase the impulse's energy, the peak was plateaued. The steeper slope of the impulse also contributed to the peak acceleration of the floor. This is partly recognized by the higher dynamic magnification factor for a rectangular pulse over a half sine pulse [Clough and Penzien, 1975].

7.3 The Bagdrop Impulse

The impulses from the bagdrop impact tests were recorded by a load cell that was mounted on the floor surface. The load was received by the floor over an area of $4780mm^2$. The softer impact induced lower peak accelerations. A trace of a typical bagdrop impulse is shown in Fig. 7.2. The trace does not settle back to zero over time because the bag remained atop the load cell for the duration of the test. The influence of the bag's mass upon the response of the system was small, particularly for the heavier I–Joist floor. The entire trace was not discretized for DYFAP. The many oscillations following the initial impulse were replaced by a flat trace as shown in Fig. 7.2. The magnitude of the bagdrop impulses were quite repeatable but each impulse's shape was slightly different. For the example shown in Fig. 7.2, the peak load is $115lb$ ($512N$). Since the impulse traces were available, DYFAP runs were made using the corresponding impulse for each test location.

7.4 Comparison of Hammer and Bagdrop Tests with DYFAP Results

The response was unique at any particular point on the floor. Although the frequency content was constant, the level of participation of each frequency made each spectrum unique. A number of factors may contribute to this phenomenon. Proximity to boundary conditions such as edges and sheathing joints, testing over or between joists and nonuniform material properties may greatly affect the level of damping or the participation for any particular frequency. The level of participation chosen by the computer solution differ from those of the experimental results largely because of the program's inability to capture all of these features in its model. Material properties such as local stiffness, connection details and mass density are considered by the computer model as more uniform than site specific.

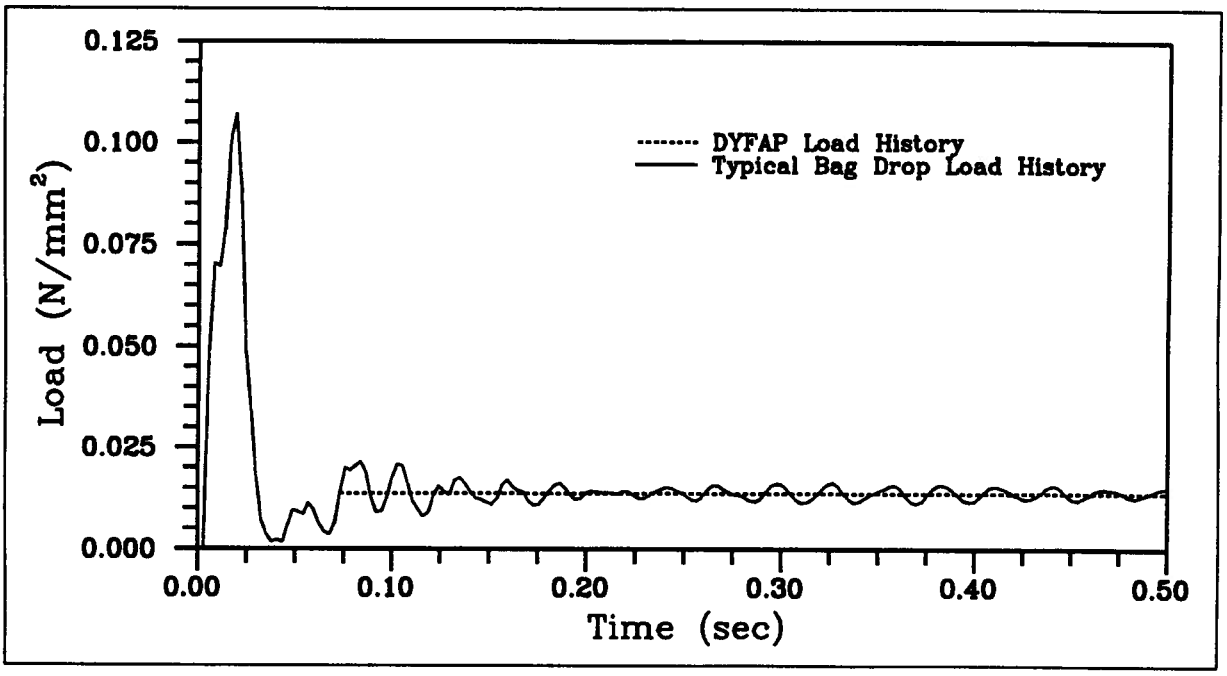

Figure 7.2: Typical recorded bagdrop time history compared with that used with DYFAP

Accepting the limitations of the model, there were still a number of features of the response and output that could be noted and compared. The peak accelerations, peak displacements and damping were key features.

Since the test data were recorded as acceleration time histories it was necessary to integrate twice to obtain the displacement record. The soft low pass nature of the integration process accentuates the low frequency content thus causing the integrated trace to show a low frequency drift. The majority of this disturbance was between $0 - 3$Hz. It was necessary to apply a digital high–pass filter to the velocity and displacement traces in order to satisfy the zeroed boundary conditions. The bag and hammer traces were filtered up to 8Hz but this was well below any system frequencies of interest (see "Designing Digital Filters", Charles Williams, 1986). The signal processing was performed using the VU–POINT software package [VU–POINT, 1988].

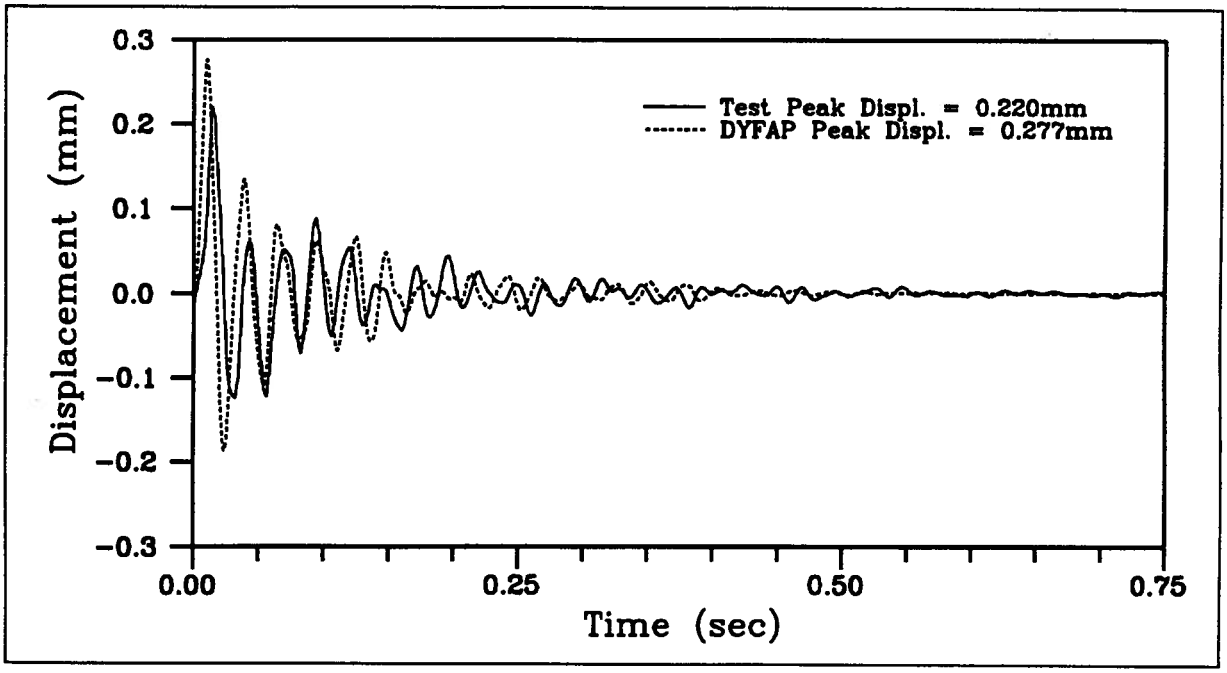

Figure 7.3: Comparison of the 2x8 floor's test and DYFAP's response to a hammer impact

The fact that DYFAP was modelling the hammer impulse from an approximation resulted in a rather poor comparison with the test results. On the other hand, the load history for every bagdrop test was available for discretization. Naturally each hammer impact must have varied in intensity, particulary between floors. A fluctuation of up to $0.5g$ from test to test is not unreasonable. The displacement time history, derived by integrating the acceleration trace twice, was not as sensitive to variations in the loading. Therefore, DYFAP's and the test's results could be conveniently overplotted as shown in Fig. 7.3 and Fig. 7.4. All of the following comparisons used the output from the same floor location. The impact location was #6 and the response was taken from accelerometer #2.

The Fourier spectrum, acceleration and displacement time histories for the bagdrop were comparable. The Fourier spectra overplots of Fig. 7.5 and Fig. 7.6 do not match

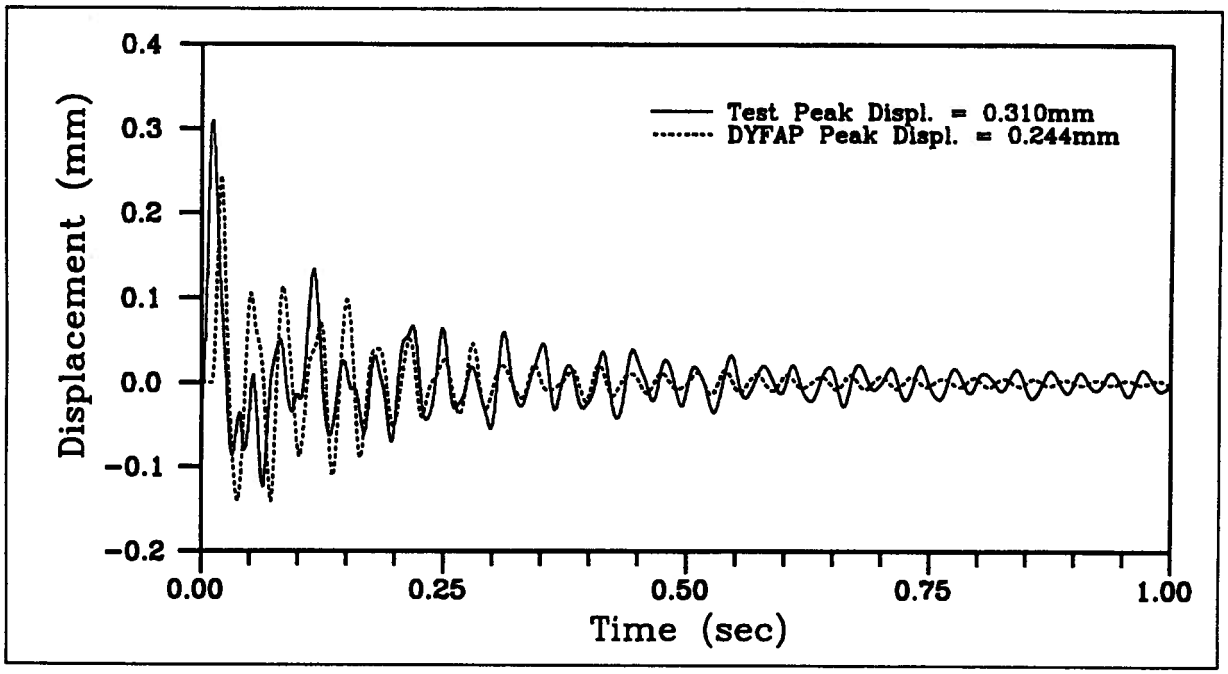

Figure 7.4: Comparison of the I–Joist floor's test and DYFAP's response to a hammer impact

closely over the entire range of frequencies but the DYFAP output does recognize the more important, dominant, low test frequencies. This is particularly evident in the case of the I–Joist floor. The strong DYFAP peak at about 30Hz and the smaller ones at 38Hz and 47Hz correspond well with the trends of the test data. Upon comparing the spectra for hammer and bag tests, the DYFAP results were able to show the shift towards the lower frequencies. The softer, longer duration of the bag drop impact allowed the lower frequencies to receive relatively more energy than the higher frequencies. The bag impact did not induce such high amplitude peaks as did the hammer impact. As a result of the lower y–axis bounds, the spectra appear to be not as clear as those from the hammer impacts.

The acceleration records from the bagdrop tests indicate that the assumed floor damping for the two floors were appropriate. The overplots of the DYFAP outputs and test

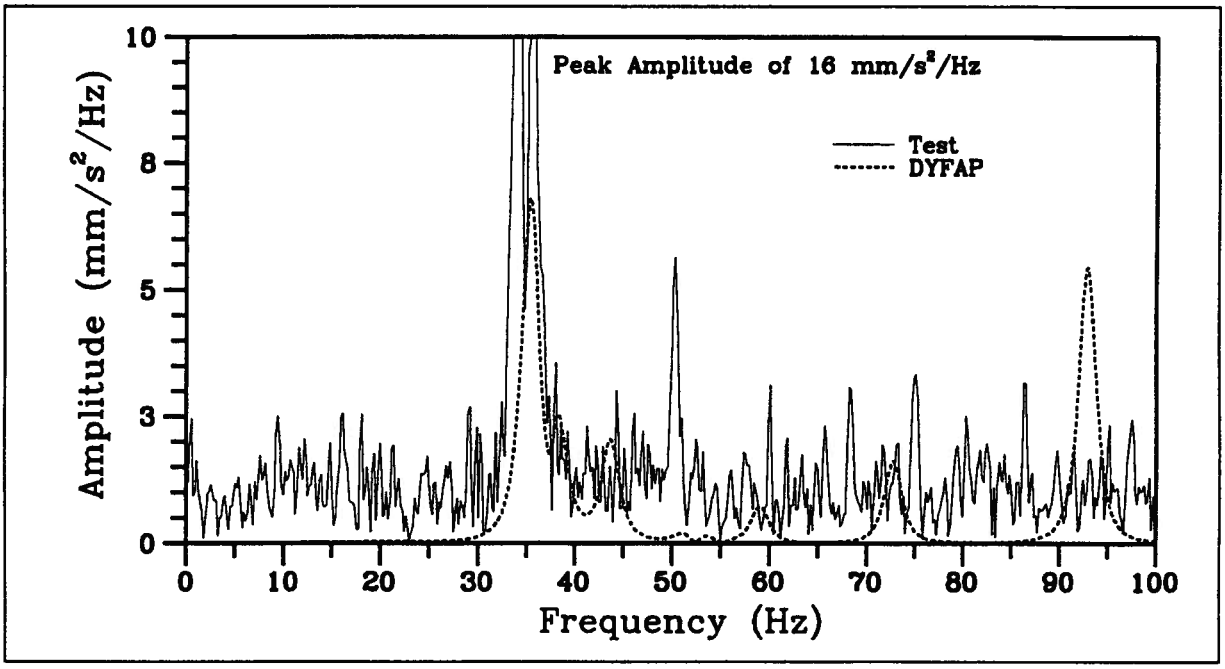

Figure 7.5: Fourier spectrum of the 2x8 floor's acceleration response to a bagdrop impact

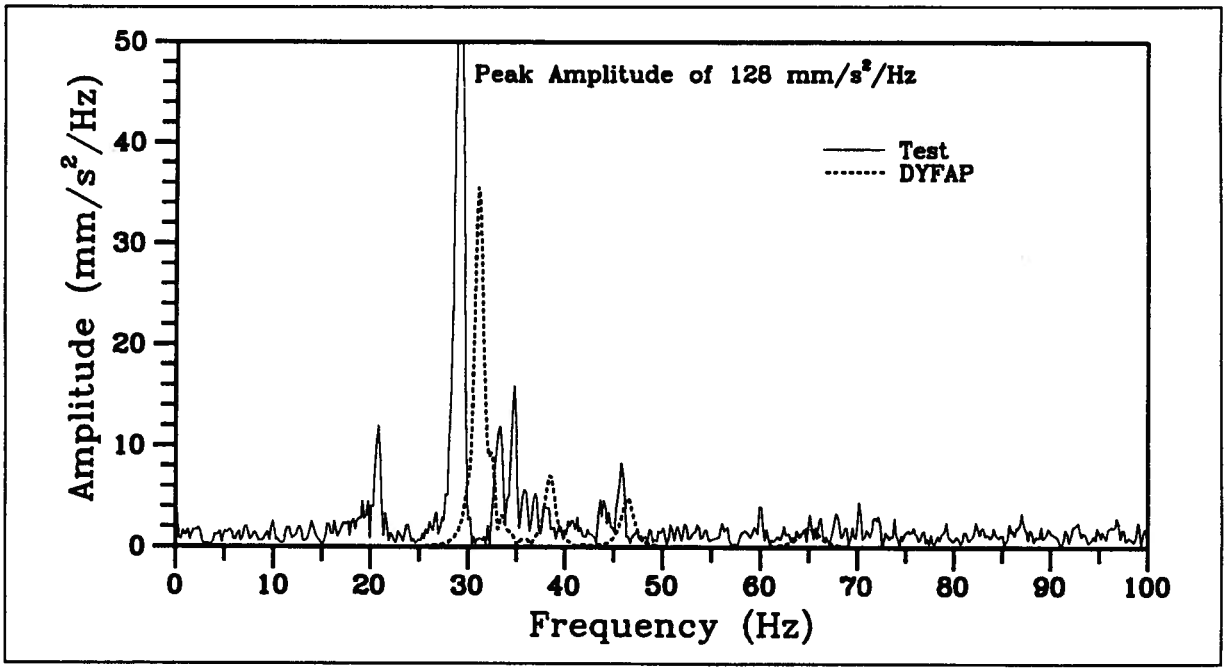

Figure 7.6: Fourier spectrum of the I-Joist floor's acceleration response to a bagdrop impact

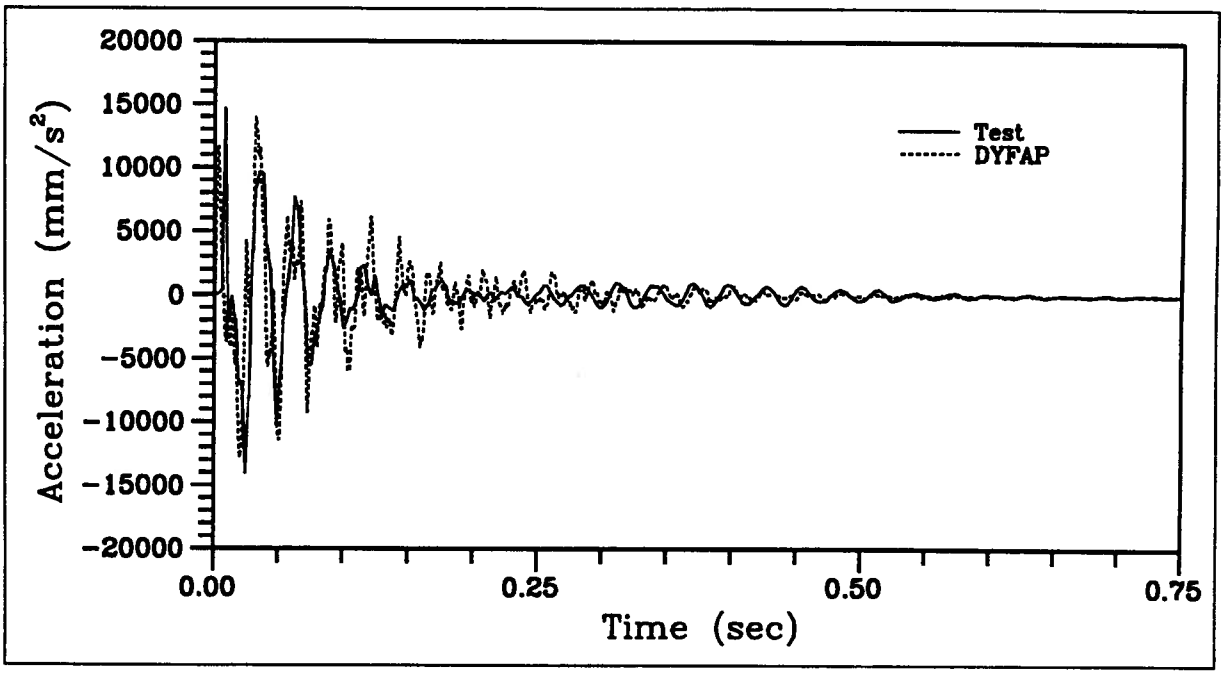

Figure 7.7: The 2x8 floor's acceleration response to a bagdrop impact

data for the 2x8 and I–Joist floors are shown in Fig. 7.7 and Fig. 7.8 respectively. Particularly for the 2x8 floor, the DYFAP trace matched the test's amplitude levels, damping to zero at 0.6 seconds.

The displacement time histories for the bagdrop tests are shown together with the DYFAP results in Fig. 7.9 and Fig. 7.10. The static displacement listed in the figures was caused by the $15lb$ ($66.7N$) sandbag. Once it was dropped it remained upon the floor for the duration of the test.

7.5 Excitation by an Oscillator

The human heel drop involves a very complicated system, namely the human. The mass of the human was a significant percentage of the entire system's mass. Particularly for the 2x8 joist floor, a $200lb$ ($890N$) man represented 29% of the system's total mass.

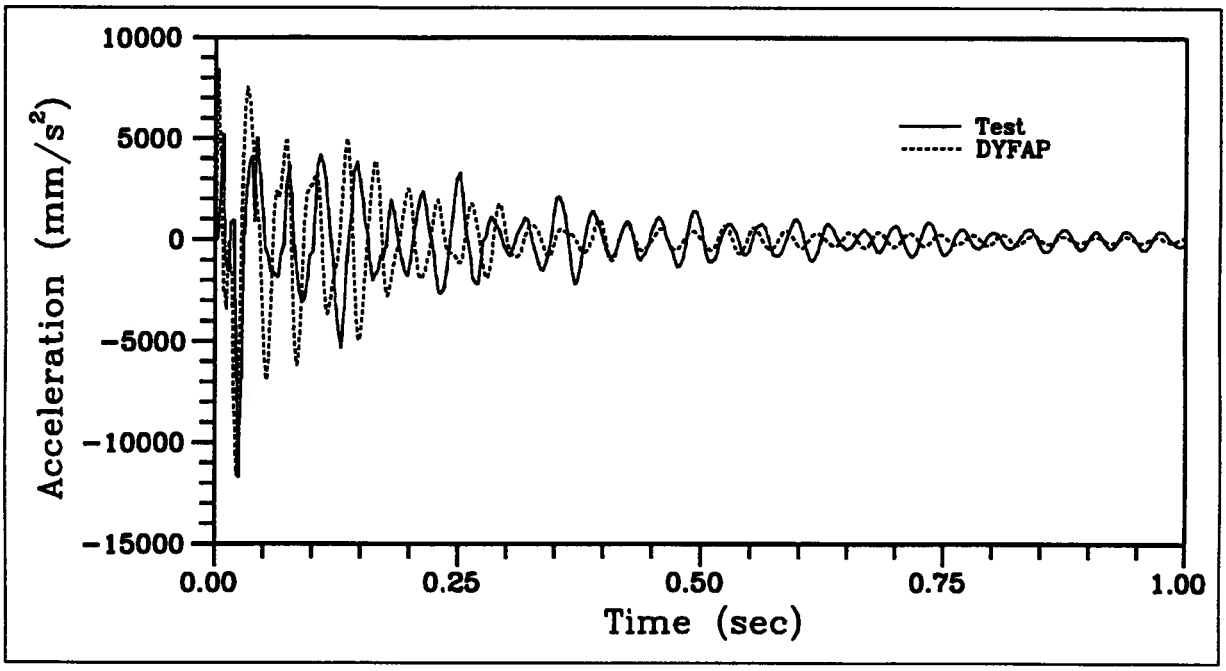

Figure 7.8: The I–Joist floor's acceleration response to a bagdrop impact

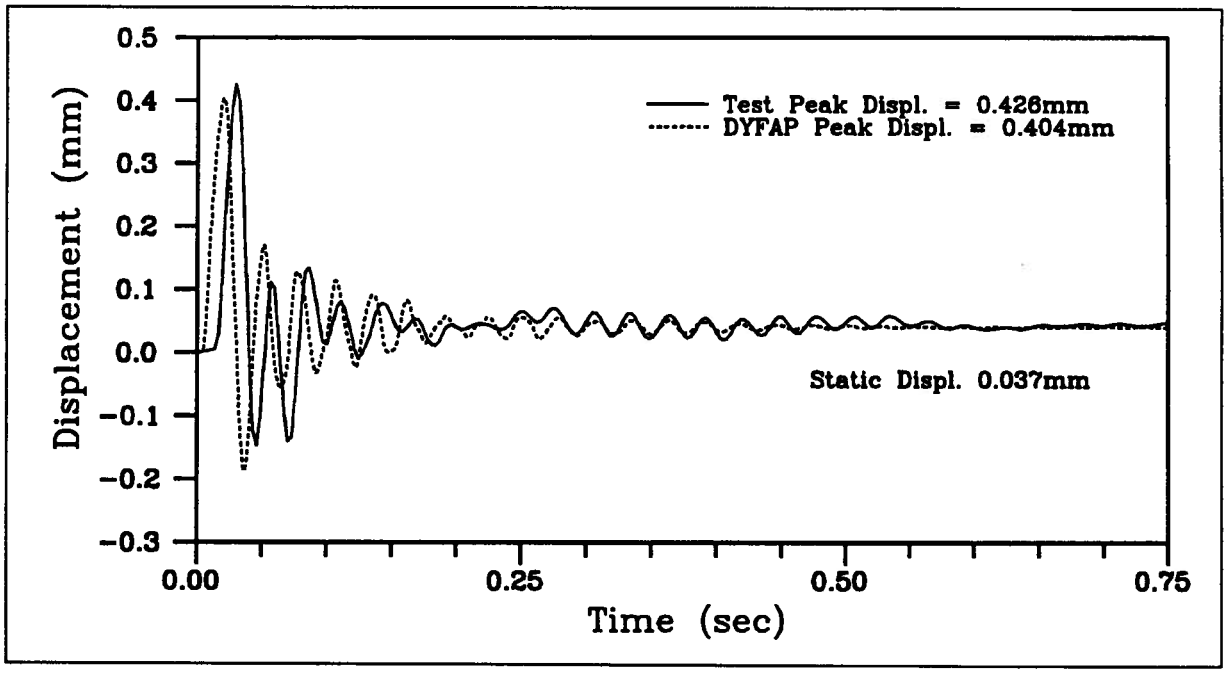

Figure 7.9: The 2x8 floor's displacement response to a bagdrop impact

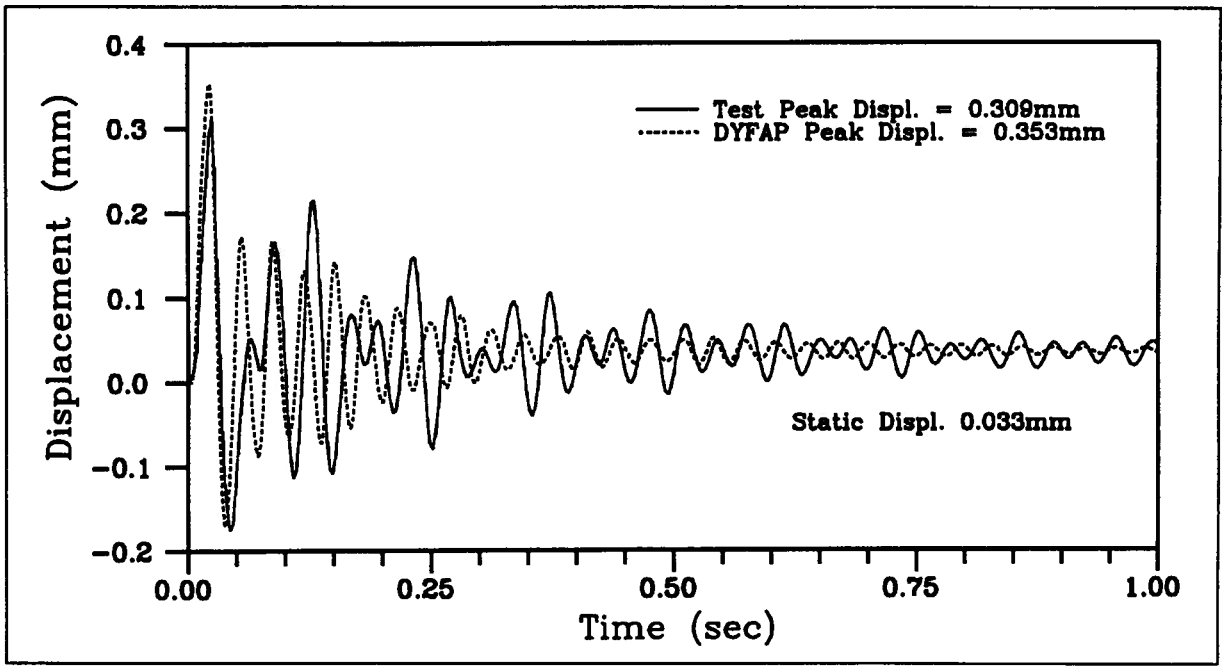

Figure 7.10: The I–Joist floor's displacement response to a bagdrop impact

It can be assumed that as this percentage rises, the influence of the occupant upon the floor's response also increases. An oscillator consisting of viscous dashpots, elastic springs and lumped masses was used with DYFAP to represent the occupant. To model the heel drop action an initial velocity equal to $\sqrt{2gh}$ was assigned to the oscillator's masses to simulate their fall to the floor. DYFAP doesn't allow the oscillator to lose contact with the floor surface.

7.5.1 DYFAP Results using the ISO Model

The ISO, International Standards Organization, have adopted a lumped parameter vibratory model for deriving the driving point impedance of the human body in a standing position [ISO 5982]. This is a simple two DOF model that was proposed by Coermann and is illustrated in Fig. 7.11 [Folz and Foschi, 1991]. Listed in Table 7.1 are the values

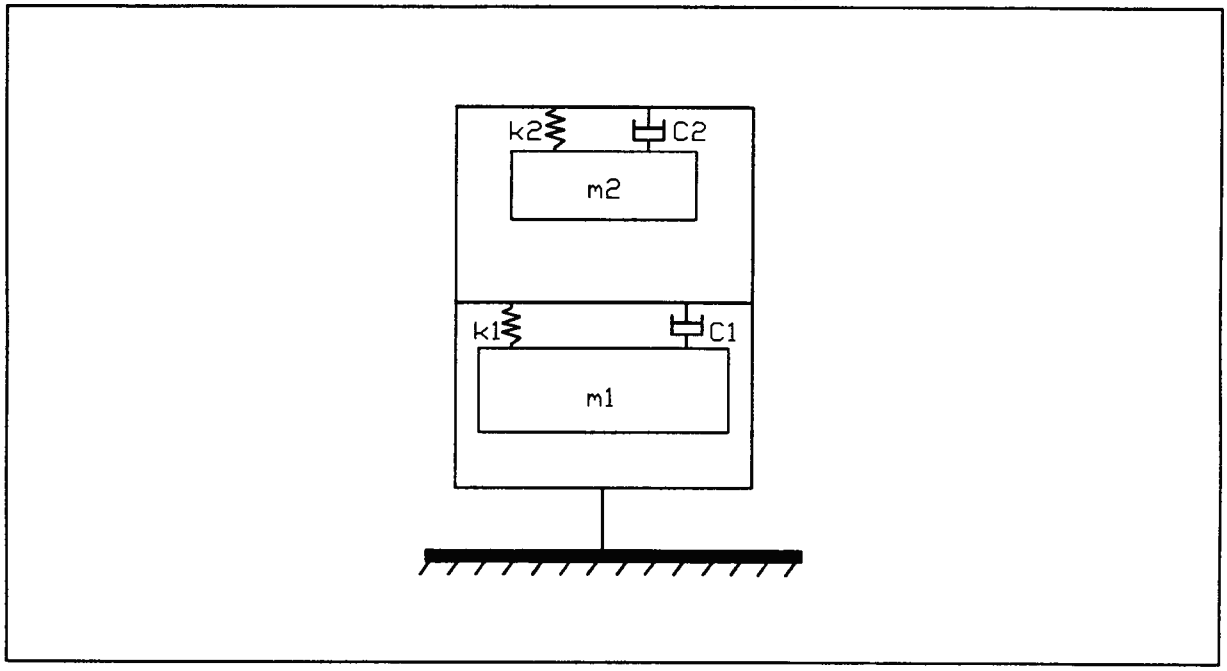

Figure 7.11: ISO, idealized lumped parameter vibratory human model

for the oscillator's lumped masses, linear springs and viscous dashpots.

DYFAP runs were done using the ISO model to assess how the output compared with the heel drop data. Although the ISO model has less mass than the test subject, displacements and damping ought to still give an indication of how well DYFAP and the ISO model work together.

The experimental results showed a significant response in the lower frequency range.

Table 7.1: Parameter values for ISO human model

Element	*Mass (kg)*	*Stiffness (N/mm)*	*Damping (Ns/mm)*
1	62.0	62.0	1.46
2	13.0	80.0	0.93

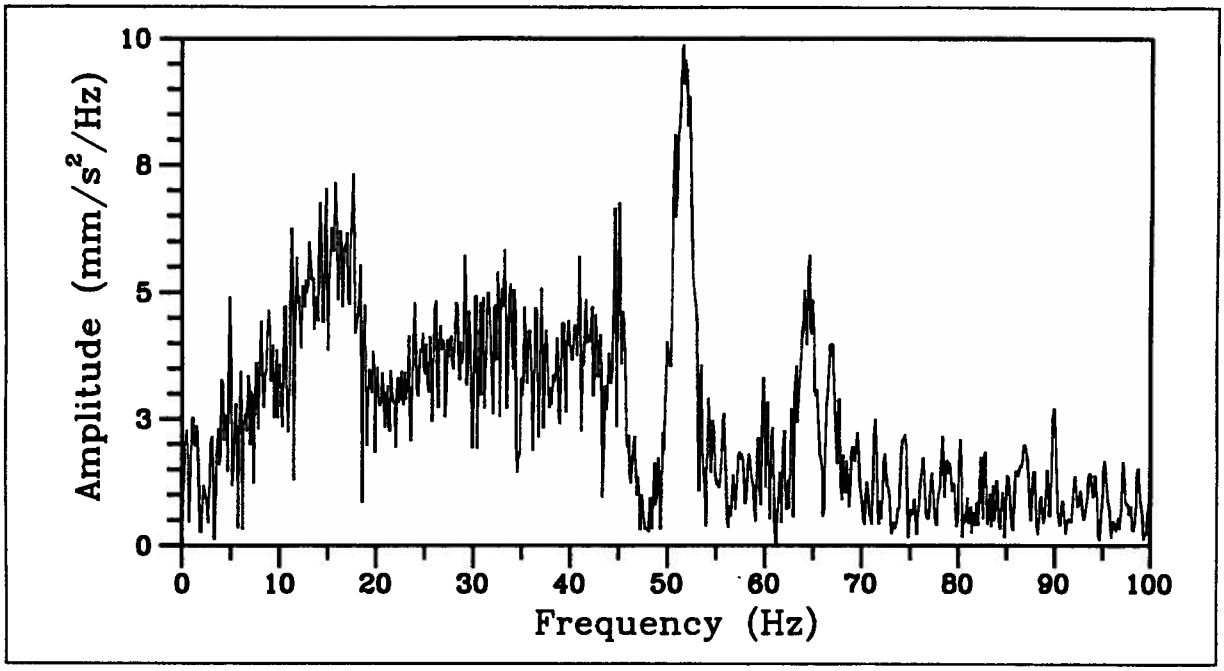

Figure 7.12: Fourier spectrum of the 2x8 floor's test response to a heel drop

The Fourier spectra of Fig. 7.12 and Fig. 7.13 show the magnitude of the human's influence when compared to the corresponding bagdrop spectra of Fig. 7.5 and Fig. 7.6. It is difficult to identify individual frequencies that belong to the human but peaks, or significant trends at 4.75Hz, $8-9$Hz, $11-12$Hz, and $16-19$Hz may be attributed to the human for they appear in both floor's responses. The large peak at 19Hz may indicate a slightly stiffer human response on the I-Joist floor when compared to the $16-17$Hz activity for the 2x8 joist floor. The ISO will contribute frequencies of 5.03Hz and 12.49Hz to the system's response. As mentioned on page 66, filtering of the test's velocity and displacement traces was required to satisfy the zeroed boundary conditions. The heel drop data required filtering up to $2-3$Hz but this was still well below any expected frequencies to be associated with the human or the floor.

DYFAP displacement time histories using the ISO model were produced for each

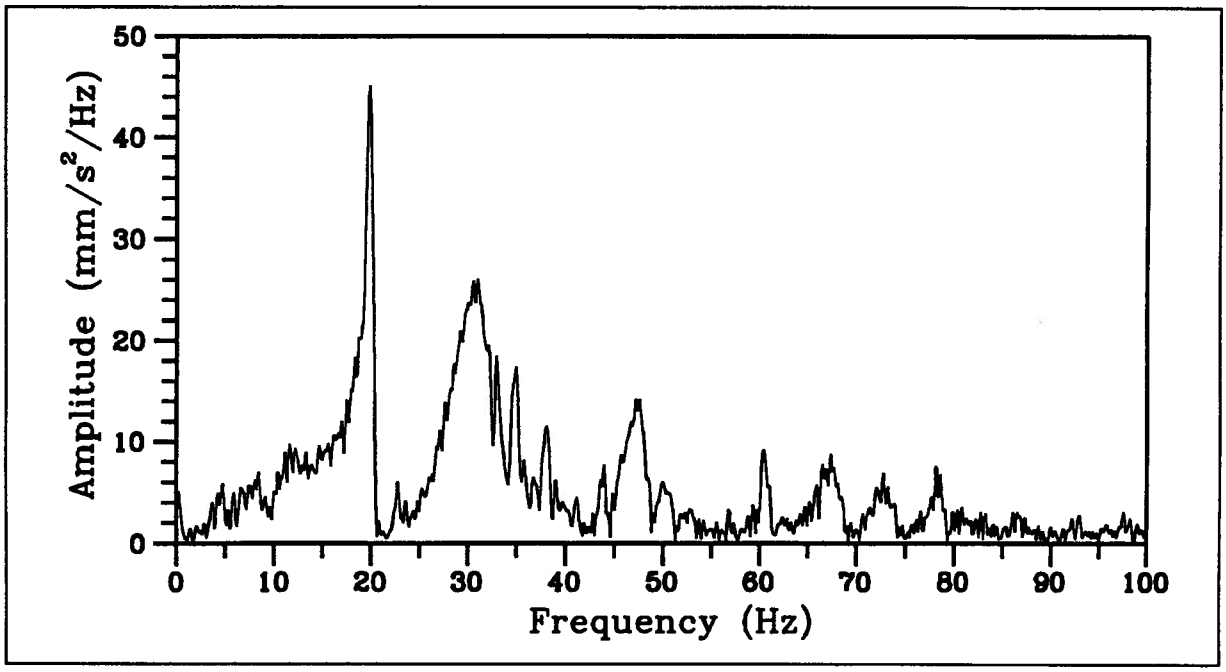

Figure 7.13: Fourier spectrum of the I–Joist floor's test response to a heel drop

floor. As shown in Fig 7.14 and Fig 7.15 the ISO results compared well with the test data. The damping appears to be at about the proper level and the trace is appropriately dominated by the low frequencies of the oscillator. The peak displacements are somewhat high but this is due to the high stiffness of the model. They are still in better agreement with the tests than the forcing function of Fig. 4.7. The forcing function failed to induce appropriate peak displacements. The forcing function exceeded the 2x8 and the I–Joist floors' displacements by 86% and 62% respectively. The high frequency oscillations of the forcing function traces also illustrate how poorly a forcing function does in representing a human impulse upon a lightweight floor. Previous research by Foschi and Folz found that the forcing function was adequate for heavy floors but that it was likely that as the occupants' mass became significant it would be necessary to replace the forcing function with an oscillator [Folz and Foschi, 1991]. Fig. 7.16 illustrates how the ISO oscillator and

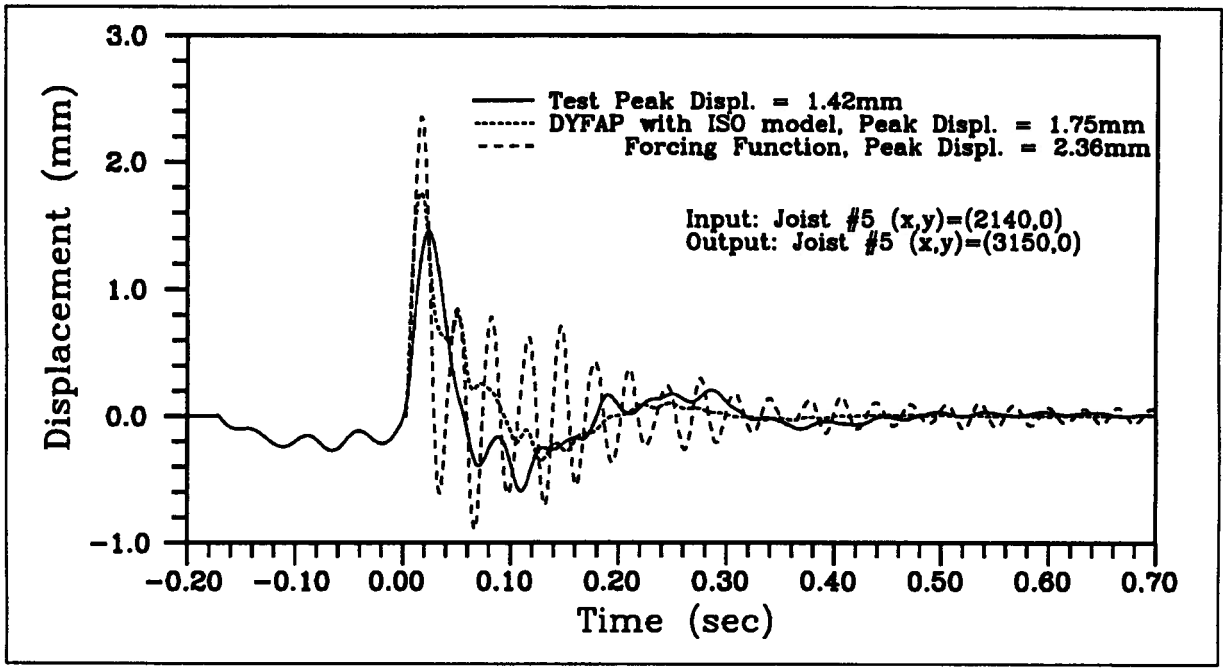

Figure 7.14: Comparison of the I-Joist floor's response to a heel drop with DYFAP's results using the ISO model or a forcing function, IJF6-2

the forcing function produced equivalent responses in the case of a heavy floor. Even though Fig. 7.16 does not include a comparison with a test trace, the fact that the oscillator and forcing function traces are very different for the lightweight floors indicate that the method of excitation does become important as the occupants' mass percentage increases.

The ISO model was shown to be appropriate but it required six input parameters. It was not clear whether the two DOF model was necessary in order for DYFAP to produce accurate results. The ISO model's second frequency was not close to the frequency range of interest, therefore a single degree of freedom model may be sufficient. A single DOF model would be preferable since tuning the ISO model would involve adjusting up to six parameters whereas a single DOF model would require only two since the mass would be well known.

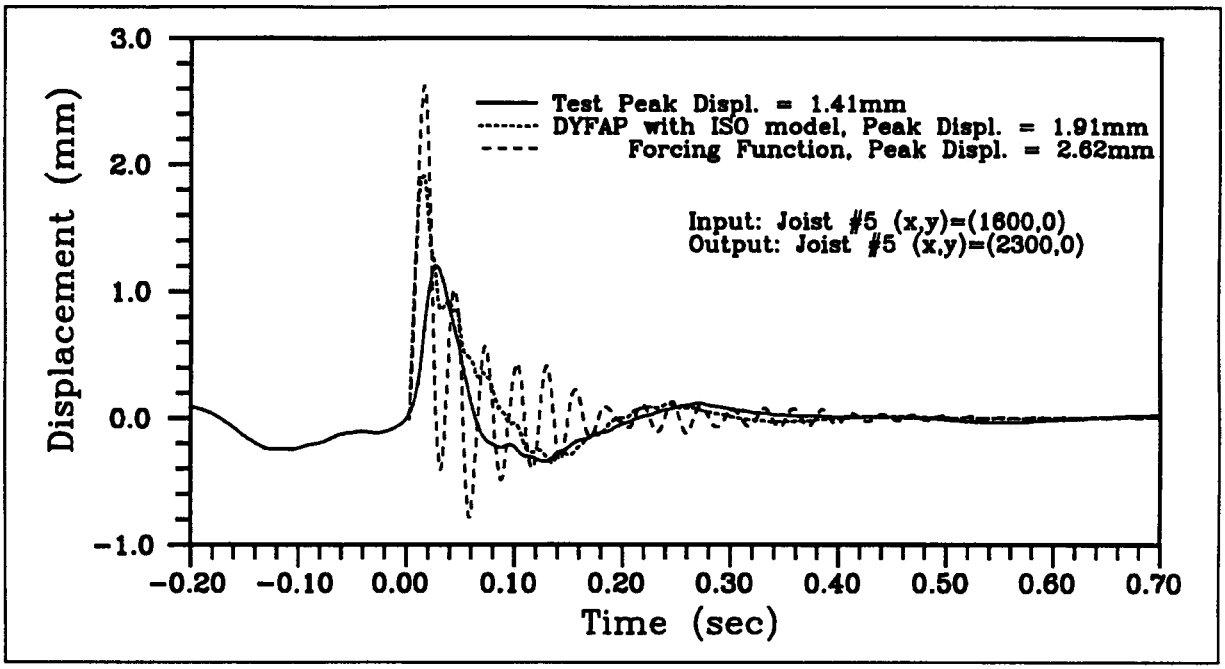

Figure 7.15: Comparison of the 2x8 floor's response to a heel drop with DYFAP's results using the ISO model or a forcing function, SLF6-2

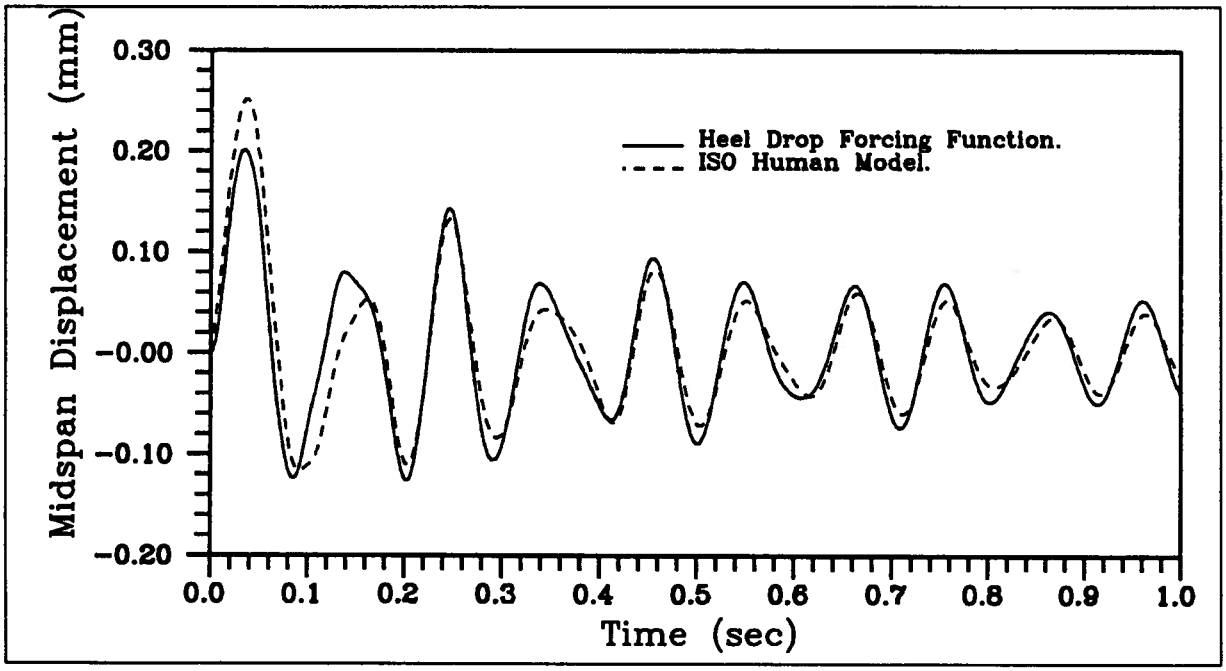

Figure 7.16: Displacement time histories for composite floor (2% damping)

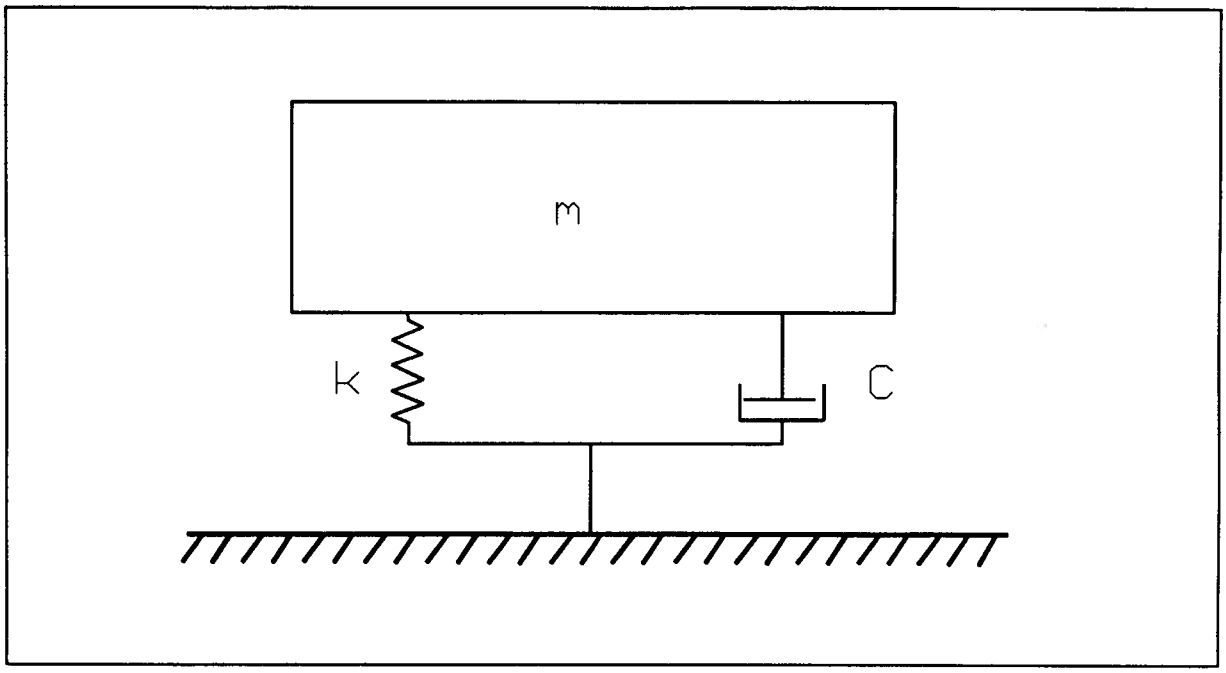

Figure 7.17: Single degree of freedom model

7.5.2 Modelling a Heel Drop with a Single Mass Oscillator

Since the floor parameters were set, only the oscillator parameters, mass, stiffness and damping were available for any adjustments in an attempt to match the DYFAP output with the experimental heel drop data. The single DOF oscillator is shown in Fig. 7.17. The mass need not be changed since the mass of the heel dropper was a well known parameter. The stiffness and damping were unknowns.

DYFAP runs were done for a number of stiffness and damping combinations. A calibration of the model was attempted using the 2x8 joist floor. The I–Joist floor would later be used to verify the applicability of the model. The acceleration time histories were not sensitive enough to changes in the oscillator parameters. DYFAP's difficulty with high accelerations when using the oscillator as an exciter overshadowed any influence that the oscillator parameters may have had. Damping has a larger influence than usual

Table 7.2: Grid of model parameters for oscillator calibration

Stiffness (N/mm)	*Viscous Damping (Ns/mm)*			
	.75	1.25	1.5	1.75
20		x		
40		x	x	
60	x	x		x
80		x		
100		x		

upon the response in the case of the DYFAP model because of how it models the heel drop action. The contribution to acceleration from the damping term in the equations of motion are quite substantial. The initial velocity that is given to the oscillator results in a high acceleration since the floor's response to this initial velocity is quite rigid. Rather than allowing some local deformation, the model forces a large portion of the floor to move immediately with an initial velocity.

The displacement time histories were much better behaved. The peak displacement, damping and the dominant period were used as keys for the calibration. Table 7.2 shows the grid of model parameters that were investigated. The results of these runs are shown in Fig. 7.19 and Fig. 7.18.

Upon comparing the plots of Fig. 7.18 one can note that as the model's stiffness increased so did the amplitude of the floor's oscillations. A stiffer model induced higher accelerations thus larger deflections. Similarly the plots of varying damping in Fig. 7.19 show increased oscillatory motion for higher damping. A highly damped oscillator will induce high accelerations just as the stiff model did. Damping and stiffness had the same effect upon the floor's peak displacements. This was quite evident when comparing their Fourier spectra. The amplitude of the oscillator's frequency became extremely large as

the viscous damping or stiffness was increased. The combination of $k = 40N/mm$ and $C = 1.25Ns/mm$ did the best at controlling the peak displacement without inducing too much oscillatory motion. For the I–Joist floor, in order to achieve better agreement with the test's peak displacement, a slightly stiffer model, $k = 60N/mm$, was required. It is known that the human body can adjust its stiffness by changing the degree of muscle tension. As previously proposed on page. 74 the "bouncier" I–Joist floor may have solicited a stiffer response from the human tester.

7.5.3 DYFAP Results using the Calibrated Single DOF Model

As with the bagdrop tests the following comparisons for the heel drop tests were made from the midfloor impact location #6. The Fourier spectra and the displacement traces for the cases in which the accelerometer was located on the same joist and two joists away from the impact site were used to compare with the DYFAP results.

The displacement traces for both floors were compared with DYFAP results using either the oscillator or a forcing function. The three traces are plotted together in Fig. 7.20 and Fig. 7.21. The time scale is labelled such that time= 0.0 marks the time of the heel's impact. The leading time of $0.16 - 0.17$ seconds corresponds to the time required for the heel dropper to shift his weight over to his heels. Starting from time= 0.0 the traces are plotted for 0.70 seconds.

The oscillator's response does a very good job with peak displacements but also in matching the general low frequency nature of the trace.

The displacement record derived from the floor's response to the heel drop impact two joists away are shown in Fig. 7.22 and Fig. 7.23. As expected the displacement amplitudes have decreased substantially. The test traces now show more influence from the floor's natural frequencies. DYFAP did well in predicting an appropriately low peak displacement. DYFAP introduced too much response participation of the floor's frequencies,

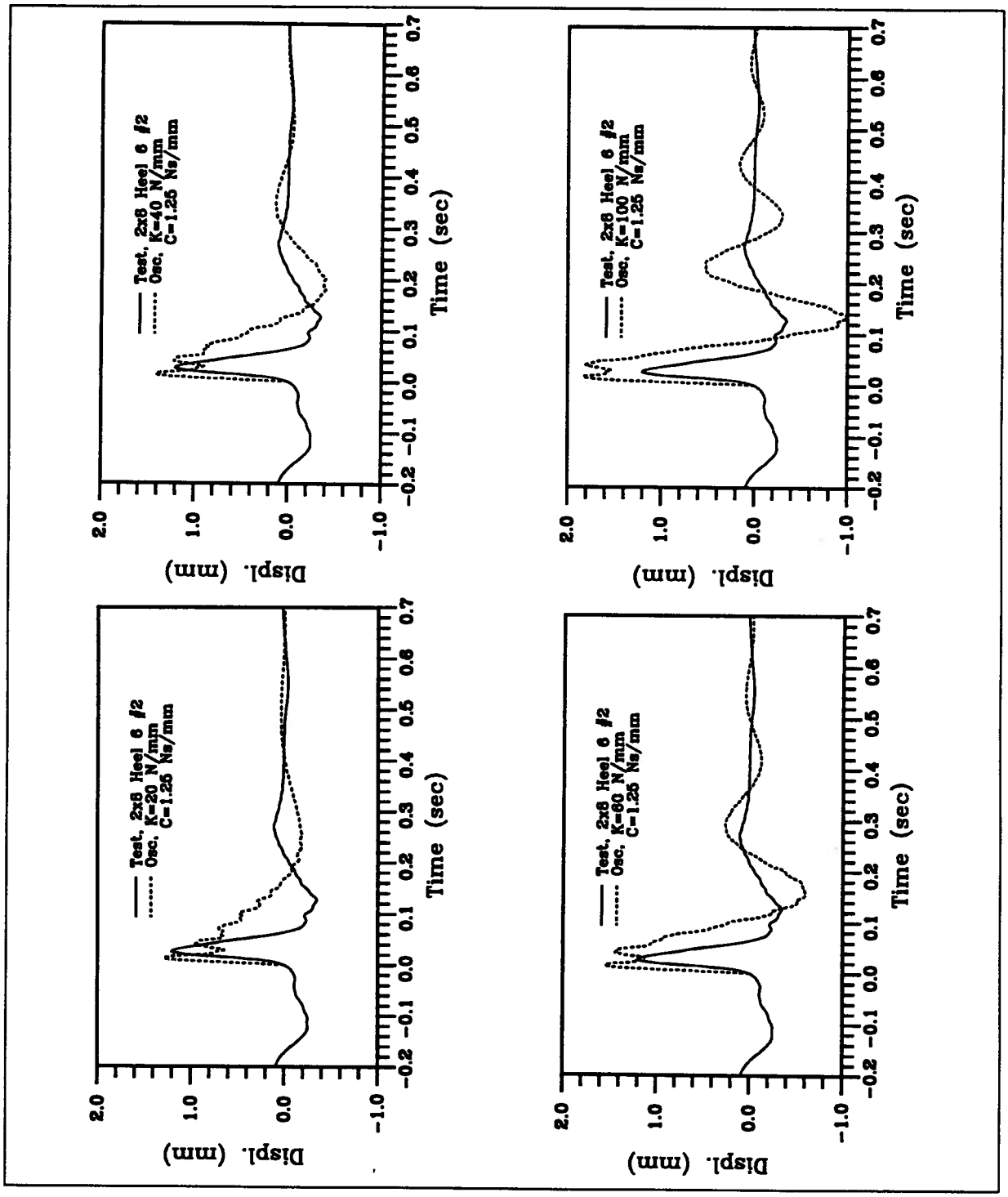

Figure 7.18: Influence of varying the stiffness of the oscillator

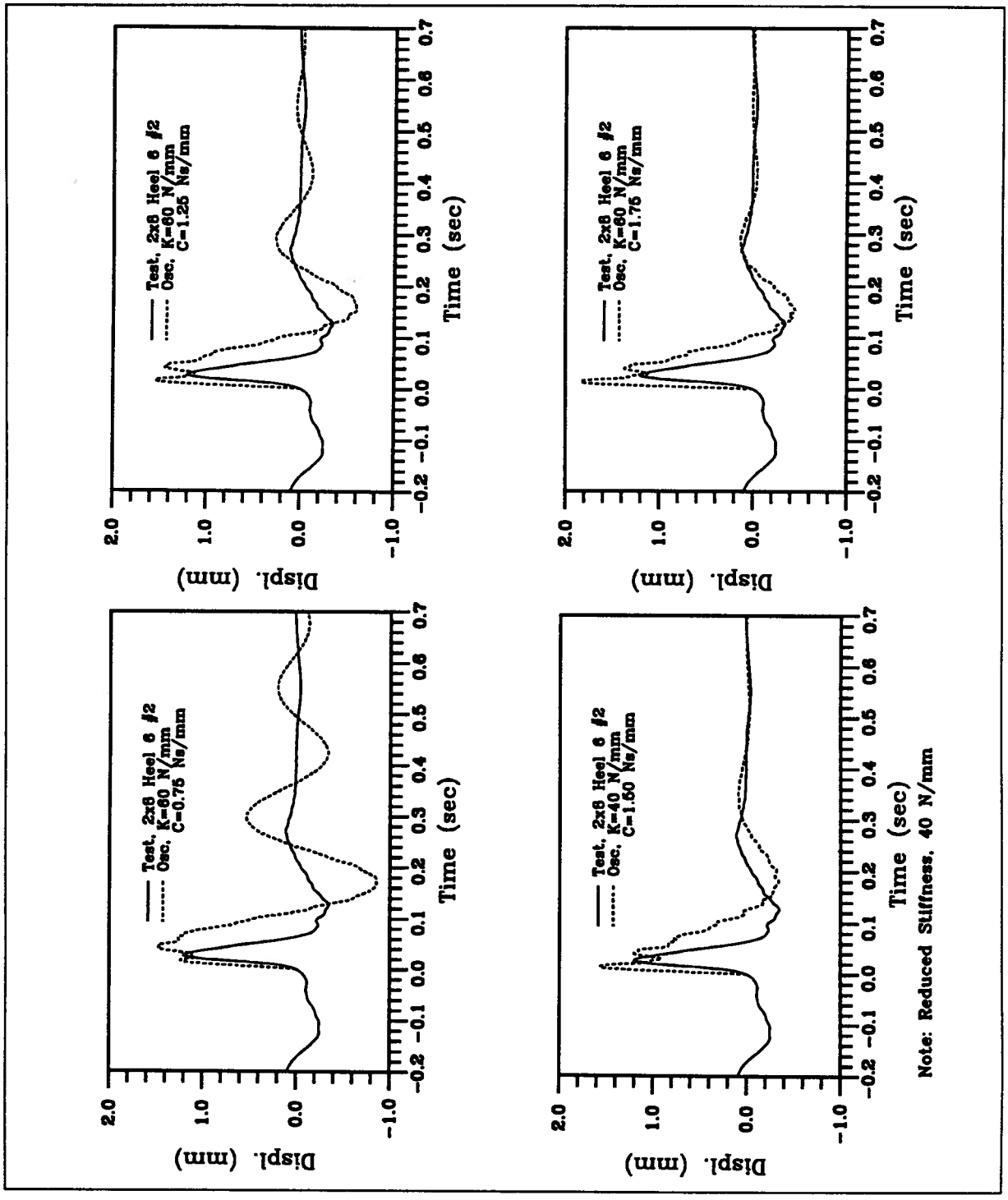

Figure 7.19: Influence of varying the viscous damping of the oscillator

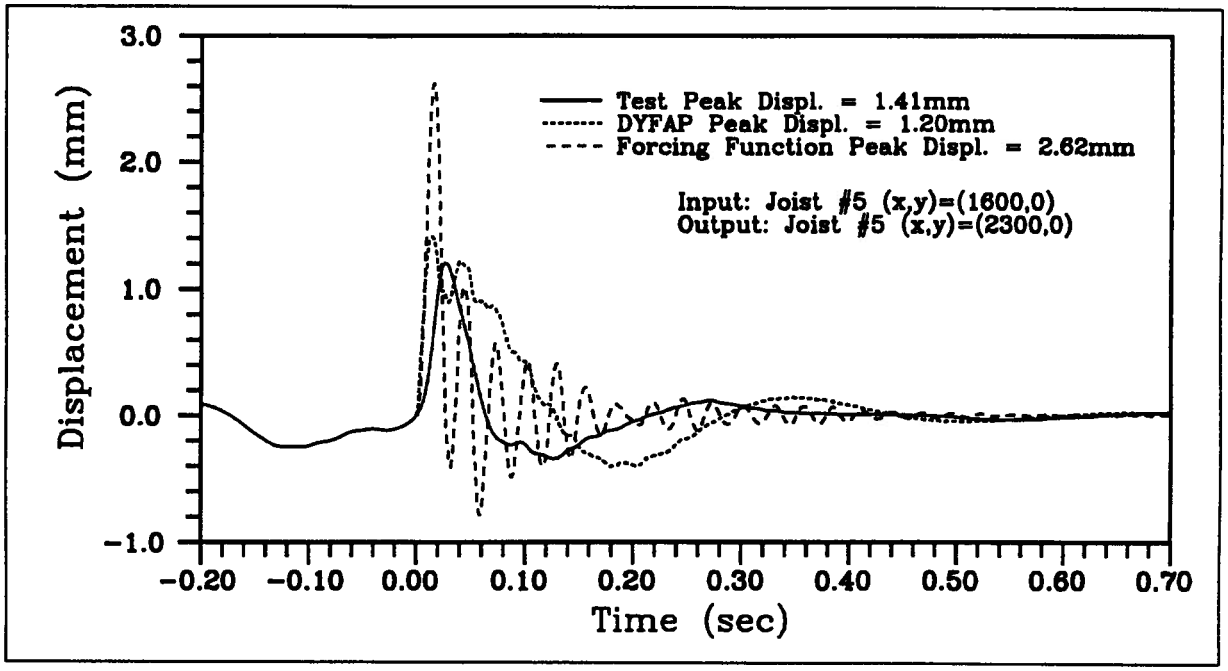

Figure 7.20: Comparison of the 2x8 floor's response to a heel drop with DYFAP's results using the 1 DOF model or a forcing function, SLF6-1

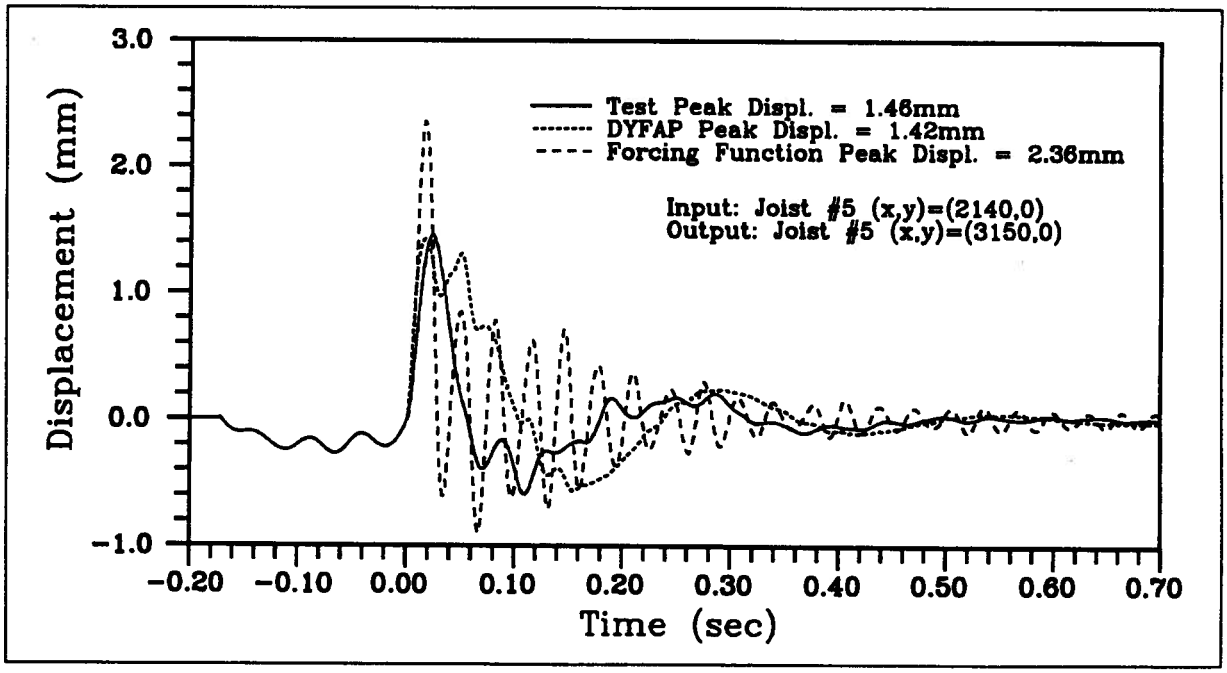

Figure 7.21: Comparison of the I-Joist floor's response to a heel drop with DYFAP's results using the 1 DOF model or a forcing function, IJF6-2

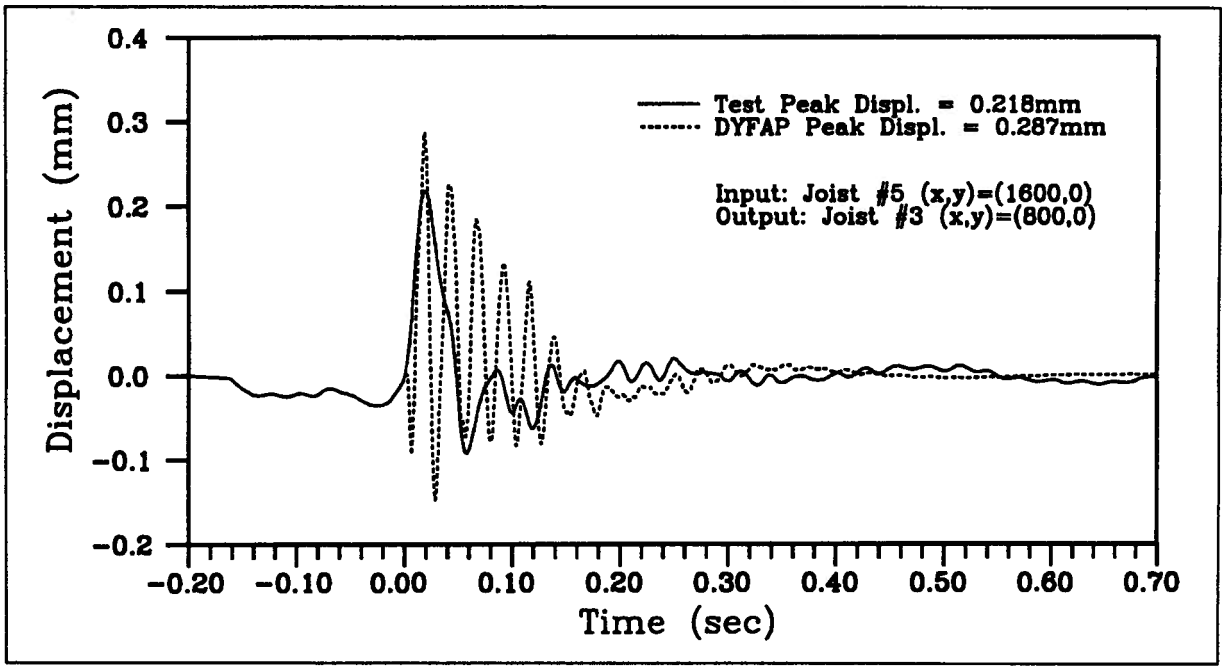

Figure 7.22: The 2x8 floor's response two joists away from the heel drop, SLF6-1

which is particularly evident for the 2x8 joist floor in Fig. 7.22.

7.5.4 Comparison of Results for the Case of Two Occupants

Up to this point all comparisons had been made for the case of only one occupant. Generally, a vibration is reported to be annoying for a passive occupant rather than the active occupant. The goal of any design criteria or the tolerance charts of Chapter 1 is to satisfy the passive occupant.

The test series #4 dealt with the case of an observer standing on the same joist or on the joist adjacent to the heel dropper. As shown by Figs. 7.24–7.27, the location of the observer relative to the heel dropper affected the output. DYFAP did well in matching the tests' peak displacements regardless of where the observer was located. The oscillators used for each floor were the same ones that were derived previously

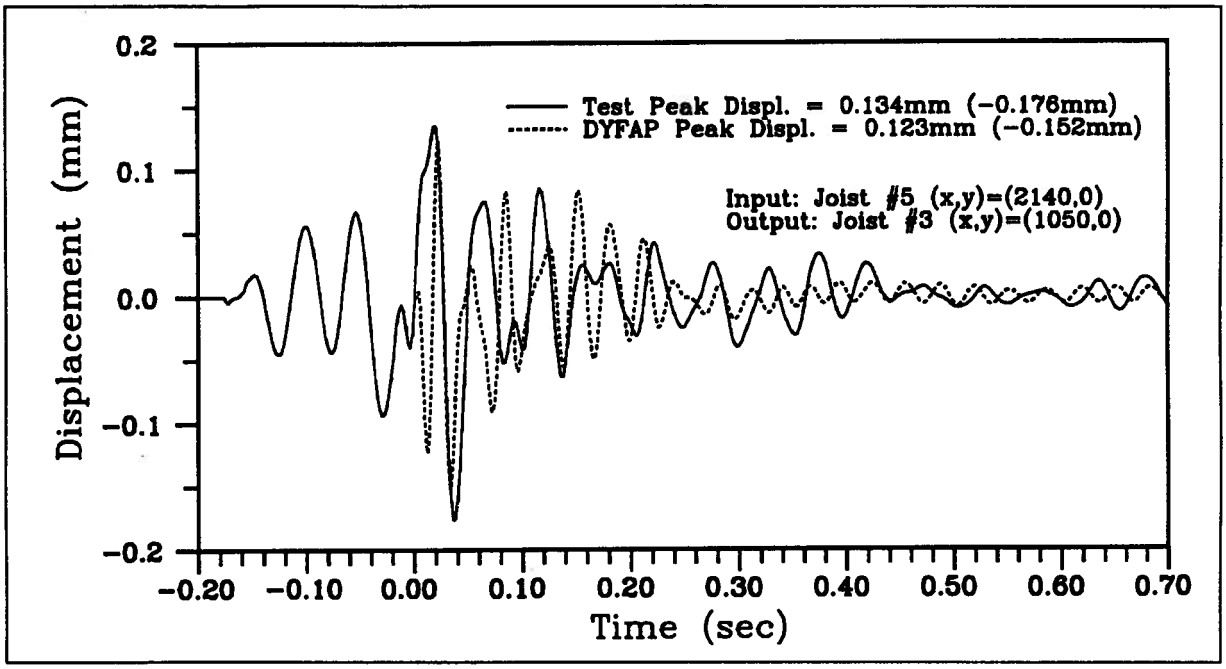

Figure 7.23: The I-Joist floor's response two joists away from the heel drop, IJF6-1

(see pg. 78).

Lastly, to relate this data with the subjective rating schemes of Wiss and Parmalee and Chui, the displacement-frequency and the RMS accelerations were calculated. Fig. 7.28 shows the test results plotted on the Wiss and Parmalee scale. The four data points correspond to a passive occupant standing on the same or adjacent joist relative to the heel dropper for each floor. Both floors received appropriate ratings of "strongly perceptible". The RMS accelerations for the plot of Fig. 7.29 were calculated from frequency weighted acceleration traces as recommended by the ISO [ISO 2631]. The frequency weighting that was followed is listed in Table 7.3. The ISO guidelines do not specify a weighting factor for frequencies greater than 80Hz due to lack of test data. Three of the four tests produced RMS values that were greater than Chui's recommended value of $0.375m/s^2$ for a satisfactory floor. The I-Joist floor was noticeably "bouncier"

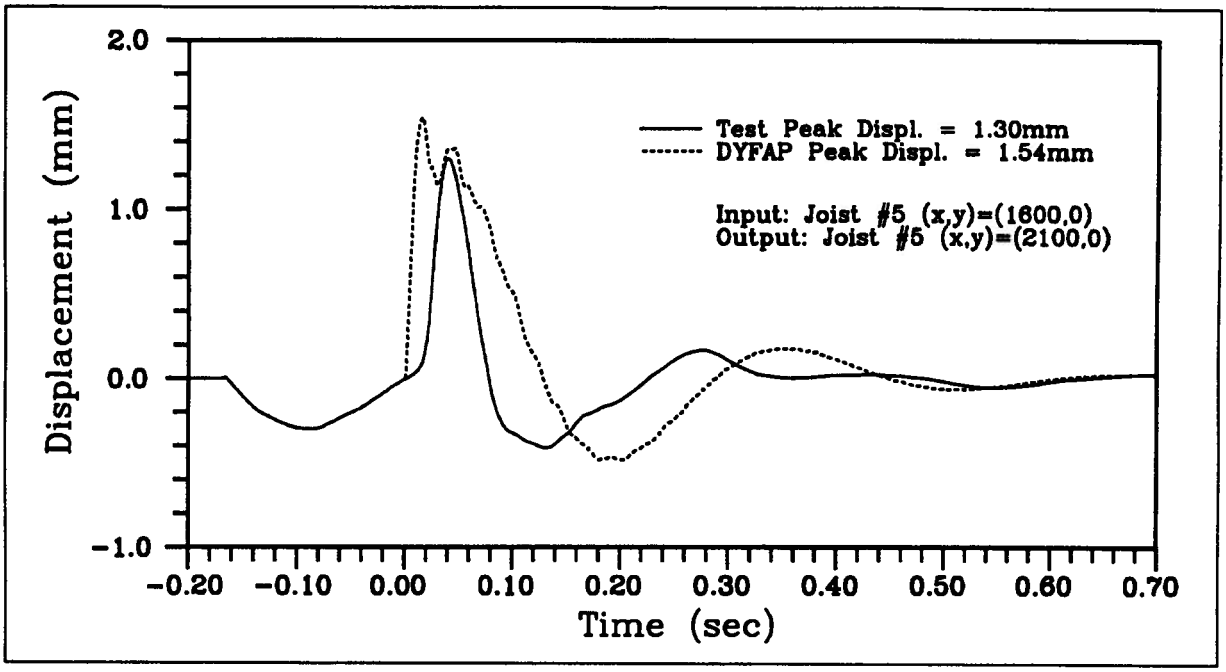

Figure 7.24: Comparison of DYFAP with the 1 DOF model and the test data for the case of a passive observer located on the same joist as the heel dropper, 2x8 floor

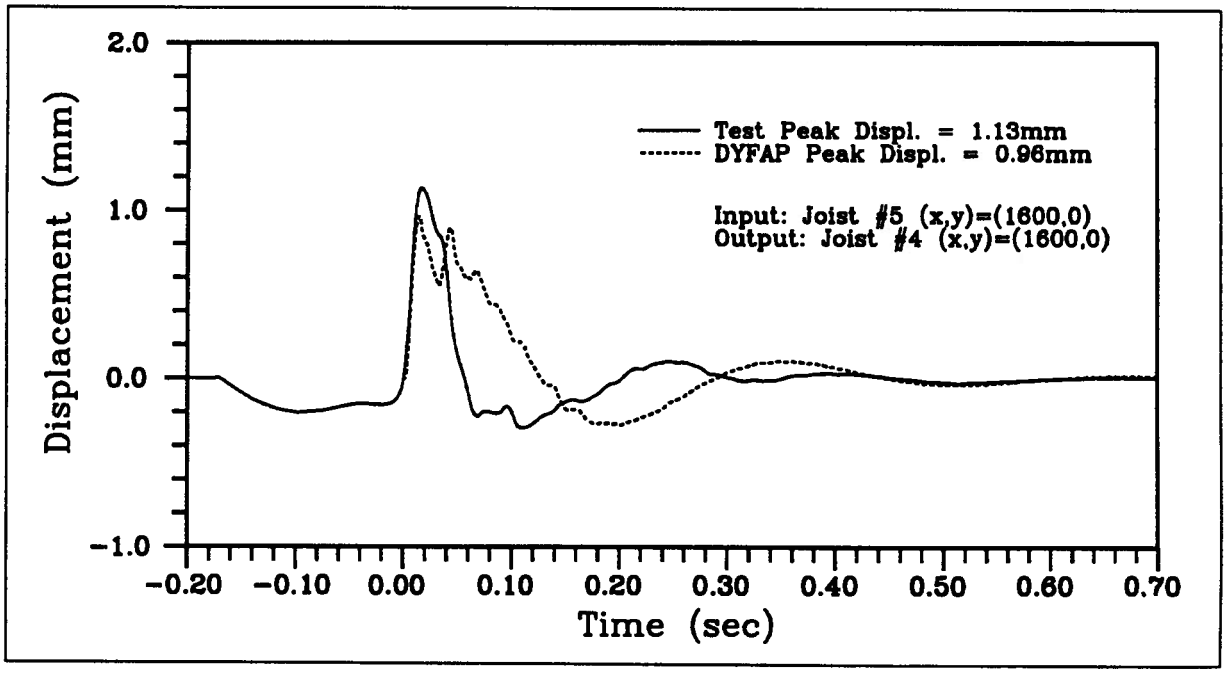

Figure 7.25: Comparison of DYFAP with the 1 DOF model and the test data for the case of a passive observer located on a joist adjacent to the heel dropper, 2x8 floor

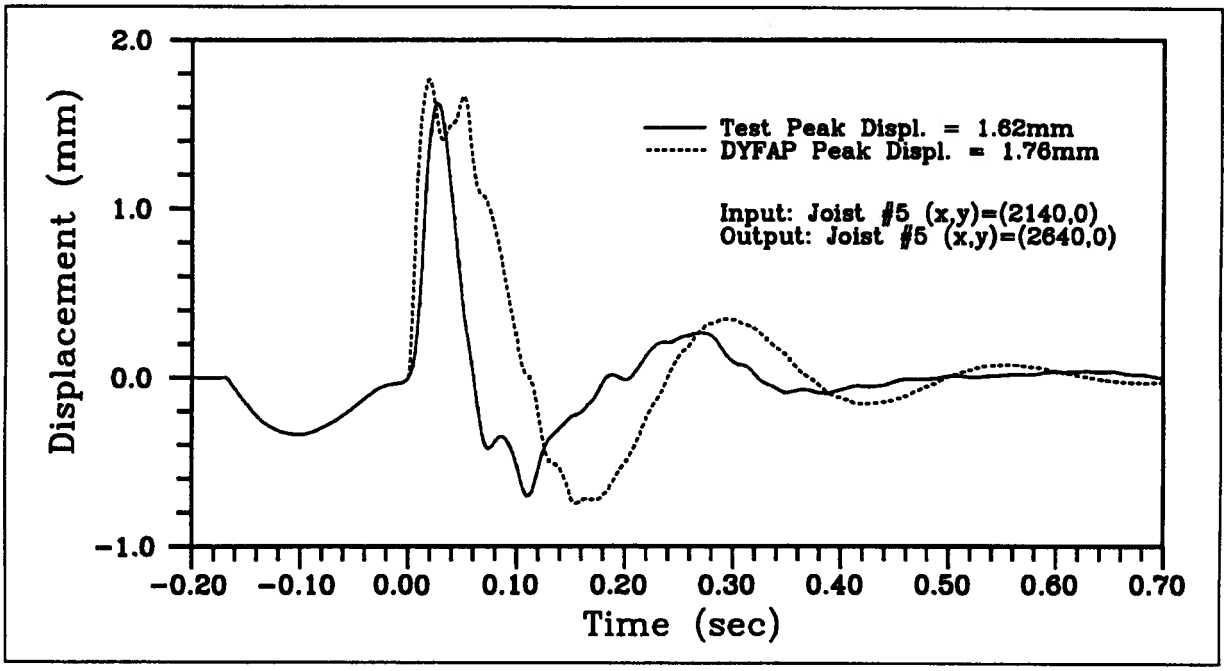

Figure 7.26: Comparison of DYFAP with the 1 DOF model and the test data for the case of a passive observer located on the same joist as the heel dropper, I-Joist floor

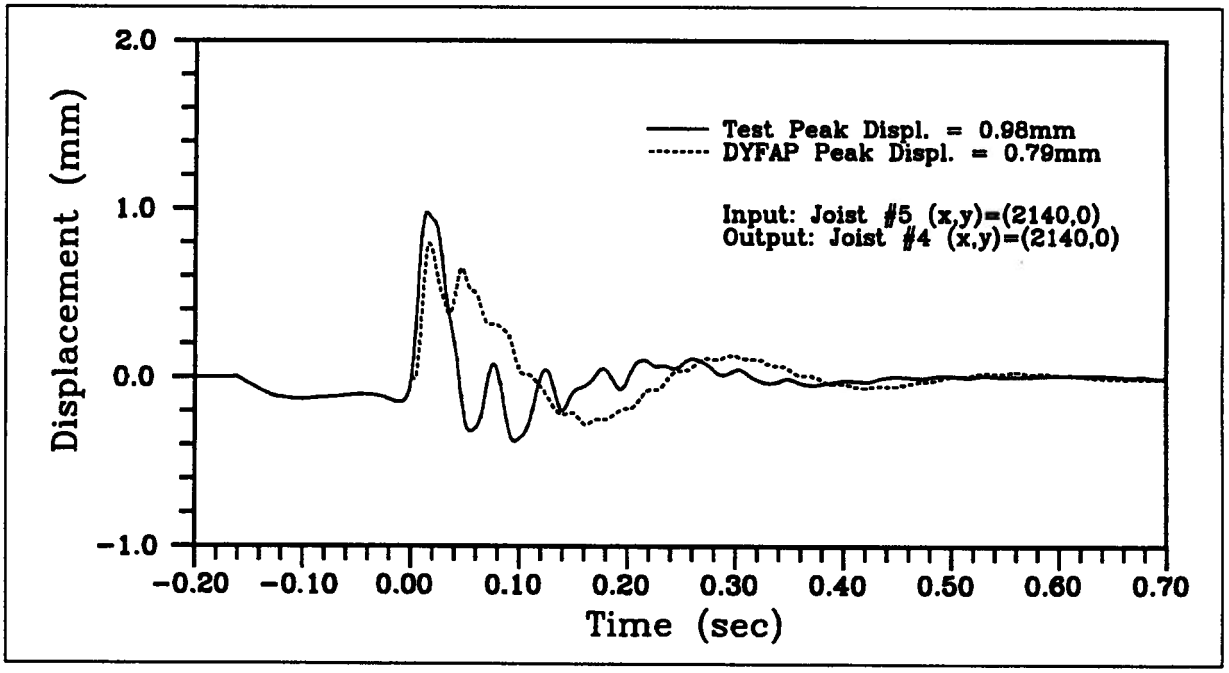

Figure 7.27: Comparison of DYFAP with the 1 DOF model and the test data for the case of a passive observer located on a joist adjacent to the heel dropper, I-Joist floor

Table 7.3: Frequency weighting factors used for calculation of RMS acceleration

Freq. Range	Weighting Factor
0Hz< f_0 <4Hz	$f_0/3$
4Hz< f_0 <8Hz	1
8Hz< f_0 <80Hz	$8/f_0$
80Hz< f_0 <500Hz	0.1

than the 2x8 joist floor. The RMS plot does illustrate this distinction but the I–Joist floor's values were expected to be somewhat higher.

Based on survey results for living room floors, Onysko has proposed static criteria to ensure satisfactory performance [Onysko, 1986]. The maximum floor system deflection, under a static concentrated load of $1kN$, at the joist's midspan, should be limited by:

$$\delta_max = (6.7/L^1.22)mm for L > 3.0m \tag{7.1}$$

As a final check, since the floors were designed as per the NBC1990, which incorporated a form of Onysko's criteria, the program FAP was used to determine the floors' static deflection under a concentrated load of $1kN$. The criteria limits the 2x8 and I–Joist floors' deflection to $1.69mm$ and $1.16mm$ respectively. The floors were satisfactory when based on FAP's results of $0.90mm$ and $0.83mm$ for the 2x8 and I–Joist floor respectively.

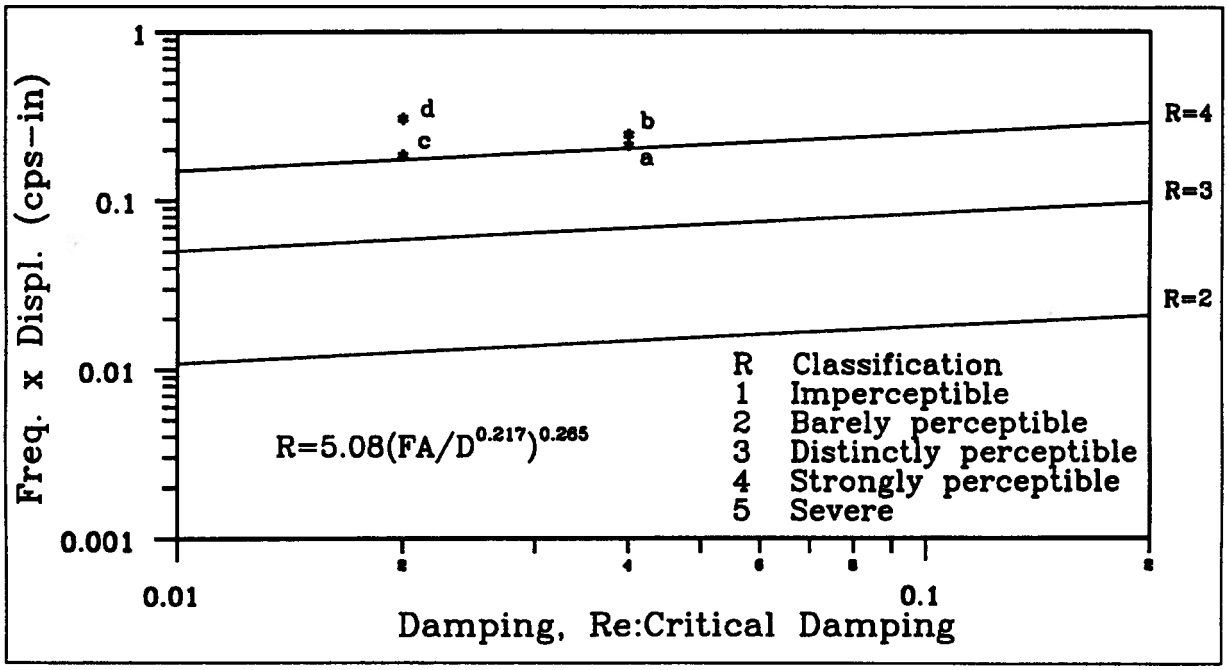

Figure 7.28: Series #4 test data, a:SLN6, b:SLS6, c:IJN6, d:IJS6, plotted on Wiss and Parmalee's mathematical model

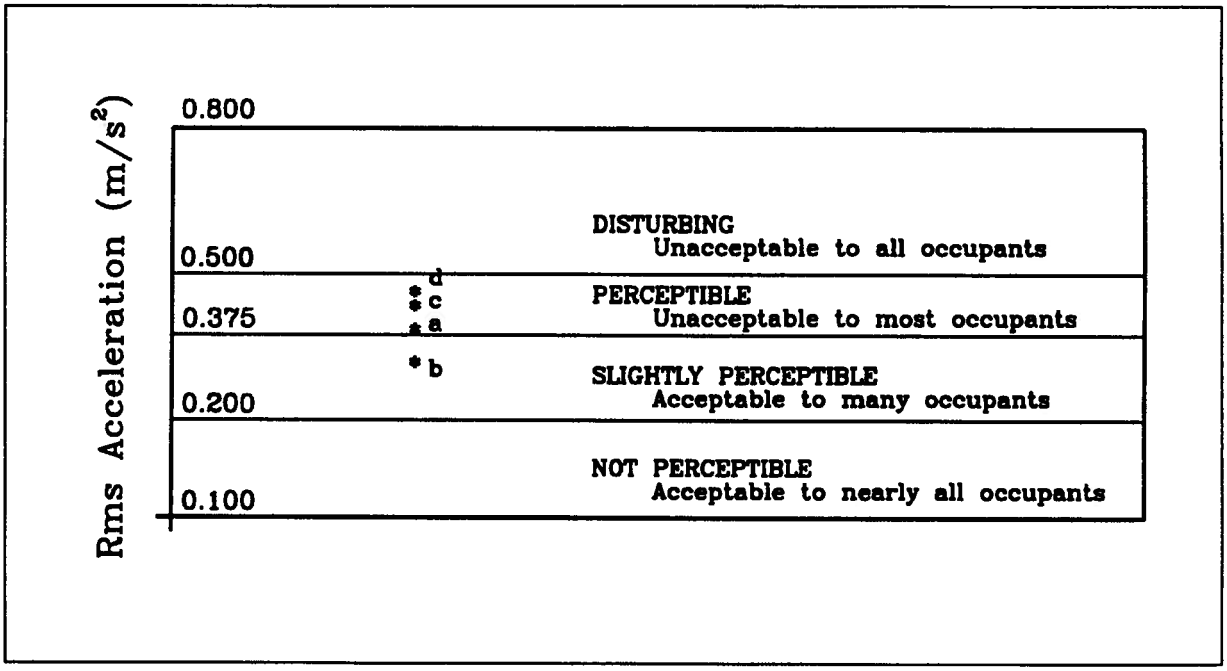

Figure 7.29: Series #4 test data, a:SLN6, b:SLS6, c:IJN6, d:IJS6, plotted on Chui's RMS scale

Chapter 8

Summary and Conclusion

8.1 Summary

Lightweight wooden floors have become prone to poor vibrational performance. The introduction of lighter, longer spanning structural members caused the floor's natural frequencies to draw closer to those that have been shown to disturb occupants. Previous work had been done in evaluating floors by a subjective procedure. People were asked to rate a floor's level of vibration on scales of perception (acceptability).

For this thesis, tests measuring the dynamic response of lightweight wooden floors were conducted for the purpose of determining the applicability of the programs NAFFAP and DYFAP for lightweight floor systems. The floor vibration problem was addressed by analytical modelling of a floor's dynamic response. The floors were impacted by means of a hammer, dropping a sandfilled bag and a human heel drop. These three types of excitation produced data that was useful in verifying and establishing the applicability of the programs NAFFAP and DYFAP.

8.2 Concluding Remarks

NAFFAP's output includes all possible frequencies for the defined floor system. An occupant is generally only aware of vertical motion, so many of the frequencies associated with degrees of freedom such as joist rotation are insignificant. The I–Joist floor, which had a relatively low joist torsional stiffness, produced many such frequencies. The output

for the 2x8 joist floor was relatively clean of these torsional frequencies.

NAFFAP's first four frequencies matched well with those from the tests. The mode shapes were useful for identifying the first two or three important frequencies but the higher modes became difficult to distinguish from insignificant modes. It was unclear from NAFFAP's output which were the predominant frequencies. The spectral analysis offered by NAFFAP is not sufficient by itself because its output of frequencies and mode shapes do not allow one to fully realize a particular frequency's level of participation.

DYFAP's time histories allows one to establish which are the more important frequencies, thus making it an appropriate program to follow a NAFFAP study. A Fourier spectrum of a DYFAP acceleration trace shows only those frequencies that are strong and are associated with vertical motion. Since DYFAP and NAFFAP employ the same floor parameters, their calculated natural frequencies are also the same. Upon comparing the two programs' frequency output, one can identify which are the predominant natural frequencies.

Reliability of DYFAP's peak accelerations depends upon how well the excitation source was modelled and what type of floor excitation was used. DYFAP's success with the bagdrop test showed that the bagdrop impulse was easily modelled as a discretized forcing function. Difficulties with the heel drop simulation using oscillators led to problems of extremely high accelerations. The oscillator results were only comparable using the displacement time histories since they were less susceptible to gross errors resulting from a poor exciter model.

The ISO have adopted a two–mass oscillator to represent a human. A DYFAP run with the ISO model was performed to show DYFAP's performance with this standardized oscillator model. DYFAP managed to provide reasonable agreement with the test's peak displacement. The dominant low frequency nature of the test traces were successfully reproduced by DYFAP.

A simpler human model, a single mass oscillator, was then used to gage how well DYFAP could match the experimental heel drop data. Runs were made for a range of oscillator damping and stiffnesses. The significant influence upon the floor's response of altering the oscillator's damping or stiffness parameters made convergence possible to a "best fit" model. It was shown that the simpler single degree of freedom model was sufficient for DYFAP to approximately reproduce the heel drop test displacement traces.

Previous research by Folz and Foschi [Folz and Foschi, 1991] demonstrated that a forcing function was sufficient to represent a heel drop impulse for the case of a heavy floor system. It was easily established that for lighter floors, where the occupants' mass is up to 30% of the system's mass, a forcing function was insufficient in modelling a heel drop. The mass and low natural frequency of the oscillator were important elements for the successful matching of the test's displacement time histories.

8.3 Further Areas of Study

The preliminary testing with multiple occupants showed that their relative position on the floor was an important factor for determining the response. DYFAP's success with the displacement time histories show promise for multiple occupants. The next logical avenue of research would be to assess DYFAP's ability to reproduce test data of two or more occupants, both passive and active, distributed randomly on the floor. Modelling of a heel drop impact may be improved by developing a time dependent damping and/or stiffness capacity for the oscillators. Modelling the impact as more of a plastic rather than a rigid impact may prove beneficial.

Bibliography

[Allen and Rainer, 1976] Allen, D.E. and Rainer, J.H., "Vibration Criteria for Long Span Floors", Canadian Journal of Civil Engineering, Vol. 3, No. 2, June, 1976, pp. 165–173.

[Billmeyer, 1984] Billmeyer, Fred W., "Textbook of Polymer Science – Third Edition", John Wiley & Sons, USA, 1984.

[Chui, 1986] Chui, Y.H., "Vibrational Performance of Timber Floors and the Related Human Discomfort Criteria", Journal of the Institute of Wood Science, Vol. 10, No. 5, 1986, pp. 183–188.

[Chui, 2/86] Chui,Y.H., "Evaluation of Vibrational Performance of Light-Weight Wooden Floors: Determination of Effects of Changes in Construction Variables on Vibrational Characteristics", TRADA Research Report 2/86, Hughenden Valley, TRADA, U.K.

[Chui, 15/86] Chui,Y.H., "Evaluation of Vibrational Performance of Light-Weight Wooden Floors: Design To Avoid Annoying Vibrations", TRADA Research Report 15/86, Hughenden Valley, TRADA, U.K.

[Chui, 1988] Chui,Y.H., "Evaluation of Vibrational Performance of Light-Weight Wooden Floors", Proceedings of the 1988

International Conference on Timber Engineering, Vol. 1, September 19–22, 1988, pp. 707–715.

[Chui and Smith, 1991] Chui, Y.H. and Smith, I., "Method of Wooden Floor Construction for Minimizing Levels of Vibration", CMHC 1989 External Research Program Project, January, 1991.

[Clough and Penzien, 1975] Clough, R., and Penzien, J., "Dynamics of Structures", McGraw–Hill, USA, 1975, pg. 94.

[Cowie, 1973] Cowie, J.M.G., "Polymers: Chemistry and Physics of Modern Materials", Intext Educational Publishers, USA, 1973.

[Filiatrault and Folz, 1989] Filiatrault, A. and Folz, B., "NAFFAP: Natural Frequency Floor Analysis Program USER'S MANUAL", version 2.0, Dept. of Civil Engineering, U.B.C., September 1989.

[Filiatrault et al, 1990] Filiatrault, A., Folz, B. and Foschi, R.O., "Finite–Strip Free–Vibration Analysis of Wood Floors", Journal of Structural Engineering, Vol. 116, No. 8, August, 1990, pp. 2127–2142.

[Folz and Foschi, 1991] Folz, B. and Foschi, R.O., "Coupled Vibrational Response of Floor Systems with Occupants", Journal of Engineering Mechanics, Vol. 117, No. 4, April, 1991, pp. 872–892.

[Foschi, 1969] Foschi, R.O., "Buckling of the Compressed Skin of a Plywood Stressed-Skin Panel with Longitudinal Stiffeners",

Department of Fisheries and Forestry Canadian Forestry Service Publication no. 1265, 1969, pp. 49–50.

[Foschi, 1982] Foschi, R.O., "Structural Analysis of Wood Floor Systems", Journal Structural Division, ASCE, Vol. 108, No. 7, July, 1982, pp. 1557–1574.

[Grether, 1971] Grether, Walter F., "Vibration and Human Performance", Human Factors, Vol. 13, No. 3, June, 1971, pp. 203–216.

[Malik and Nigam, 1987] Malik, M. and Nigam, S.P., "A Study on a Vibratory Model of a Human Body", Journal of Biomechanical Engineering. Trans. ASME, Vol. 109, May, 1987, pp. 148–153.

[Ohlsson, 1982] Ohlsson, S., "Floor Vibrations and Human Discomfort", Ph.D. Thesis, Chalmers University of Technology, Div. of Steel and Timber structures, Gothenburg, Sweden, 1982.

[Onysko, 1986] Onysko, D., "Serviceability Criteria for Residential Floors Based on a Field Study of Consumer Response", Forintek Canada Corp., Ottawa Laboratory, Ottawa, Ontario, 1986.

[Pechhold, 1973] Pechhold, W., "Deformation of Polymers as Explained by the Meander Model", Battelle Institute Materials Science Colloquia, September 11–16, 1972, pp. 301–313.

[Pernica and Rainer, 1986] Pernica, G. and Rainer, J.H., "Vertical Dynamic Forces from Footsteps", Canadian Acoustics, Vol. 14, No. 2, April, 1986, pp. 12–21.

[Polensek, 1970] Polensek, Anton, "Human Response to Vibration of Wood-Joist Floor Systems", Wood Science, Vol. 3, No. 2, October, 1971, pp. 111–119.

[Rainer, 1980] Rainer, J.H., "Dynamic Tests on a Steel-Joist Concrete-Slab Floor", Canadian Journal of Civil Engineering, Vol. 7, No. 2, June, 1980, pp. 213–224.

[Sazinski and Vanderbilt, 1979] Sazinski, R.J. and Vanderbilt, M.D., "Behaviour and Design of Wood Joist Floors", Wood Science, Vol. 11, No. 4, April, 1979, pp. 209–220.

[Wiss and Parmelee, 1974] Wiss, J.F. and Parmelee, R.A., "Human Perception of Transient Vibrations", ASCE Journal of the Structural Division, Vol. 100, No. ST4, April, 1974, pp. 773–787.

[CMHC, 1984] CMHC, "Canadian Wood–frame House Construction", Publication NHA 5031 M 08/84, Canada Mortgage and Housing Corporation, Ottawa.

[TRUS JOIST] "Residential Products Reference Guide", TRUS JOIST CANADA LTD., January, 1991.

[VU–POINT, 1988] "VU–POINT: A Digital Data Processing System for IBM PC/XT/AT and Compatible Personal Computers", version 1.21, S–CUBED, a division of Maxwell Laboratories inc., March 1988.

[ISO 2631] "Guide for the evaluation of human exposure to whole-body vibration", (1987) Standard No. 2631, Int. Organization for Standardization, Geneva, Switzerland.

[ISO 5982] "Vibration and Shock-Mechanical driving point impedance of the human body", (1987) Standard No. 5982, Int. Organization for Standardization, Geneva, Switzerland.